

# Behavioral Performance and Neurobiology of Sound Localization in the Chicken

**Gianmarco Maldarelli**

Vollständiger Abdruck der von der TUM School of Life Sciences der Technischen Universität München zur Erlangung des akademischen Grades eines

**Doktors der Naturwissenschaften (Dr. rer. nat.)**

genehmigten Dissertation.

**Vorsitz:**

Prof. Dr. Martin Klingenspor

**Prüfer der Dissertation:**

1. Prof. Dr. Harald Luksch
2. Prof. Dr. Bernhard Seeber

Die Dissertation wurde am 22.11.2022 bei der Technischen Universität München eingereicht und durch die TUM School of Life Sciences am 19.03.2023 angenommen.

# Summary

Birds mainly rely on vision and most avian species lack any auditory specialization – such as asymmetric ears, external pinnae or hypertrophied auditory brain nuclei – for a high-resolution sound localization in the 3-D space. However, a proper localization of auditory signals seems necessary for vital cognitive functions, such as recognition of salient calls or audio-visual integration. Therefore, I used the chicken (*Gallus gallus*) as a representative of the auditory generalist birds and investigated behavioral and neurophysiological aspects related to sound localization.

In the first study, I quantified the accuracy for azimuthal sound localization and investigated possible head movement strategies used during the task. I trained roosters to locate broad-band noise along azimuth and discovered that the chicken has high localization acuity compared to other auditory generalist bird species tested so far. The interaural difference in time of arrival and level (ITD and ILD, respectively) at the corresponding minimum audible angles are comparable to what was measured in other non-auditory specialist bird species, suggesting that they are sufficiently informative for azimuthal sound localization. The comparatively good localization acuity thus appears to result from the relatively large head of the chicken. Moreover, during the presentation of sounds with long duration, I discovered characteristic head turns which might be beneficial for localization.

In the second study, I investigated the neural representation of auditory space in specific areas of the midbrain. I conducted *in vivo* extracellular recordings of single neurons in the optic tectum (OT) – known as a hub for multimodal integration – and in the external portion of the *formatio reticularis lateralis* (FRLx) in anaesthetized chickens of either sex. I found that most of the auditory spatial receptive fields (aSRFs) were spatially confined both in azimuth and elevation, divided into two main classes: round aSRFs, mainly present in the OT, and annular aSRFs, with a ring-like shape around the interaural axis, mainly present in the FRLx and arranged in a topographic map. Furthermore, ITD and ILD seem to play a role in the formation of both aSRF classes. These results suggest that, unlike mammals and owls, which have a congruent representation of visual and auditory space in the OT, generalist birds separate the computation of auditory space in two different midbrain

structures, with possible implications in multimodal integration and behavioral strategies related to sound localization.

# Zusammenfassung

Vögel verlassen sich hauptsächlich auf das Sehen, und den meisten Vogelarten fehlt jegliche auditive Spezialisierung - wie asymmetrische Ohren, äußere Ohrmuscheln oder hypertrophierte auditorische Hirnkerne - für eine hochauflösende Schalllokalisierung im 3-D-Raum. Eine korrekte Lokalisierung von Hörsignalen scheint jedoch für lebenswichtige kognitive Funktionen notwendig zu sein, wie z. B. das Erkennen von markanten Rufen oder die audiovisuelle Integration. Daher habe ich das Huhn (*Gallus gallus*) als Vertreter der auditiven Generalisten unter den Vögeln verwendet und verhaltens- und neurophysiologische Aspekte im Zusammenhang mit der Schalllokalisierung untersucht.

In der ersten Studie quantifizierte ich die Genauigkeit der azimuthalen Schalllokalisierung und untersuchte mögliche Kopfbewegungsstrategien, die bei dieser Aufgabe eingesetzt werden. Ich habe Hähne darauf trainiert, Breitbandgeräusche entlang des Azimuts zu lokalisieren, und festgestellt, dass Hühner im Vergleich zu anderen bisher getesteten auditiven Generalisten eine hohe Lokalisierungsschärfe besitzen. Die interaurale Differenz der Ankunftszeit und des Pegels (ITD bzw. ILD) bei den entsprechenden minimalen Hörwinkeln ist vergleichbar mit dem, was bei anderen, nicht auf das Gehör spezialisierten Vogelarten gemessen wurde, was darauf hindeutet, dass sie für die azimuthale Schalllokalisierung ausreichend informativ sind. Die vergleichsweise gute Lokalisationsleistung scheint daher durch den relativ großen Kopf der Hühner bedingt zu sein. Außerdem konnte ich während der Präsentation von Tönen mit langer Dauer charakteristische Kopfdrehungen beschreiben, die für die Lokalisierung von Vorteil sein könnten.

In der zweiten Studie untersuchte ich die neuronale Repräsentation des auditorischen Raums in bestimmten Bereichen des Mittelhirns. Ich führte *in vivo* extrazelluläre Ableitungen einzelner Neuronen im Tectum Opticum (OT) - bekannt als Zentrum für multimodale Integration - und im äußeren Teil der *Formatio reticularis lateralis* (FRLx) bei betäubten Hühnern beiderlei Geschlechts durch. Ich fand heraus, dass die meisten auditorischen räumlichen rezeptiven Felder (aSRFs) sowohl in Azimut als auch in Elevation räumlich begrenzt sind und in zwei Hauptklassen unterteilt werden können: runde aSRFs, die hauptsächlich im OT vorhanden sind, und ringförmige aSRFs, die ringförmig um die



interaurale Achse verlaufen, hauptsächlich im FRLx vorhanden und in einer topographischen Karte angeordnet sind. Außerdem scheinen ITD und ILD eine Rolle bei der Bildung beider aSRF-Klassen zu spielen. Diese Ergebnisse deuten darauf hin, dass im Gegensatz zu Säugetieren und Eulen, die eine kongruente Repräsentation des visuellen und auditiven Raums im OT haben, generalistische Vögel die Berechnung des auditiven Raums in zwei verschiedenen Mittelhirnstrukturen trennen, was möglicherweise Auswirkungen auf die multimodale Integration und Verhaltensstrategien im Zusammenhang mit der Schalllokalisierung hat.

# Contents

|  |            |
|--|------------|
| <b>Summary</b>   | <b>ii</b>  |
| <b>Zusammenfassung</b>   | <b>iv</b>  |
| <b>List of Figures</b>   | <b>x</b>   |
| <b>List of Tables</b>  | <b>xi</b>  |
| <b>Abbreviations</b>   | <b>xii</b> |
| <b>1 Introduction</b>  | <b>1</b>   |
| 1.1 Function of sound localization in birds . . . . .                    | 1          |
| 1.2 Physical cues of sound localization . . . . .                        | 2          |
| 1.2.1 Binaural cues and azimuthal localization . . . . .                 | 2          |
| 1.2.2 Monaural cues and elevational localization . . . . .               | 3          |
| 1.3 Behavioral measurement of sound localization . . . . .               | 5          |
| 1.4 Auditory pathway in birds . . . . .                                  | 6          |
| 1.4.1 Auditory pathway in the barn owl . . . . .                         | 7          |
| 1.4.2 Difference between barn owl and chicken auditory pathway . . . . . | 8          |
| 1.5 Optic tectum and multimodal integration . . . . .                    | 11         |
| 1.6 Objective of the Ph.D. . . . .                                       | 12         |
| <b>2 Azimuthal sound localization in chickens</b>                        | <b>13</b>  |
| 2.1 Materials and Methods . . . . .                                      | 13         |
| 2.1.1 Animals . . . . .  | 13         |
| 2.1.2 Stimuli presentation . . . . .                                     | 14         |
| 2.1.3 Behavioral setup . . . . .   | 15         |
| 2.1.4 Behavioral training . . . . .                                      | 16         |

|          |  |           |
|----------|--|-----------|
| 2.1.5    | Experimental paradigm and data collection . . . . .  | 17        |
| 2.1.6    | IR-Marker application . . . . .  | 18        |
| 2.1.7    | Data analysis . . . . .  | 18        |
| 2.1.8    | Statistical analysis . . . . .   | 20        |
| 2.2      | Results . . . . .  | 21        |
| 2.2.1    | Training . . . . .   | 21        |
| 2.2.2    | Final experiment . . . . .   | 21        |
| 2.2.3    | Calculation of ITD and ILD at the MAA . . . . .  | 23        |
| 2.2.4    | Localization in elevation . . . . .  | 24        |
| 2.2.5    | Head movements . . . . .   | 24        |
| 2.3      | Discussion . . . . .   | 30        |
| 2.3.1    | Azimuthal localization accuracy . . . . .  | 30        |
| 2.3.2    | Head movements during localization . . . . .   | 33        |
| <b>3</b> | <b>Two Types of Auditory Spatial Receptive Fields in Different Parts of the Chicken's Midbrain</b> | <b>35</b> |
| 3.1      | Materials and Methods . . . . .  | 35        |
| 3.1.1    | Animals . . . . .  | 35        |
| 3.1.2    | Surgery . . . . .  | 36        |
| 3.1.3    | Stimulus generation and recording . . . . .  | 37        |
| 3.1.4    | Stimuli presentation . . . . .   | 38        |
| 3.1.5    | Data analysis . . . . .  | 38        |
| 3.1.6    | Statistical analysis . . . . .   | 42        |
| 3.2      | Results . . . . .  | 43        |
| 3.2.1    | VAS stimuli . . . . .  | 43        |
| 3.2.2    | Basic properties . . . . .   | 43        |
| 3.2.3    | Monaural responses . . . . .   | 44        |
| 3.2.4    | aSRFs . . . . .  | 45        |
| 3.2.5    | ITD and ILD tuning properties . . . . .  | 47        |
| 3.2.6    | The units in FRLx and OT show different aSRFs . . . . .  | 49        |
| 3.2.7    | Topographic map in FRLx and OT . . . . .   | 50        |
| 3.3      | Discussion . . . . .   | 51        |
| 3.3.1    | Role of ITD and ILD tuning in aSRF formation . . . . .   | 53        |

|          |   |           |
|----------|---|-----------|
| 3.3.2    | Auditory spatial tuning along the pathway ICx–FRLx–OT . . . . .             | 55        |
| 3.3.3    | Implications for auditory localization and multimodal integration . . . . . | 56        |
| <b>4</b> | <b>General Discussion and Outlook</b>                                       | <b>57</b> |
|          | <b>Bibliography</b>   | <b>65</b> |
|          | <b>Acknowledgments</b>  | <b>77</b> |
|          | <b>Supporting documents concerning copyright</b>                            | <b>78</b> |

# List of Figures

|      |  |    |
|------|--|----|
| 1.1  | Interaural time and level differences (ITD and ILD) as azimuthal cues . . . . .                              | 4  |
| 1.2  | External pinnae generate spectral cues for elevational localization . . . . .                                | 5  |
| 1.3  | Monaural gain from HRTF of auditory generalist birds . . . . .   | 7  |
| 1.4  | Midbrain auditory pathway and visual input to optic tectum in the barn owl. . . . .                          | 9  |
| 2.1  | Sketch of the experimental setup . . . . .   | 16 |
| 2.2  | Overview of behavioral training and final task. . . . .  | 22 |
| 2.3  | Psychometric curves of responses to the right key. . . . .   | 23 |
| 2.4  | Histogram of the response time after target presentation. . . . .  | 25 |
| 2.5  | Time series of the head position and orientation. . . . .  | 25 |
| 2.6  | Head position during trial periods. . . . .  | 27 |
| 2.7  | Head position across periods for each axis. . . . .  | 28 |
| 2.8  | Head orientation across periods for each plane. . . . .  | 29 |
| 2.9  | Histogram of the frontal axis orientation for each period. . . . .   | 30 |
| 2.10 | Comparison of localization acuity across species. . . . .  | 31 |
| 3.1  | ITDs and ILDs of the VAS stimuli. . . . .  | 44 |
| 3.2  | Neural responses to auditory stimulation in FRLx and OT. . . . .   | 45 |
| 3.3  | Properties of the auditory spatial receptive fields. . . . .   | 46 |
| 3.4  | ITD tuning properties. . . . .   | 48 |
| 3.5  | ILD tuning properties. . . . .   | 49 |
| 3.6  | Distribution of aSRFs in FRLx and OT. . . . .  | 50 |
| 3.7  | Anatomical reconstruction of recoding sites and topographic map of the annular aSRFs<br>in the FRLx. . . . . | 52 |
| 3.8  | Projection of aSRFs onto the OT surface. . . . .   | 53 |
| 3.9  | Schematic of the representation of the auditory space in FRLx and OT. . . . .                                | 54 |

|    |   |    |
|----|---|----|
| A1 | Authors permission for reproduction from <i>The Journal of Neuroscience</i> . . . . . | 79 |
| A2 | License for reproduction from <i>Elsevier</i> . . . . .                               | 80 |
| A3 | Copyright for reproduction from <i>PLOS ONE</i> . . . . .                             | 81 |
| A4 | Copyright for reproduction from <i>PLOS ONE</i> . . . . .                             | 82 |

## List of Tables

|     |   |    |
|-----|---|----|
| 2.1 | Summary of data collection for the closed-loop condition. . . . .   | 22 |
| 2.2 | Summary of data collection for the open-loop condition. . . . .   | 23 |
| 3.1 | Count and percentage of units in the OT classified by the combination of monaural response types. . . . .   | 45 |
| 3.2 | Count and percentage of units in the FRLx classified by the combination of monaural response types. . . . . | 45 |

# Abbreviations

**2AFC** Two-alternative forced choice

**aSRF** Auditory spatial receptive field

**BB** Broadband

**BF** Best frequency

**DV** Dorso-ventral

**FRLx** External part of the formatio reticularis lateralis

**HRTF** Head-related transfer function

**ICC-core** Core of the central inferior collicular nucleus

**ICC-ls** Lateral shell of the central inferior collicular nucleus

**ICE** Internally coupled ears

**ICx** External nucleus of the inferior colliculus

**IC** Inferior colliculus

**ILD** Interaural level difference

**IPD** Interaural phase difference

**IR** Infrared

**ISI** Interstimulus interval

**ITD** Interaural time difference

**LLDp** Posterior part of the dorsal lateral lemniscus



|             |                             |
|-------------|-----------------------------|
| <b>LS</b>   | Loudspeaker                 |
| <b>MAA</b>  | Minimum audible angle       |
| <b>ML</b>   | Medio-lateral               |
| <b>MRA</b>  | Minimum resolvable angle    |
| <b>NA</b>   | Nucleus angularis           |
| <b>NL</b>   | Nucleus laminaris           |
| <b>NM</b>   | Nucleus magnocellularis     |
| <b>OT</b>   | Optic tectum                |
| <b>PSTH</b> | Peristimulus time histogram |
| <b>RC</b>   | Rostro-caudal               |
| <b>RI</b>   | Regio intermedius           |
| <b>RT</b>   | Response time               |
| <b>VAS</b>  | Virtual auditory space      |

# 1 Introduction

---

Parts of this introduction are modified from sections of the following publication:

“Two types of auditory spatial receptive fields in different parts of the chicken’s midbrain” (Maldarelli et al., 2022a)

The article is published in *The Journal of Neuroscience*, which permits authors the reproduction of published articles for dissertations without charge or further license (see Figure A1).

---

## 1.1 Function of sound localization in birds

The ability to locate sound sources may well have been the driving force behind the development of airborne sound perception, and has been observed across several animal taxa, from insects to mammals. Sound localization is a fundamental process to form auditory objects that are distinguishable from each other and from the background noise (Bregman, 1990). In birds, sound localization is fundamental for survival, and is present in several behaviors, examples of which will be described below.

One example regards predator-prey interaction, where predators and preys would increase their chances to not be detected by each other, and successfully hunt or not be preyed upon, respectively. For example, Passerines such as the chaffinch (*Fringilla coelebs*) and the wren (*Troglodytes troglodytes*) emit characteristic alarm calls which would be hardly localized by predators (Marler, 1955). In contrast to the previous case, another strategy of preys is to emit alarm calls that are well detectable by predators. The advantage of such behavior is to let the predator know that the prey will hide and flee, discouraging the predator from starting or continuing the chase (Klump and Shalter, 1984). From the predator side, several birds of prey show remarkable hunting abilities relying on auditory cues. Typical examples are the marsh hawk (*Circus cyaneus*), which can successfully hunt rodents hiding in the scrub with exceptional accuracy (Rice, 1982), and the barn owl (*Tyto alba*), which shows

outstanding abilities in hunting in total darkness (Payne, 1971), and its flight can be extremely silent to not be detected by preys (Wagner et al., 2017).

Another example is territorial interaction and defense. Towhees (*Pipilo erythrophthalmus*), for instance, are a quite territorial species, and respond aggressively to conspecific intruders. To accomplish this task, they do not only rely on visual cues but also on auditory ones. In playback experiments, they can accurately localize calls of conspecifics and approach the corresponding loudspeaker (Nelson and Stoddard, 1998).

Moreover, some bird species make use of echolocation for spatial navigation in dark environments. This phenomenon has been observed in the oilbirds (*Steatornis caripensis*; Griffin, 1953; Konishi and Knudsen, 1979) and the cave swiftlets (genera *Aerodramus* and *Collocalia*; Novick, 1959; for a review of echolocating birds: Brinkløv et al., 2013). These species emit bio-sonar signals in order to form a 3D representation of the surrounding environment in darkness, when vision would not be of help. This peculiar feature seems to allow them to nest in dark caves, and it might be evolved to reduce the predation pressure. However, the biosonar calls of these avian species are broadband click-type signals within the audible frequency range, thus providing a lower resolution of the space representation compared to the ultrasonic system of bats and toothed whales.

## 1.2 Physical cues of sound localization

Sound localization is a three-dimensional problem. The position of a sound source can be defined using three parameters within a head-centered spherical coordinate system: 1) the horizontal distance from the sagittal plane or azimuth, 2) the vertical distance from the horizontal plane or elevation, and 3) the distance between the listener and the sound source. The following section will focus on the physical cues used by animals in general – and birds in particular – to locate sounds along azimuth and elevation.

### 1.2.1 Binaural cues and azimuthal localization

Several sensory modalities extract spatial information by means of the difference between two sensory organs. This phenomenon, for instance, is used in stereopsis using the image disparity between the retinae (Patterson and Martin, 1992), in olfactory navigation by comparing the odors between nostrils (Catania, 2013) and in electrolocalization by the change of the electric field on two body areas of the

weakly electric fish (Heiligenberg, 1991). This principle is valid also for auditory localization. But what are the auditory cues that are compared between the two ears?

A sound presented exactly in front – or at the back – of an animal would reach the two ears at the same time and with the same loudness. However, if the stimulus comes from a lateral position, the sound will arrive slightly earlier and louder at the ipsilateral ear compared to the contralateral one. These two binaural cues are called interaural time difference (ITD) and interaural level difference (ILD), respectively (Figure 1.1). When pure tones are presented, the difference in time is encoded by the phase difference between the two ears – called interaural phase difference (IPD). These binaural cues are computed along the auditory pathway and provide information about the location of the sound source along azimuth (see section 1.4). According to the ‘duplex theory’, ITDs are more informative at low frequencies, whereas ILDs are more informative at high frequencies (Rayleigh, 1907).

In mammals and auditory generalist birds, ITD and ILD are mainly used for azimuthal localization. The barn owl, however, uses ITDs and ILDs for sound localization along both azimuth and elevation, thanks to specific anatomical specializations which influence the directionality of the ears (see next paragraph).

### 1.2.2 Monaural cues and elevational localization

The binaural cues alone are not sufficient for an unambiguous localization of sound sources in 3D space – e.g., there are ambiguities for the localization of sounds along elevation, as well as for the discrimination of sounds coming from the front and the back. In a 3D spherical coordinate system, constant ITDs and ILDs lie on the surface of a cone – known as “cone of confusion”. The apex of the cone is at the center of the head, whereas the cone axis is parallel to the interaural axis. Thus, in principle, ITDs and ILDs alone are ambiguous for frontal and back positions along azimuth, and between top and bottom locations along elevation.

However, mammals have external ear structures which introduce attenuations of certain frequencies as a function of elevation. These notches in the spectrum allow the auditory system to estimate the elevation of the sound source (Figure 1.2). Interestingly, elevational localization seems to be a learned behavior: after insertion of ear molds in human participants, their performance in sound localization decreased in elevation – but did not change along the horizontal plane -, but over time the performance slowly improved, until reaching, after around 1 month, the level before ear mold insertion (Hofman et al., 1998).

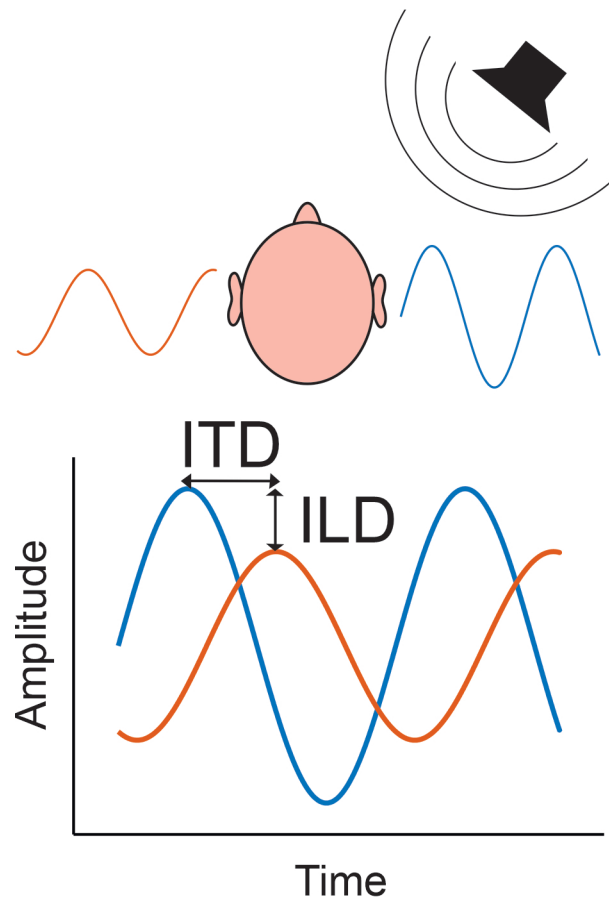


**Figure 1.1** Interaural time and level differences (ITD and ILD) as azimuthal cues. When a sound comes from the side, the sound reaching the ipsilateral ear (blue sound wave) arrives earlier and louder than the contralateral ear (the red soundwave). This difference generates ITDs and ILDs, which are used for azimuthal localization by the auditory system.

Birds, reptiles and amphibia lack external pinnae that can be used for elevational localization. However, there are some species that evolved specific auditory adaptations. For example, the barn owl has asymmetric ears and a facial ruff (von Campenhausen and Wagner, 2006). The ruff consists of two types of feathers, called auricular and reflector feathers (Koch and Wagner, 2002). The former are poorly ramified and acoustically transparent, present in the facial disc, while the latter are present at the ruff border, are densely ramified and reflect sounds to the ear openings (Koch and Wagner, 2002). Both the ears asymmetry and the reflector feathers cause a vertical disparity in the directionalities of the two ears, providing ILDs that change as a function of elevation (von Campenhausen and Wagner, 2006). As a result, in the auditory pathway an ITD/ILD map is formed, where ITDs mainly encode azimuth and ILDs mainly encode elevation. This has been shown with behavioral studies (Moiseff, 1989b; Poganiatz and Wagner, 2001; Poganiatz et al., 2001) as well as electrophysiological recordings (Moiseff, 1989a; Takahashi et al., 2003). However, ILDs are also used for azimuthal localization, especially to resolve ambiguities given by the ITDs (Kettler et al., 2017).

While sound localization in the barn owl has been studied for decades, most bird species are not specialists for auditory localization, and typically have symmetric ears and lack any peripheral adaptations. Thus, while the ability to locate sound in azimuth has been broadly acknowledged, the ability of generalist birds to locate sound in elevation is not clear. Even though a study published some years ago provided evidence for the introduction of elevation-dependent monaural cues by the head shape of generalist birds (Schnyder et al., 2014), the role and contribution of these cues in auditory localization remained untested.

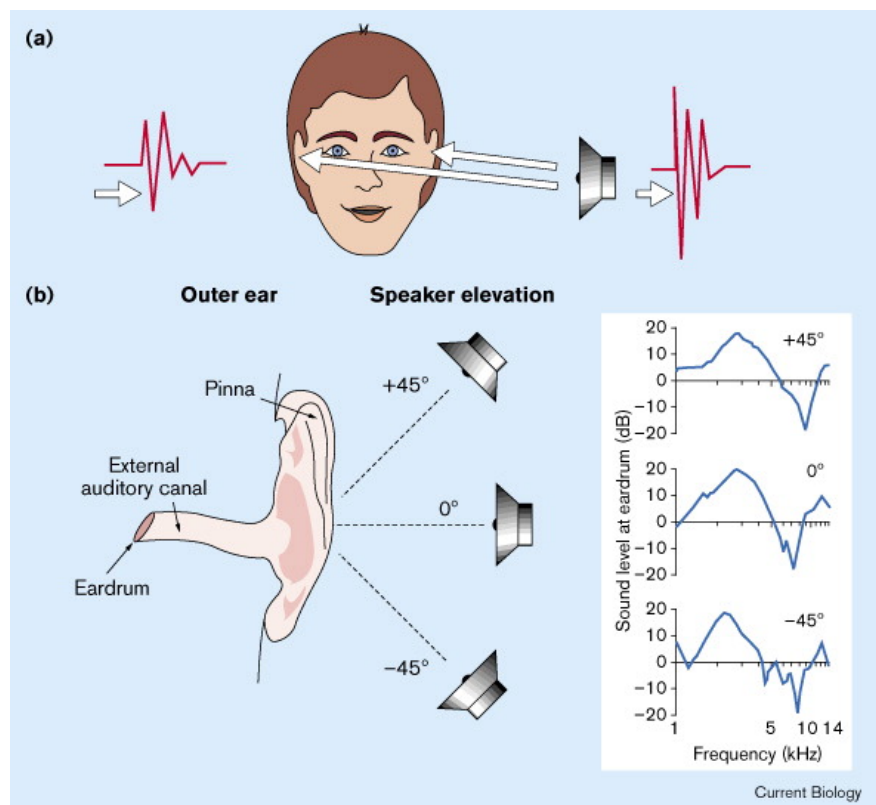


**Figure 1.2** External pinnae generate spectral cues for elevational localization. The same sound reaching the eardrum from different angles in elevation has different spectra due to the filtering property of the external ear. These notches are informative for localization along elevation. (Moore and King, 1999; reproduced with permission from *Elsevier*, see Figure A2)

### 1.3 Behavioral measurement of sound localization

Sound localization acuity along azimuth has been measured in several animal species during the last decades using psychophysical experiments. One seminal study by Mills (1958) measured sound localization in humans using a two-alternative forced choice (2AFC) task, where the participants located the sound direction in respect to a central reference sound. From the resulting psychometric function showing the subject response as a function of the angle between target and reference sound

sources, it was possible to quantify the localization accuracy by calculating the so-called minimum audible angle (MAA). Similar experiments have been conducted in other animals, such as mammals (e.g., in cat: Heffner and Heffner, 1988) and birds (see below). These experiments also used different paradigms, such as absolute localization tasks – i.e., where the subject locates a sound source between two possible locations –, which are quantified by the minimum resolvable angle (MRA).

In birds, the species most studied behaviorally is the barn owl. Several experimental paradigms have been developed to measure the behavioral response to change in sound location, such as tracking saccadic head movements toward the target stimulus with the search coil technique (Knudsen and Konishi, 1979; Knudsen et al., 1979), measuring the pupillary dilation response (Bala and Takahashi, 2000; Bala et al., 2003), and behavioral training in a Go/NoGo task (Krumm et al., 2019). All of these studies showed a notable high resolution of the auditory space with an MAA as small as 3-4° for broadband (BB) noise. Regarding the auditory generalist birds, several studies measured the sound localization accuracy in a number of species, such as the great tit (*Parus major*; MAA=21°; Klump et al., 1986), the budgerigar (*Melopsittacus undulatus*; MAA=29°), the canary (*Serinus canarius*; MAA=27°), the zebra finch (*Poephila guttata*; MAA=101°; Park and Dooling, 1991), the European starling (*Sturnus vulgaris*; MAA=17°; Feinkohl and Klump, 2013), the bobwhite quail (*Colinus virginianus*; Gatehouse and Shelton, 1978), the red-tailed hawk (*Buteo jamaicensis*; MAA=9°) and the American kestrel (*Falco sparverius*; MAA=11°; Rice, 1982). In general, these species show inferior localization accuracy than the barn owl due to a small-sized head – implying small binaural cues – and lack of auditory specializations. A recent study was also conducted in chicken females (*Gallus gallus*), measuring the MAA for BB noise and for pure tones in the range between 0.5 and 4 kHz (Krumm et al., 2022). The results show that chickens have a remarkable localization accuracy and that, in line with the duplex theory, ITDs are informative at low frequencies, whereas ILDs are informative at high frequencies.

## 1.4 Auditory pathway in birds

The difference between the original acoustic signal and the filtered version reaching the eardrums is expressed in the head-related transfer function (HRTF; Wightman and Kistler, 1989; Keller et al., 1998) and represents the input used by the auditory system for the coding of the auditory space (Figure 1.3). In the following section, I will describe the general structure of the auditory pathway in the avian brain, which mainly refers to studies conducted in the barn owl (Figure 1.4; for a review see Singheiser et al., 2012; Takahashi et al., 2021).

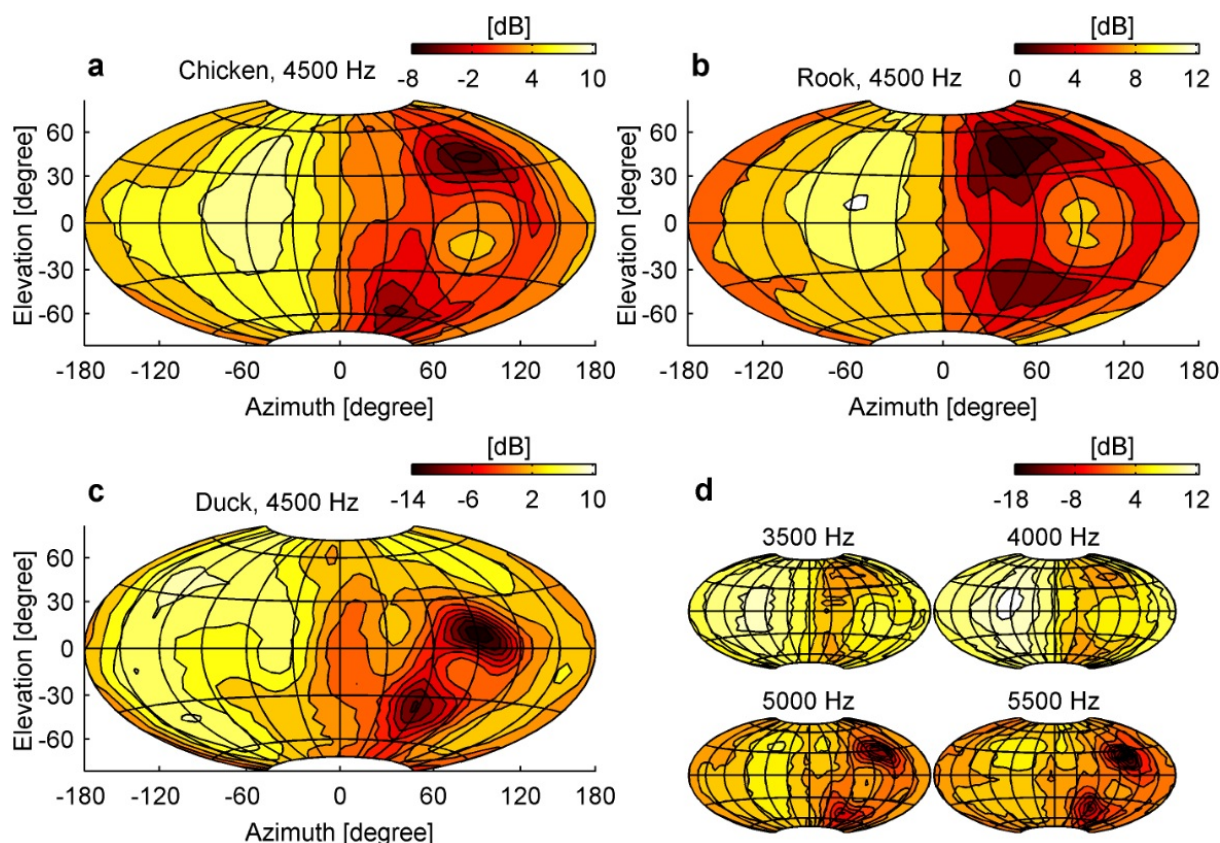


**Figure 1.3** Monaural gain from the head-related transfer function (HRTF) of auditory generalist birds [chicken (a, d), rook (b) and duck (c)]. Monaural gain [dB] is displayed at the right ear for multiple sound positions. Coordinates of  $0^\circ$  azimuth and  $0^\circ$  elevation face the beak,  $-90^\circ$  azimuth and  $0^\circ$  elevation face the right ear. Sound intensity is projected according to the Hammer projection. Meshgrid spacing is  $30^\circ$ , iso-contourline spacing is 2 dB. (reproduced from Schnyder et al., 2014; It is an open-access article distributed under the terms of the Creative Commons Attribution License, which permits unrestricted use, distribution, and reproduction in any medium, provided the original author and source are credited, see Figure A3)

### 1.4.1 Auditory pathway in the barn owl

The first step is the encoding of frequency-specific amplitude and phase of the sound at each ear. In the auditory nerve, the amplitude is coded by the spike rate, whereas the phase is coded by phase-locking, i.e., spikes are evoked at a certain phase of the sound wave. The auditory nerve bifurcates and projects to two cochlear nuclei, the *nucleus magnocellularis* (NM) and *nucleus angularis* (NA), which provide the monaural inputs for the independent and parallel pathways for the computation of IPD/ITD and ILD, respectively (Takahashi et al., 1984).

The processing of IPD/ITD takes place first in the *nucleus laminaris* (NL), which receives inputs from both ipsilateral and contralateral NMs (Parks and Rubel, 1975). The ITD processing is frequency dependent and similar to a place-code model proposed by Jeffress (1948). It is based on delay lines – i.e., the axons coming from the NMs – and coincidence detectors – i.e., the NL neurons –: each neuron is innervated by both NMs, and the NMs axons projecting to the NL have a different length.



Each NL neuron fires when the spikes from the two axons arrive at the same time. The difference in length between the two axons compensates for the difference in the time of arrival of the sound at the two ears. Consequently, each neuron will fire at a specific ITD; thus, the ITD is topographically represented (Carr and Konishi, 1988, 1990). The NL projects to the core of the contralateral central inferior collicular nucleus (ICc-core; Wagner et al., 1987) and from there to the lateral shell of the central inferior collicular nucleus (ICc-ls; Takahashi et al., 1989). In these areas, neurons are arranged in columns according to the best frequency and with roughly the same best ITD. ICc-ls neurons also receive ILD input from the posterior segment of the dorsal lateral lemniscal nucleus (LLDp; see next paragraph). Each neuron in the external nucleus of the inferior colliculus (ICx) receives input from ICc-ls neurons of the same column, merging the information across frequencies and endowing the ICx neurons to be tuned to the space-specific ITDs across frequencies (Takahashi and Konishi, 1986). As a result, ICx presents a map of best ITDs. ICx projects to the optic tectum (OT), where the best ITD map and the spatial tuning are preserved (Knudsen and Konishi, 1978; Knudsen and Knudsen, 1983).

The processing of ILD is less well delineated. The first site involved in the ILD computation is the LLDp, where neurons are excited by stimulation of the contralateral ear and inhibited by stimulation of the ipsilateral ear ('EI' cell types); thus, the ILD response curves are sigmoidal. The LLDp projects to the ICc-ls and this provides the ICc-ls with both ITD and ILD information. However, only in areas further along the auditory pathway a clear ILD sensitivity has been recorded, such as in the ICx (Singheiser et al., 2012) and the OT. In the ICx a neural map of auditory space is formed by the multiplicative computation at each neuron of a specific ITD-ILD combination (Peña and Konishi, 2001), forming narrowly tuned spatial receptive fields (Singheiser et al., 2012).

#### **1.4.2 Difference between barn owl and chicken auditory pathway**

The organization of the auditory system of owls in general is likely a derived character and differs in many aspects from that of other birds. This is evident from the major differences in the auditory pathway between the chicken and the barn owl, as a result of a different development of the auditory brainstem (for a review, see Kubke and Carr, 2000). In general, in the barn owl the auditory nuclei have peculiar specializations and hypertrophied structures.

The barn owl has an extremely elongated papilla and an extended high-frequency hearing range. On the contrary, the chicken and other generalist birds have a shrunk frequency representation at the papilla apex, which endows an extension of the lower-frequency hearing range (Gleich et al., 2004).

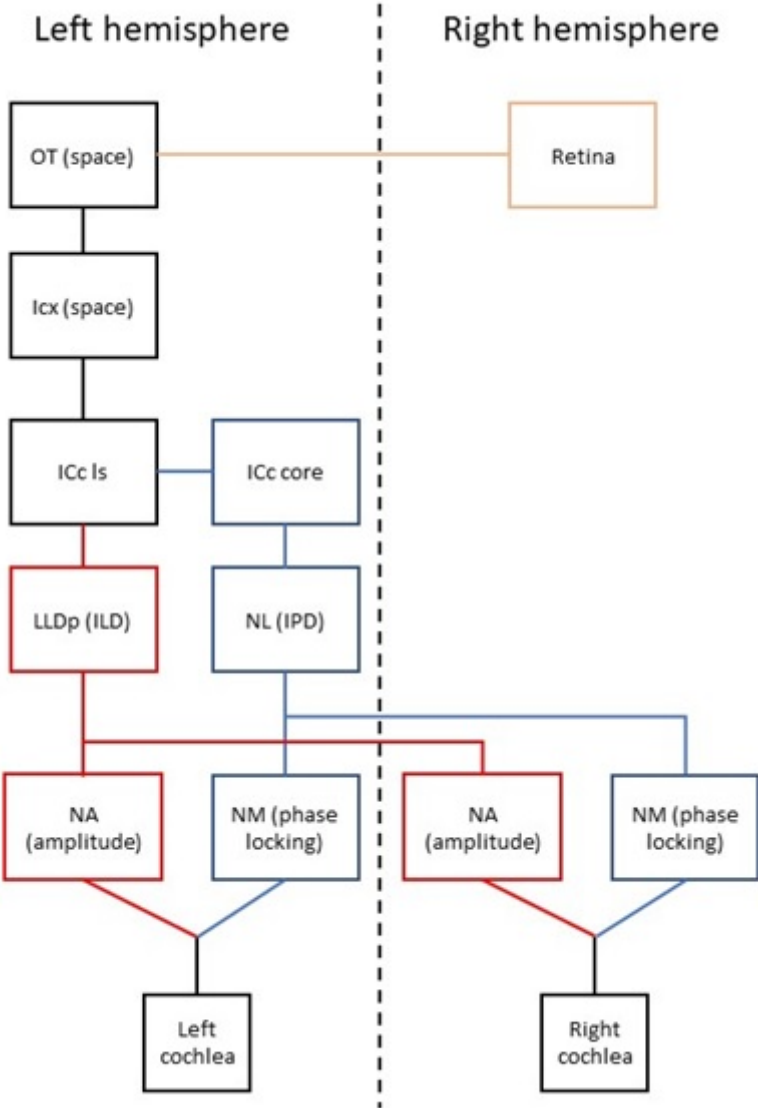


**Figure 1.4** Midbrain auditory pathway and visual input to optic tectum in the barn owl. Red and blue indicate the parts where the amplitude and phase information are processed, respectively. Black indicates where both auditory cues are computed together, whereas orange indicates the visual input that reaches the OT.

Thus, the chicken is sensitive to infrasound, up to a frequency as low as 9 Hz (Hill et al., 2014). On the other hand, the barn owl has an over-representation of high frequencies, called ‘auditory fovea’ (Köppl et al., 1993) and a wider frequency hearing range (0.1-10 kHz) compared to the chicken (0-5 kHz).

Moreover, the auditory nerve in the barn owl has a high-frequency phase-locking, which is necessary to successfully transmit the high-frequency phase information to the cochlear nuclei (Köppl, 1997), while, there is a deterioration of phase locking at high frequencies in the chicken between the auditory nerve and the cochlear nuclei (Salvi et al., 1992).

At higher-level nuclei along the pathway, the NL of chicken and barn owl have different characteristics, in order to provide a more accurate detection (for a review, see Carr and Friedman, 1999). First, the adult chicken NL is a single layer of bipolar neurons, while the barn owl NL is a thick neuropil. On closer look, it is evident that it is because the structure observed in the chicken - i.e. a line of detection neurons – is a ‘module’ that is replicated several times in the barn owl. Second, the NM projections to the NL are asymmetric in the chicken, as only the contralateral axons have a different length in a gradient (Parks and Rubel, 1975; Young and Rubel, 1983), thus only that side operates as delay lines (Overholt et al., 1992). In contrast, the barn owl NM axons form delay lines on both sides (Carr and Konishi, 1988, 1990).

The structure of the inferior colliculus (IC) is quite similar between chicken and barn owl, since both have distinct areas receiving contralateral inputs from NA and NL, where the NL-receiving area projects to the contralateral NA-receiving area (Wang and Karten, 2010). In the barn owl, these regions correspond to the ICc-core and ICc-ls, respectively (see section 1.4.1). This nomenclature has also been adopted by some authors for the chicken (Puelles et al., 1994; Puelles, 2007). However, in the chicken it is not clear whether ICc-core and ICc-ls correspond to the NA and NL receiving areas, respectively. Moreover, in the chicken there is a rostro-medial region of ICc that receives bilateral projections from an interposed region of cells lying at a caudal level, between the NL and NA, called *regio intermedius* (RI). The RI-receiving area in ICc shows reciprocal commissural projections (Wang and Karten, 2010), and projects to separate regions of the *nucleus ovidalis* (Ov), the target of ICc in the thalamus (Wang et al., 2017). The RI pathway seems to play a role in the processing of infrasound (Wang and Karten, 2010), and no equivalent area has been described in any other bird.

In addition, another brain area along the auditory pathway has been discovered in the chicken, called *formatio reticularis lateralis pars externa* (FRLx). The FRLx is located in the midbrain, it receives input from the ICx and projects to the OT, and it is discussed as the plesiomorphic connection between the ICx and the OT (Niederleitner et al., 2017). Thus, in the chicken the auditory information from ICx reaches the OT through a direct – but rather weak – connection, as well as through the FRLx. However, little is known about the neural activity and the functional role of the FRLx. As a comparison, in the barn owl the ICx – OT connection is mainly direct, and this might be an adaptation to provide high localization acuity for hunting in dark environment (Niederleitner et al., 2017).

The lack of auditory specializations in generalist birds raises the question of how the auditory space is represented in the auditory system with a reliable resolution, especially in elevation. Several electrophysiological studies investigated the auditory spatial receptive fields (aSRFs) in the auditory

midbrain of generalist birds, but the results are ambiguous. As an example, the aSRFs in the ICx of hawks and owls with symmetrical ears show responses with no elevational features (Calford et al., 1985; Volman and Konishi, 1990); another study in the pigeon OT, however, found auditory responses spatially confined along both azimuth and elevation (Lewald and Dörrscheidt, 1998). As mentioned earlier, there is evidence that the simple head shape of some generalist bird species, including the chicken, provides monaural cues which change systematically across elevation and which, therefore, could be used by the animal for elevational localization (Schnyder et al., 2014).

## 1.5 Optic tectum and multimodal integration

Birds – like most animal species – possess several types of sensory organs, and this sensory abundance has the advantage of providing an enriched input for a more accurate representation of the surrounding environment compared to the resolution of only one sense. However, this requires an accurate alignment and integration of the sensory information streams in the brain. This process is called multimodal integration and is encoded by precise computational rules – such as the “superadditivity” rule –, where multimodal neurons dramatically enhance their activity in response to weak multisensory stimuli compared to only one modality (Stein and Meredith, 1993). In birds, multimodal integration takes place in the OT, which is homologous to the mammalian superior colliculus (Knudsen and Brainard, 1995). The OT is part of both visual and auditory pathways, where the visual input comes directly from the retinal ganglion cells (review in Luksch, 2003). There are several studies that have investigated multimodal processing in the avian OT: in the barn owl, for instance, the visual and auditory space maps overlap well (Knudsen, 1982); there is an overlap of the auditory and visual receptive fields in the pigeon (Lewald and Dörrscheidt, 1998); both visual and auditory stimuli are processed in the OT of the chicken (Cotter, 1976), and young chicks exhibit audio-visual integration as shown in a behavioral study (Verhaal and Luksch, 2016).

In contrast to the barn owl, which possesses auditory specializations and frontally oriented eyes as adaptations for the nocturnal hunting (Harmening and Wagner, 2011; Wagner et al., 2013), the generalist birds, which are mostly preyed upon, mainly rely on vision and have a laterally eye orientation to inspect the surroundings to full extent (Iwaniuk et al., 2008). Even though the generalist birds OT has a topographic map of visual space (Clarke and Whitteridge, 1976), it is not known how the auditory space might be represented and how it could coherently match the visual map for multimodal integration.

## 1.6 Objective of the Ph.D.

In my Ph.D., I used the domestic chicken (*Gallus gallus domesticus*) as a representative of non-auditory-specialist birds with the aim of investigating the behavioral accuracy and the neurophysiological mechanisms underlying sound localization. The auditory system of the chicken has been studied for decades and it has already been considered a representative of generalist birds, in comparison to the auditory specialist barn owl (Kubke and Carr, 2000); however, as described in the Introduction, some basic aspects of its sound localization were still unexplored.

My work can be divided into two main studies:

In the first study (Chapter 2), I investigated the psychophysics and the behavior underpinning azimuthal sound localization, and also attempted to measure elevational sound localization. The aim was to calculate the accuracy in azimuthal localization of BB noise and to analyze the head orientation to understand what behavioral strategy was used to maximize the sound localization accuracy.

The second study (Chapter 3) investigated the neural response to auditory stimuli in the midbrain, in particular in the FRLx and OT. The aim was to verify whether a map of auditory space is represented in the midbrain, how good the resolution is, and whether the elevational component is also encoded.

## 2 Azimuthal sound localization in chickens

---

This chapter is modified from the Materials and Methods, Results and Discussion sections that correspond to the following publication:

“Azimuthal sound localization in the chicken” (Maldarelli et al., 2022b)

The article is published in *PLOS One*, distributed under the terms of the Creative Commons Attribution License. This permits unrestricted use, distribution, and reproduction in any medium, provided the original author and source are credited (see Figure A4).

---

### 2.1 Materials and Methods

#### 2.1.1 Animals

In total the behavioral training involved 15 chickens (*Gallus gallus*, White Leghorn; 13 males, 2 females). However, as in the first behavioral cohort the female subjects did not learn the final task (see section 2.2.1), I continued to train males and eventually collected data for the final task from 3 male chickens aged between 100 and 160 days post-hatch. Fertilized eggs were provided by the Chair of Reproductive Biology, TUM School of Life Sciences, incubated at 37 °C and 70 % humidity and, after hatching, reared at the animal facility of the Chair of Zoology, TUM School of Life Sciences. The animals were kept in groups in cages with access to sand, perches, water, and food *ad libitum*. The bird housing facilities were artificially illuminated with UV-balanced light in a 12 h/12 h light-dark cycle. After the period where the animals were tested for this study, they were used in electrophysiological experiments. At the end of those experiments the animals, which were kept anaesthetized by a constant injection of anesthetic (ketamine: 13mg/kg/h; xylazine: 4mg/kg/h), were sacrificed with an intrapulmonary injection of sodium-pentobarbital (200mg/kg, Narcoren) and decapitated with poultry scissors. All experiments were performed according to the principles regarding the care

and use of animals adopted by the German Animal Welfare Law for the prevention of cruelty to animals. This study (including the mentioned electrophysiological experiments) was approved by the Government of Upper Bavaria, Germany (permit no. ROB-55-2-2532-Vet\_02-18-154).

### 2.1.2 Stimuli presentation

The stimuli were broadband (BB) noise (0.4 – 4 kHz), in the frequency range corresponding to the highest chicken's sensitivity, according to its audiogram (Hill et al., 2014). A ramp function of 10 ms was applied at the beginning and the end of the stimuli; the time duration was 0.1 s or 1 s, depending on the experimental paradigm. In this study, the experimental condition with presentation of BB noise with 1 s duration is called "closed-loop condition", whereas the presentation of BB noise with 0.1 s duration is called "open-loop condition". In the literature the terms "closed-loop" and "open-loop" typically refer to the presence or absence of an orienting head movement used to enhance sound localization, as observed, e.g., in the barn owl (*Tyto alba*) (Knudsen et al., 1979). In our study I use these terms because, regarding the long duration sounds, an active head movement was observed (see section 2.2.5), whereas, for the short duration stimuli, a duration of 100 ms would not be long enough to allow the chicken to respond with a head movement. The barn owl, for example, which is an auditory specialist, has a head turn latency of about 100 ms (Knudsen et al., 1979; Wagner, 1993). Thus, the localization accuracy in this case would solely depend on the 'snapshot' binaural cues. The stimuli were generated by a custom-written script in MATLAB (MathWorks, USA), converted to analogue signals via an external sound card (Fireface 400, RME, Germany), amplified (AX-396, Yamaha, Japan) and presented through the loudspeakers (Cougar NSW1-205-8A, AuraSound, USA).

11 loudspeakers were mounted on a semi-circular aluminum structure (radius = 50 cm; from now on called 'loudspeakers hoop') mounted at the chamber wall opposite from the entrance. The center of the loudspeaker hoop semi-circle was at the position where the head of the chicken was supposed to be during the stimuli presentation. The loudspeakers were covered with an acoustically transparent but optically opaque cloth to prevent visual cues from membrane movement. Each loudspeaker had been calibrated to 60 dB SPL RMS using a measuring amplifier (type 2636, Brüel & Kjaer, Denmark) and a microphone positioned at the center of the loudspeaker hoop semicircle. In order to cancel out differences between loudspeakers characteristics which could be used by the bird as a discrimination cue, I compensated the loudspeakers to obtain a flat frequency response for each of them.

### 2.1.3 Behavioral setup

The behavioral experiments took place in a chamber (width: 1.5 m W, 1.5 m D x 1.5 m H), coated with a 10-cm thick layer of pyramid-shaped sound-absorbing foam. The floor area where the animals could freely move was covered with a carpet to avoid sound reflections. The chamber was illuminated with two LED lightbulbs, one of which was always on, while the second one could be turned off to lower the illumination as punishment for incorrect response of the animal during training or experimental sessions (see section 2.1.5). A keys box was located between the loudspeaker hoop and the chicken, consisting of 3 plastic buttons, each of them placed on top of a switcher (D45U-V3LD, ZF Friedrichshafen AG, Germany). The central button was pressed by the subjects to initiate the trial, while the two lateral keys were pressed as a behavioral response to the stimuli presentation. Next to each button there was a 5-mm diameter LED (Conrad Electronic, Germany), used to provide a visual cue to the subject indicating the pre-trial period and the response period (see Section 2.1.5, Figure 2.1). A plastic-coated steel fence (1.06 m high; HEV Heimwerkermarkt GmbH & Co. KG, Germany) was mounted between the keys box and the loudspeaker hoop, in order to prevent the animals to access the loudspeakers area. In front of the chamber entrance, and behind the bird when it was facing the loudspeakers, there was a glass plate where the food pellets (Gallogold Küken Alleinkorn C, BayWa, Germany) were provided through a pipe and delivered by a custom-made food feeder placed on top of the chamber (components and assembly instructions available: [www.jonasrose.net](http://www.jonasrose.net)). The food plate was surrounded by an LED band (Josef Barthelme GmbH, Germany) which turned on during the food delivery, as a reward cue. A camera (30 fps, 720p; W15, Jelly Comb, USA), connected to an external Windows-operated laptop, was fixed on the door wall to monitor and record the behavior of the subjects during training and experimentation. The control and execution of the experiments (including receiving inputs from the keys box switchers, presentation of stimuli, control of the feeder and the punishment lightbulb) was done with a custom-written MATLAB script, which allowed to control a general-purpose input/output device (K8055, Velleman, Belgium).

### Mocap system

The mocap system (Flex 13, NaturalPoint Inc. DBA Optitrack, USA) consisted of 6 infrared (IR) cameras (refresh rate: 120 Hz) placed on the 4 walls of the behavioral chamber (2 on the back wall, 2 on the frontal wall, and 1 on each lateral wall), at a height between 80 and 90 cm above the floor. These cameras detected the IR-reflective markers placed on the chicken's head for a continuous recording of the 3D position and orientation during the task performance.



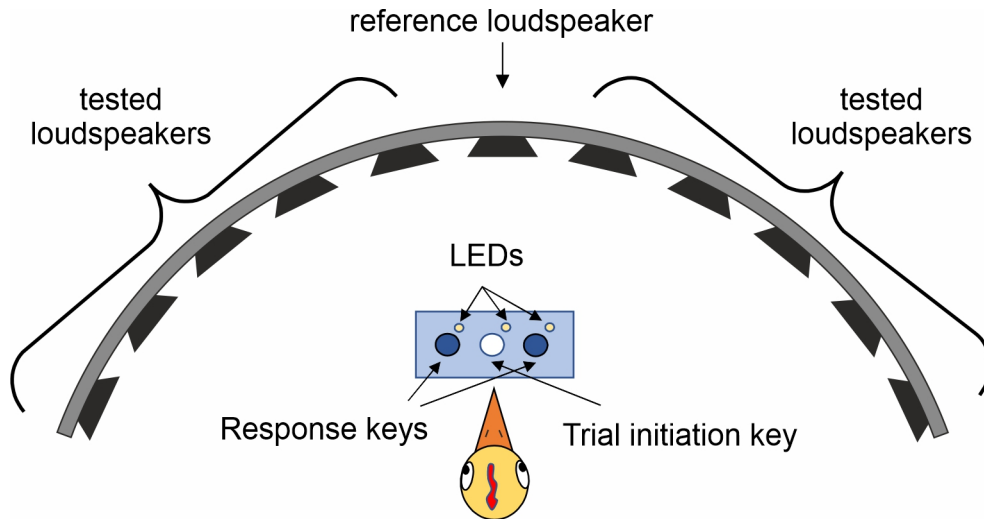


Figure 2.1 Sketch of the experimental setup

## 2.1.4 Behavioral training

### Azimuthal localization task

The behavioral training involved 15 chickens (13 males, 2 females). The choice to train mainly males was justified by previous preliminary training (tested in 3 males and 5 females, where 2 roosters learned the final task), in which females showed a motivational drop during the last steps of the training paradigm and could not even learn to localize the most lateral sounds (at  $-65^\circ$  and  $+65^\circ$  azimuth). The training started from the age of 5-12 days post-hatch and was divided into different tasks with increasing difficulty until reaching the final experimental task. It was based on operant conditioning and positive reinforcement. At the beginning, after familiarization with the trainers, the birds were rewarded every time they pressed a button with the beak. Then, the animals were trained to press only the buttons indicated by a visual cue, i.e., the corresponding LED. Starting from the third week post-hatch, the birds could be trained alone without social isolation distress. When the animals reached high performance at following the visual cues, the auditory cues were also included, by playing sounds at the most lateral positions. At this stage, the LED of the correct response key was turned on with a delay after the target sound presentation, creating an advantage in reward time for the animals that used the sound as a main cue. Then, both lateral LEDs were turned on, removing any information content of the visual cues. When the animal reached high performance at this task (i.e., the performance was higher than chance level according to the binomial test,  $p \leq 0.01$ ; see section 2.1.8), the target sounds at smaller angles were gradually included, until the presentation of all of them. At this point the animal could be tested in the final task.

### **Elevational localization task**

I also attempted to measure the sound localization accuracy in elevation. To switch from the azimuthal to the elevational paradigm, I progressively tilted the LS hoop across sessions until reaching the vertical position. The reference LS, previously located at  $0^\circ$  elevation and  $0^\circ$  azimuth, was then repositioned at around  $45^\circ$  elevation  $0^\circ$  azimuth. This means that the chicken had to discriminate between locations from above (elevation between  $45^\circ$  and  $90^\circ$ ) and frontally (elevation between  $0^\circ$  and  $45^\circ$ ). The response keys box remained in the usual position and the response protocol did not change. Therefore, in the case that the LS hoop was tilted counterclockwise, in the final vertical position the chicken had to press the right response key for sounds coming from above, and the left key for sounds coming frontally.

#### **2.1.5 Experimental paradigm and data collection**

The task was a relative sound localization task, i.e., the subject had to localize the direction of a target sound in relation to a reference sound, tested using a 2-alternative-forced-choice (2AFC) paradigm. The trials were grouped into sessions, each of them containing 30 - 48 trials. Within each session, the number of repetitions for each target sound location ranged between 3 and 4, and the order of the stimuli presentation was pseudo-randomized. Between sessions there was a 5-minute break. At the beginning of each session, the animal was placed into the chamber, and the experiment was performed with the door closed. Each trial consisted of the following sequence of events: the subject pressed the central key for the trial initiation; a BB noise was presented from the central loudspeaker (the reference stimulus); after 0.5 s of inter-stimulus interval, the same sound was presented from one of the lateral loudspeakers (the target stimulus); at the end of the second stimulus presentation, the subject pressed one of the lateral keys to report the direction of the second sound in relation to the first one. The response period was indicated by illumination of both lateral LEDs. The correct response was pressing the key at the same side of the second target sound. In that case, the food plate LEDs turned on for 3 s and the reward food was delivered onto the plate. In case of wrong responses (i.e., pressing the key at the opposite side of the target stimulus) the illumination was dimmed for a period of 2 - 3 s. In case the subject pressed the central key, the same punishment was applied. The response period had a duration of 4 - 5 s, therefore if the subject did not respond within that time window, a new trial could be initiated by pressing the central button.

### 2.1.6 IR-Marker application

For one chicken (subject n.1) the head movements were tracked during the localization task. To do so, 4 spherical IR-reflective markers were attached to the subject's head to be detected by the IR cameras array. Two metal rods with thread endings were pierced through the comb, and one was pierced through the skin at the neck. The rods at the comb had one spherical marker on one side, and a nut on the opposite side; the rod at the neck had markers on both endings. To obtain an unambiguous pattern and hence a better detection by the cameras, an asymmetric arrangement of the markers was chosen. The whole procedure was performed under general anesthesia: an initial dose was injected (ketamine: 40 mg/kg; xylazine: 12 mg/kg), followed by maintained anesthesia with injections every half an hour (ketamine: 13 mg/kg; xylazine: 4 mg/kg). Moreover, a local analgesic lidocaine (Xylocain, AstraZeneca GmbH, Germany) was applied to the skin regions before the piercing operation. All protocols and procedures were in accordance with the institutional guidelines of the authorities of Upper Bavaria, Germany (permit no. ROB-55-2-2532-Vet\_02-18-154).

### 2.1.7 Data analysis

#### Behavioral data

Given the high variability in the subjects' motivation across time, I applied some criteria for the selection of the valid sessions to be included for the data analysis, divided into two steps.

During the response time window of each trial, the subject could show 2 behaviors in addition to the typical lateral responses: 1) pressing the central key or 2) not providing any response. Since a high rate of these undesired behaviors indicates a lack in motivation or inability of performing the task, as a first step I discarded the sessions where the rate of lateral pecking responses was < 75% of the total trials.

Secondly, when the animal consistently reported lateral responses, I expected the localization performance to be above chance level for wide angles between reference and target stimuli. Considering that the MAA of the starling (*Sturnus vulgaris*), another generalist bird, is equal to 17° (Feinkohl and Klump, 2013), I assumed that angles  $\geq 52^\circ$  are sufficiently wide to be easily localized by the chicken. These angles corresponded to the two leftmost and two rightmost loudspeakers on the loudspeaker hoop (- 52°, - 65° and + 52°, + 65°). However, in some cases I observed a biased response strategy, where the subject responded systematically (or preferentially) to one of the two lateral keys, regardless of the target location. In order to discard these inappropriate sessions, I only considered the sessions

where the proportion of correct responses to the external loudspeakers was significantly high and not due to chance (see section 2.1.8). The appropriate sessions were used for the calculation of the MAA.

The procedure to calculate the MAA is comparable to what has been done in a similar study on humans (Mills, 1958). The proportion of the responses to the right key has been plotted as a function of the angle between reference and target stimulus. After fitting the curve to the data (see section 2.1.8), it was possible to calculate the angle at which the proportion of responses was equal to 0.25 and 0.75 ( $A_{25}$  and  $A_{75}$ , respectively). The MAA was calculated as the mean of the absolute values of  $A_{25}$  and  $A_{75}$ .

### **Mocap data**

For one chicken (subject n.1) the head movements were tracked during the localization task. During each trial the chicken performed the closed-loop condition task as before the application of the markers. The acquisition and representation of the 3D data of the head was accomplished online by the commercial software Motive:Tracker (Optitrack, USA). The 3D configuration of the markers was treated by the software as a rigid body. The center of the rigid body was the medial point along the interaural axis, and 3 axes were identified, orthogonal to each other: 1) the interaural axis; 2) the frontal axis, connecting the interaural axis to the beak tip; 3) a third axis orthogonal to the plane where the 2 other axes laid on. The position and orientation of the head in the following analysis refer to the distance and angle from the standard condition, respectively: the standard position is defined as the distance along the 3 axes of the rigid body center from the calibration point, placed close to the entrance of the chamber; the standard orientation corresponds to the head position when the animal is facing toward the central loudspeaker (LS) with a beak angle of  $45^\circ$ . The standard orientation was recorded by the software when the animal was placed in the behavioral box, after the marker application and still under anesthesia. The head was held in the desired position using a head holder with ear bars covered with foam.

Thus, 6 parameters were recorded during each frame: the position of the head along the 3 axes (defined as the distance from the calibration point), and the angles along the 3 orthogonal planes (called yaw, on the horizontal plane; pitch, on the sagittal plane; and roll, on the frontal plane). Moreover, I defined 3 periods of interest: 1) the reference sound presentation; 2) the target sound presentation; 3) the response time, between the end of the target presentation and the pecking of the response key by the subject. During the data analysis, the raw data were first pre-processed in 2 steps: discarding trials with big data loss, and data smoothing.

In some trials, the rigid body defined by the software was not continuously detected. In those cases, a continuous ‘frozen’ value in the position/rotation of the rigid body was recorded for a relative long time. If this data collection interruption was too long (>70 consecutive frames, corresponding to 0.6 s), the corresponding trial was discarded from further analysis.

Moreover, in some cases the markers were not continuously detected during all recordings due to particular positions/orientations of the head or temporary displacement of the markers. This resulted in artifacts especially in the reconstruction of the head orientation. In order to get rid of these artifacts, a smoothing was applied to the raw data by using the averaged mean (smoothing window length = 50 frames; MATLAB function ‘movmean’). All data analysis was performed by custom-written scripts in MATLAB (MathWorks, USA).

### 2.1.8 Statistical analysis

I discarded the sessions where the subject had a low performance for the most external stimuli (absolute angles  $\geq 52^\circ$ ; see section 2.1.7). To do so, for each session, given the number of lateral responses for the most external stimuli, I run a binomial test to calculate the theoretical number of correct responses that would be significantly higher than chance level ( $p \leq 0.01$ , chance level probability=0.5). If the number of correct responses for the recorded session was below this threshold, the data from that session was not included in the MAA calculation. For the MAA calculation, a logistic function was fitted to the data points (i.e., the proportion of the responses to the right key as a function of the angle between reference and target stimulus). The logistic function had the following equation:

$$f(x) = \frac{1}{1 + e^{-k(x-x_0)}} \quad (2.1)$$

Where  $x_0$  is the curve’s midpoint and  $k$  is the logistic growth rate or steepness of the function. The regression curve was fitted to the data using the non-linear least squares method. All the mentioned analyses were performed using custom-written scripts in MATLAB.

## 2.2 Results

### 2.2.1 Training

For the subjects which could be tested in the final task ( $N = 3$ ), the training period ranged between 91 and 100 days. Another trained subject could perform the final task, but it was not possible to conduct enough sessions for a precise estimation of the MAA. The total number of trials that the animals could perform every day was either stable over time (subjects 2 and 3) or increased up to 80 days old (subject 1) until reaching a plateau (Fig 2.2 A, D, G). After that age, the subjects had also learned to respond by pressing the lateral keys, as the percentage of lateral responses was stably above 75%, even though subject 1 showed an unstable progress (Fig 2.2 B, E, H). The subjects were able to learn and stably perform the localization task starting from 70-80 days post-hatch. This is evident from the remarkable increase of performance in localizing sounds widely distant from the reference sound ( $\geq 52^\circ$ ), followed by a stable performance above chance level (binomial test,  $p \leq 0.01$ ; Fig 2.2 C, F, I). The other subjects which could not reach the final task ( $N=9$ ) were trained as long as possible, in a range between 84 and 140 days. However, they did not show any notable performance increase or sustained high-performance level. This indicates that the behavioral training had a relatively low rate of success ( $3/15 = 20\%$ ).

### 2.2.2 Final experiment

The data collection period ranged between 100 - 108 days post-hatch and 135 - 160 days post-hatch (29 - 60 days; Fig 2.2). This limited time window was because the roosters, when they were around 4-5 months old, lost the motivation to perform the task (evident for subjects 2 and 3 from Fig 2.2 F, I). Around that age the roosters reached sexual maturity and developed territorial and crowing behavior, the latter of which they also displayed in the experimental box. Nevertheless, all 3 subjects completed a high number of sessions and repetitions per each tested loudspeaker for the closed-loop condition (Table 2.1). Subjects 2 and 3 were presented also with the open-loop condition, and they could complete a lower number of repetitions per tested loudspeaker (Table 2.2). In general, the animals were better at localizing BB noise in the closed-loop condition compared to the open-loop one (average MAA: closed-loop =  $16 \pm 2^\circ$ ; open-loop =  $26 \pm 6^\circ$ , Fig 2.3 A, B), in line with what observed in the starling (Feinkohl and Klump, 2013). Moreover, the analysis of the head position and orientation in 3D space in one subject showed that the chickens moved the head during the closed-loop condition, and it seems to be an anticipatory movement toward the response keys (see section 2.2.5). Conversely,

the brief sounds of the open-loop condition (0.1 s) would not have allowed the animal to use the orienting head behavior to enhance the sound localization.

**Table 2.1** Summary of data collection for the closed-loop condition.

| Subject | Number of sessions | Number of trials | Averaged number of repetitions per sound location | $R^2$ | MAA ( $^\circ$ ) |
|---------|--------------------|------------------|---|-------|------------------|
| 1       | 16                 | 575              | 57  | 0.980 | 14               |
| 2       | 20                 | 573              | 54  | 0.990 | 11               |
| 3       | 20                 | 572              | 57  | 0.981 | 23               |

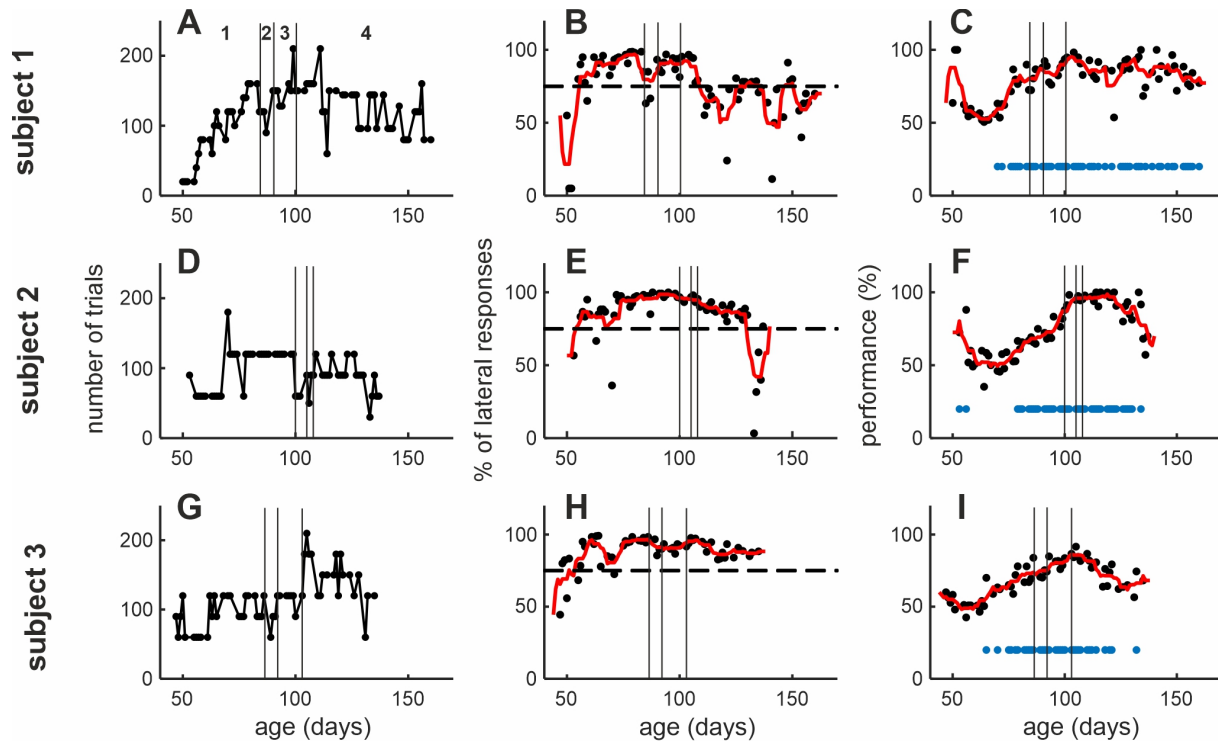


**Figure 2.2** Overview of behavioral training and final task. Data about the 3 subjects which learned the sound localization task are shown. Each row refers to one subject. The time window of each plot covers a total of 4 periods between the training (from stage 1 to 3) up to the end of the experimental recording (stage 4): 1= stimuli presentation from only external LSs, trial initiation by trainer; 2= stimuli presentation from only external LSs, trial initiation by the subject by pressing the central key; 3= progressive addition of stimuli with smaller angles from the reference LS; 4= stimuli presentation from all LSs (final task). A, D, G) Each data point represents the daily number of trials done by the subject. Note that all 3 subjects could perform a relatively high number of trials. B, E, H) Each data point represents the daily proportion of lateral pecking responses over the total number of trials performed. The red line is a moving mean of the data using a sliding window of 7 days. The dashed line shows the threshold used for valid session selection at 75%. C, F, I) The data points show the daily percentage of correct responses over the lateral key responses for the most lateral sound sources (absolute angle  $\geq 52^\circ$ ). The red line is a moving mean of the data using a sliding window of 7 days. The dots at the bottom of the plot represent the days when the performance was significantly above chance level (binomial test,  $p \leq 0.01$ ).

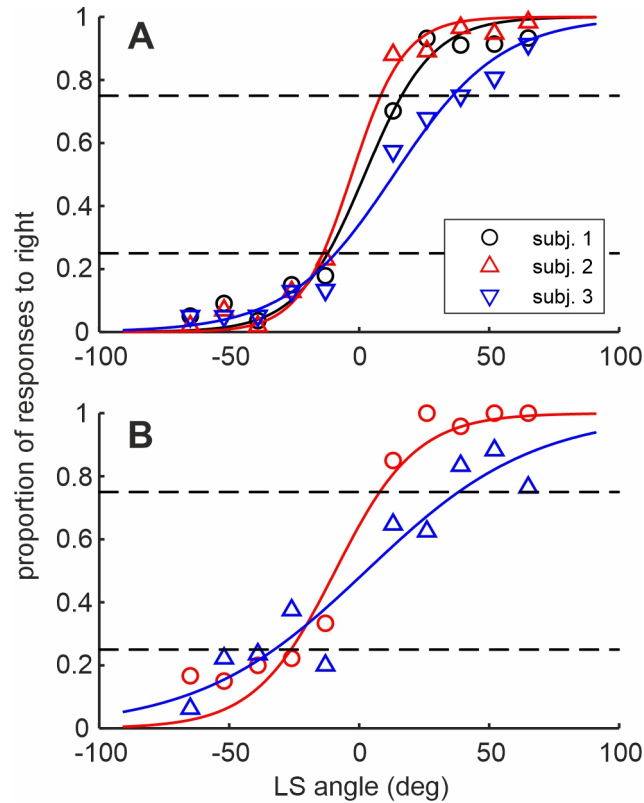


**Figure 2.3** Psychometric curves of responses to the right key. Proportion of responses to the right during (A) closed-loop condition (stimuli duration = 1 s) and (B) open-loop condition (stimuli duration = 0.1 s). In both plots the lines represent the logistic curves fitted to the data of each subject. The dashed lines indicate the response proportion at 0.25 and 0.75. The MAA is calculated as the average of the absolute angles where the logistic curve is equal to 0.25 and 0.75.

**Table 2.2** Summary of data collection for the open-loop condition.

| Subject | Number of sessions | Number of trials | Averaged number of repetitions per sound location | $R^2$ | MAA ( $^\circ$ ) |
|---------|--------------------|------------------|---|-------|------------------|
| 1       | -                  | -                | -   | -     | -                |
| 2       | 8                  | 211              | 21  | 0.956 | 17               |
| 3       | 6                  | 161              | 16  | 0.895 | 35               |

### 2.2.3 Calculation of ITD and ILD at the MAA

I calculated the ITD and ILD available at the chicken's MAA (the "minimum audible ITD and ILD"), in order to quantify the size of these binaural cues for the azimuthal sound localization. To do so, I used 4 head-related transfer function (HRTF) datasets of adult chickens from a previous study Schnyder et al. (2014). For each HRTF sound source location, I calculated the ITDs in the tested frequency range (0.4 – 4 kHz) and averaged them across subjects. Then, from the linear interpolation of the averaged ITDs along azimuth, I estimated the ITDs at the positive and negative values of the MAA around the



0° azimuth. The final ITD was the average of the two estimated ITDs. The same logic was followed for the ILDs. For the closed-loop condition (mean MAA = 16°), the estimated ITD and ILD were 56  $\mu$ s and 2.1 dB, respectively, whereas for the open-loop condition (mean MAA = 26°), the ITD and ILD were 92  $\mu$ s and 3.1 dB. Given the ITD enhancement effect of the interaural canal that in the chicken can reach a factor of up to 1.8 (Köppl, 2019), the ‘heard’ ITDs could broaden up to 101  $\mu$ s for the closed-loop condition and 166  $\mu$ s for the open-loop condition.

#### 2.2.4 Localization in elevation

The elevational paradigm was tested only in one subject (subject n.1). After the data collection along azimuth, the LS hoop was tilted of 30° counterclockwise for 11 sessions (N. trials= 440) and 45° for 10 sessions (N. trials=400), in each case for a period of 6 days. During this procedure the subject had already reached sexual maturity (age: 149 - 160 days post-hatch). As already observed towards the end of the data collection for the azimuthal task, the animal was generally not motivated to perform the task, spending most of the time crowing and scratching the response keys box with the paws. This was reflected by the very low rate of suitable sessions performed (3/21=14%), as the animal often pressed the central key with the paws during the response period. Because of these problems, I stopped the training procedure. Aware of this time limit in data collection, for the other subjects I focused on the azimuthal paradigm, testing closed and open-loop conditions.

#### 2.2.5 Head movements

Mocap data from 310 trials were collected from subject 1. Only a small percentage of trials were removed due to a relatively high data loss (39/310; 13%; see section 2.1.7 for preprocessing methods). In order to investigate the head movement strategies for sound localization, I only considered the trials with correct responses (192/271; 71%), that is, in cases when the localization had been successful. The analysis spanned 3 time periods: during 1) the reference sound presentation – when the animal is supposed to be in the standard position –; 2) the target sound presentation – when the sound localization would take place –; 3) the response time – when the animal reports the response by pressing one of the response keys. The reference and target presentation periods had a duration of 1 s each – i.e., the duration of the sound presentation –, whereas the response time had a variable duration based on the subject behavior for each trial. This response time (RT) was counted from the end of the target presentation and usually lasted less than 1 second (Fig 2.4).

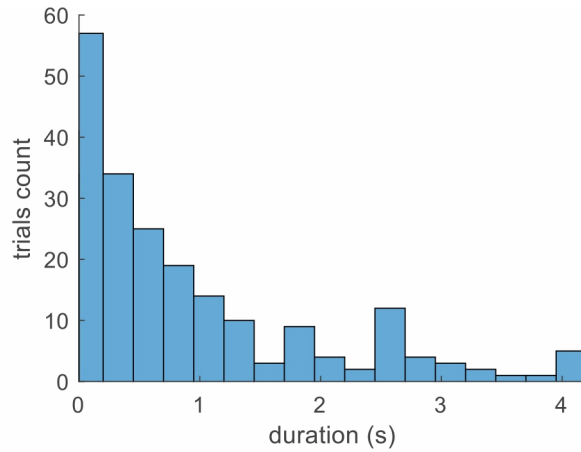


Figure 2.4 Histogram of the response time after target presentation.

For each trial, the time series of the head position along each axis was extracted - defined as the distance from the calibration point - as well as the head orientation on each plane - defined as the angle from the standard orientation (see section 2.1.7; Fig 2.5).

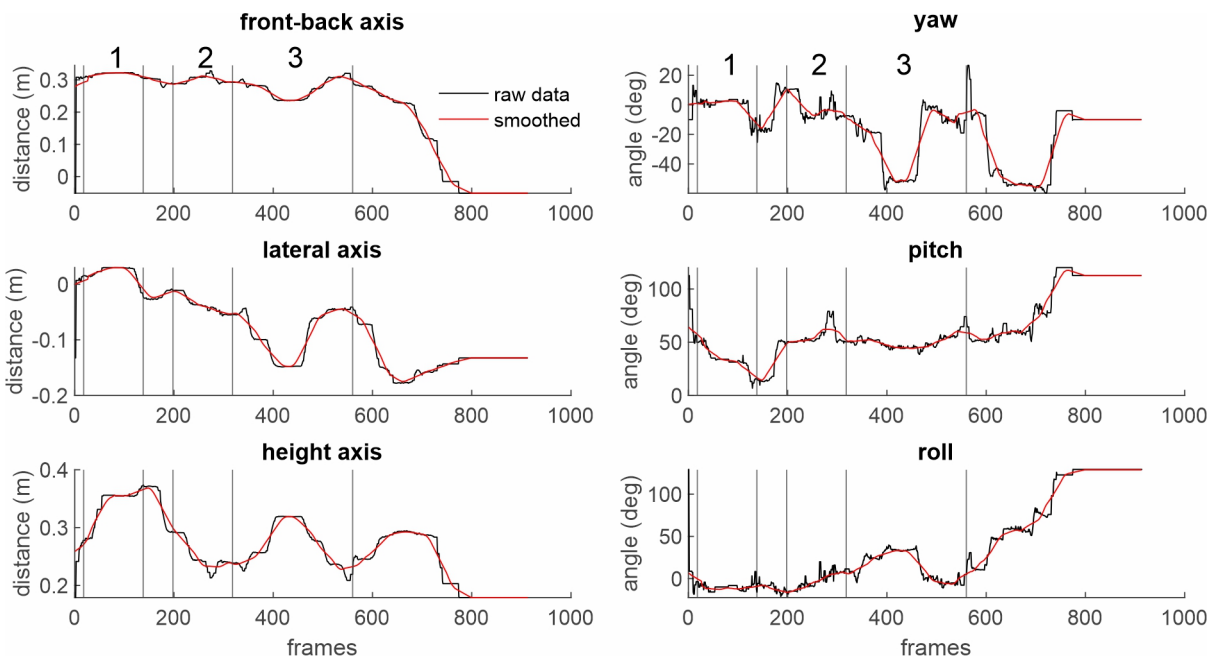


Figure 2.5 Time series of the head position and orientation. Example of raw and smoothed data of the head position track along the 3 axes and the orientation along the 3 planes. The periods labeled as 1, 2 and 3 refer to the reference stimulus, target stimulus presentation and response period, respectively.

In the following, I first investigated the head position, then the head rotation, and finally I combined the position and orientation – limited to the azimuthal plane – to see where the chicken’s head was pointing at.

### Head position

From the smoothed data it was possible to 3D-reconstruct the position of the head during the 3 periods of interest (Fig 2.6). In general, the chicken actively moved the head during both sound presentations. The average distance traveled was  $13 \pm 3$  cm (mean  $\pm$  S.D.) during reference sound and  $13 \pm 4$  cm (mean  $\pm$  S.D.) during the target sound. During the reference presentation, the head usually moved from the initiation key up to the center of the LS hoop, in front of the reference LS (Fig 2.6A). However, after 0.5 s, during the target presentation, the head mainly moved toward two areas, which correspond to the lateral response keys (Fig 2.6B). It is noteworthy that the period when the response was valid – thus, recorded – was limited to the post-target period, when the lateral LEDs also turned on, as an additional visual cue. Any response during the target presentation did not elicit reward (or punishment), but still the animal showed a tendency to at least approach the response key during the 1-s long target presentation. Indeed, during the response period the subject either pressed the key where the beak was already positioned above, or made a circular trajectory, most likely because it pressed the response key in advance – without any reward – followed by a movement back to the response key for a second peck (Fig 2.6C).

Another way to represent the position pattern across periods is shown in Fig 2.7. For each trial, the median position along each axis and within each period was calculated. Thus, each boxplot contains as many data points as the trials. It is shown that the head was in general slightly frontal compared to the hoop center (dashed line) during all the trial duration (Fig 2.7A); considering the lateral position, during the reference sound the head was placed in front of the central LS but, interestingly, it was biased to the left during the target sound (Fig 2.7B); regarding the height, the head was centered to the hoop during the reference, but already lowering toward the keys height starting from the target period (Fig 2.7C). In general, these results support the idea that during the target presentation the chicken was already directing toward the response keys. The new result shown here is the leftward bias during the target presentation, which would suggest that the chicken had a response preference to the left, at least as first choice. In the case of a rightward target sound, this behavior might have been followed by a deviation to the right toward the correct response key.

### Head orientation

Similar to the position analysis, in Figure 2.8 for each trial the median orientation along each plane within each period was calculated. This analysis confirms what has been already observed with the analysis in Figure 2.7: a rotational bias to the left during the target presentation (Fig 2.8A), together

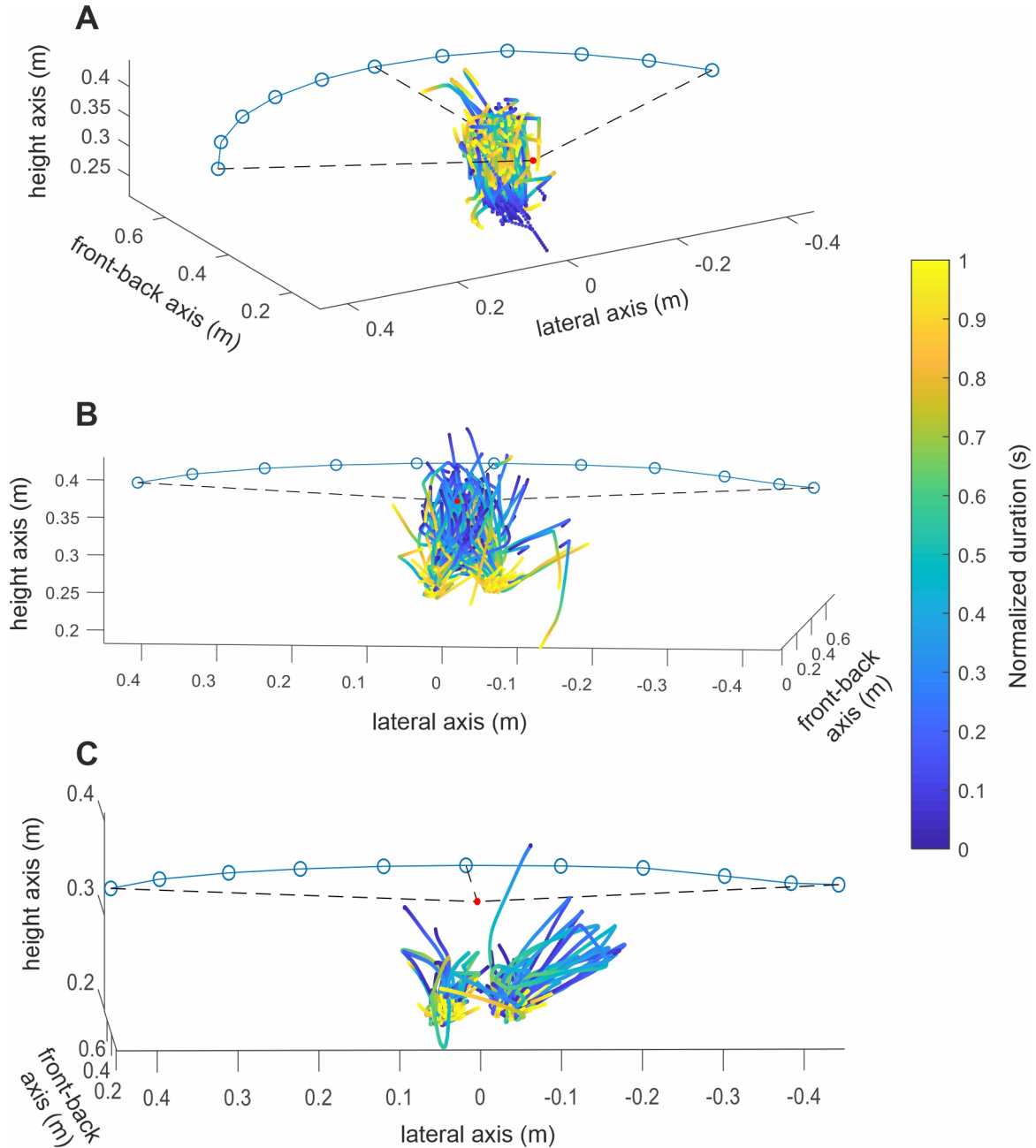


**Figure 2.6** Head position during trial periods. Each line indicates the 3D head position trajectory for a single trial during A) the reference presentation, B) the target presentation and C) the response period. The color code indicates the time dimension within the period of interest. The blue circles represent the LSs, the red dot indicates the LS hoop center, connected to the most lateral and central reference loudspeakers by the dashed black lines.

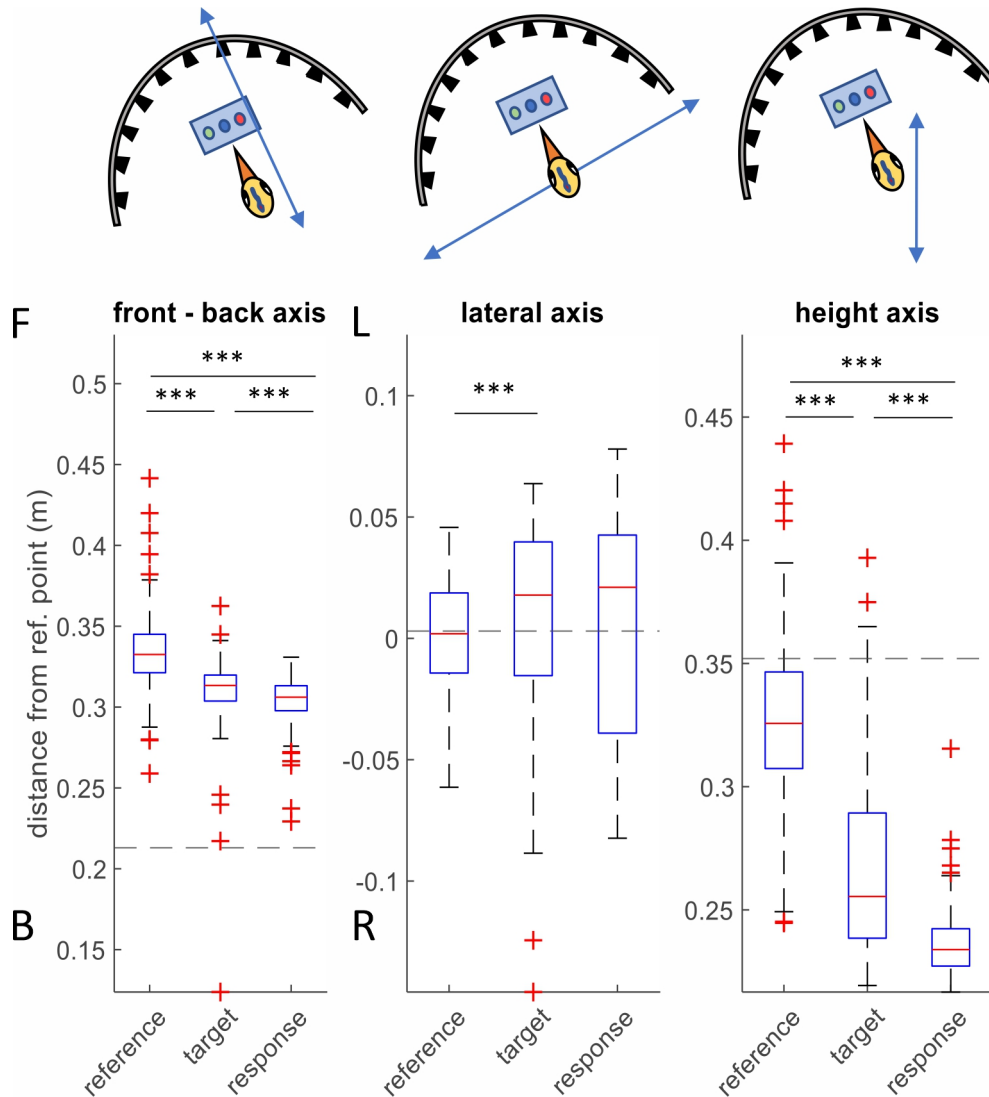


**Figure 2.7** Head position across periods for each axis. Distribution of the head position along the front-back axis, the lateral axis, and the height axis, analyzed within the periods of interest (reference, target, response). The dashed lines indicate the position of the LS hoop center. Difference in the variance between time periods was tested using the Tukey-Kramer post-hoc test (\*\*= $p < 0.001$ ). F=front, B=back, L=left, R=right.

with a downward rotation toward the response keys (Fig 2.8B), both statistically significant compared to the reference presentation (Tukey-Kramer test,  $p < 0.001$ ). In addition, the roll orientation did not change significantly between reference and target periods, indicating that the chicken did not use roll movements to improve sound localization (Fig 2.8C, Tukey-Kramer test,  $p = 0.92$ ).

### Yaw and position in azimuth

After analyzing the position and orientation separately, I investigated the combination of both along the azimuthal plane, to verify what LS the subject was pointing at during different time windows. To do so, I took into account both the 3D head position and axes orientation and I projected onto the azimuthal plane the intersection of the frontal axis with the LS hoop. Figure 2.9 shows a histogram

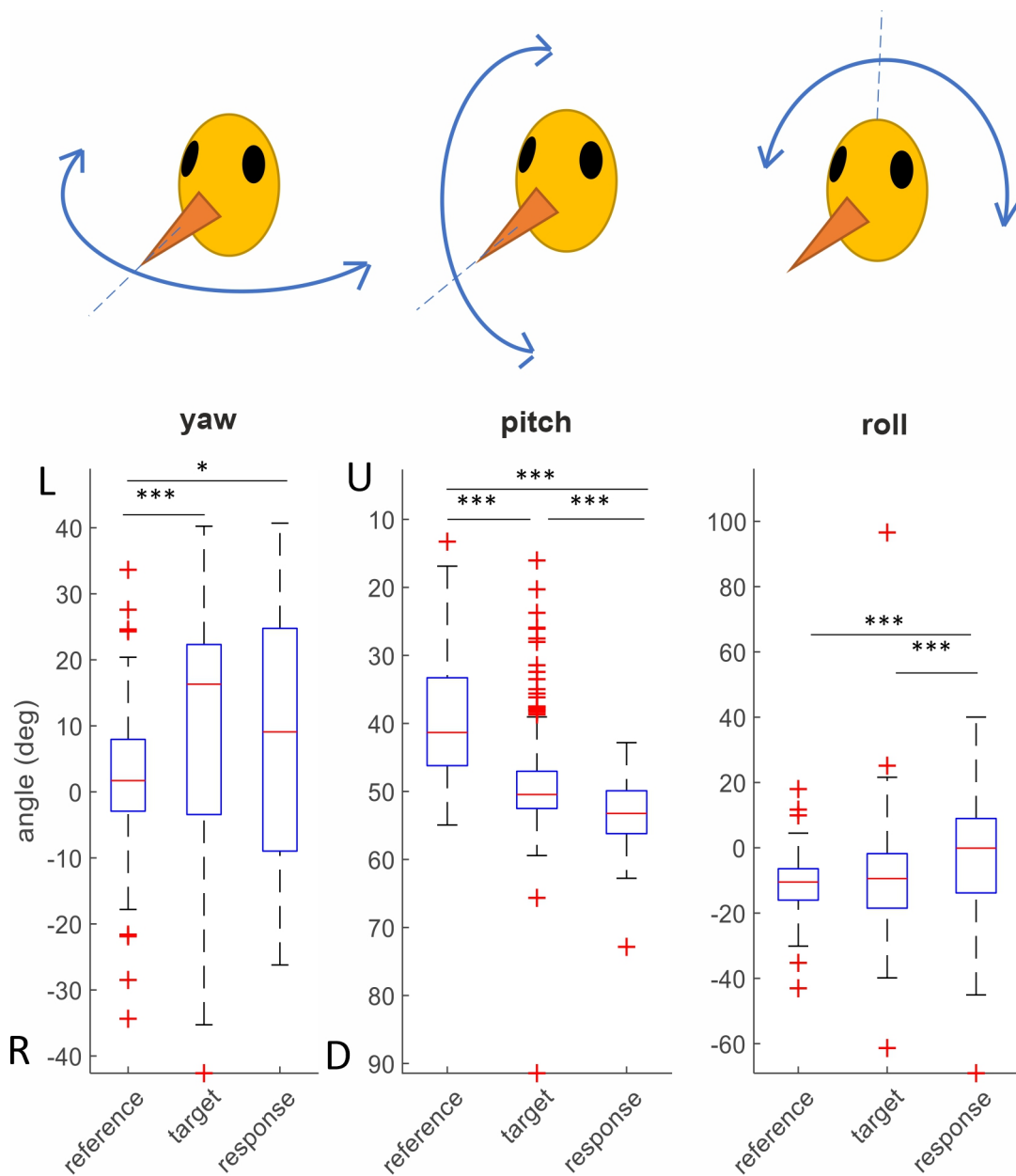


**Figure 2.8** Head orientation across periods for each plane. Distribution of the head orientation: yaw, pitch, and roll, analyzed within the periods of interest (reference, target, response). Difference in the variance between time periods was tested using the Tukey-Kramer post-hoc test (\*= $p < 0.05$ , \*\*\*= $p < 0.001$ ). L=leftwards, R=rightwards, U=upwards, D=downwards.

of the target locations of LS hoop pointed by the frontal axis: during the reference sound the subject is mainly facing toward the central LS, whereas during the target sound the head has two preferred orientations, corresponding to the position of the 2 response keys, and with a biased orientation to the left. The pattern during the target sound well overlaps with the response time orientation, when the animal is supposed to peck one the lateral response keys.

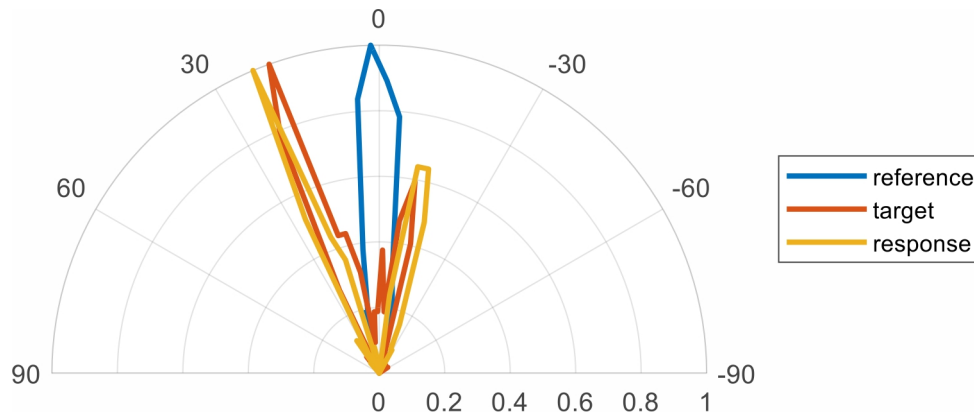


Figure 2.9 Histogram of the frontal axis orientation for each period. Each 'bin' covers a range of  $3^\circ$ .

## 2.3 Discussion

### 2.3.1 Azimuthal localization accuracy

This study shows that freely moving roosters can localize noise along azimuth with relatively good localization acuity among the generalist bird species tested so far (Fig 2.10). Our data are in line with what shown for hens by Krumm et al. (2022), where the MAA for broadband noise was  $12.2^\circ$ . However, in their study the hens performed a Go/NoGo task, while I used a 2AFC task. It is noteworthy that the methodological difference might affect the MAA results. The better localization acuity of chickens compared to other generalist birds might be due to the availability of wider binaural cues, which depends on factors such as the head size and the role of the interaural canal. It is known that the size and shape of the head have a relevant impact in generating the interaural differences in time of arrival and intensity (ITD and ILD, respectively) that the animal can experience at the level of the eardrums (Grothe et al., 2010). The head size of the chicken is notably bigger than most of the generalist birds shown in Figure 2.10 (subject 1 from the present study = 34.0 mm, starling = 15.5 mm (Klump and Larsen, 1992), budgerigar (*Melopsittacus undulatus*) = 15.1 mm, canary (*Serinus canarius*) = 13.5 mm (Park and Dooling, 1991), great tit (*Parus major*) = 12 mm (Klump et al., 1986)) and might be comparable to the head size of the tested diurnal raptors (Rice, 1982). Moreover, the chicken head shape induces monaural cues, but they are thought to be relevant for localization along elevation, rather than along azimuth (Schnyder et al., 2014).

The "minimum audible ITD and ILD" presented at the ear drums of the chicken for closed-loop condition are  $56 \mu\text{s}$  and 2.1 dB, respectively. Budgerigars can lateralize broadband noise based on presentation of ITDs and ILDs as small as  $16 \mu\text{s}$  and 1.5 dB, respectively (Welch and Dent, 2011), which suggests that in the chicken both binaural cues are big enough to be informative for azimuthal sound

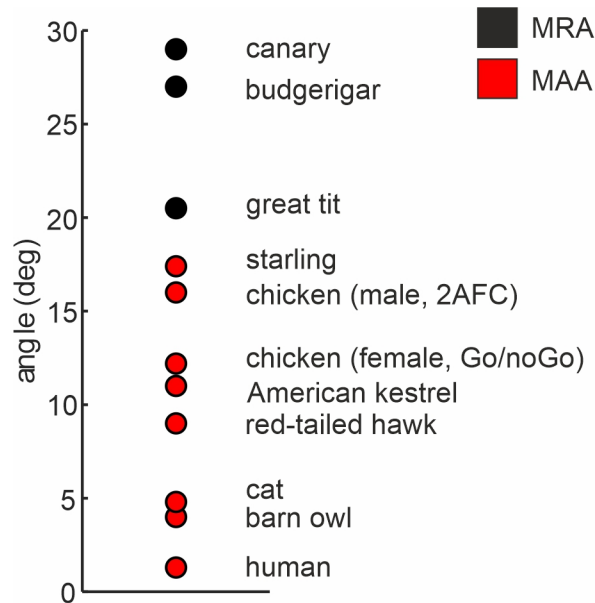


**Figure 2.10** Comparison of localization acuity across species. Localization acuity measurements – minimum audible angle (MAA) or minimum resolvable angle (MRA) – of generalist birds – canary and budgerigar (Park and Dooling, 1991), great tit (Klump et al., 1986), starling (Feinkohl and Klump, 2013), chicken, male (present study, closed-loop condition), chicken, female (Krumm et al., 2022), red-tailed hawk (*Buteo jamaicensis*) and American kestrel (*Falco sparverius*) (Rice, 1982) – and auditory specialists such as the barn owl (Krumm et al., 2019), cat (Heffner and Heffner, 1988) and human (Heffner and Heffner, 1988). Note that the chicken shows relatively good localization accuracy among the generalist birds, but it is much worse than avian specialists such as the barn owl or mammal species.

localization. For the other mentioned generalist bird species, the ITD corresponding to the MAA or minimum resolvable angle (MRA) was calculated using a model by Kuhn (1977), which considers only the influence of the head size and the head shadowing in the generation of the binaural cues (within the range 1-4 kHz: budgerigar = 50-62  $\mu$ s, canary = 25-55  $\mu$ s (Park and Dooling, 1991), great tit = 18-24  $\mu$ s (Klump et al., 1986), starling = 22-30  $\mu$ s (Feinkohl and Klump, 2013)). The minimum audible ITD of the chicken from our study is similar to the ITD calculated for these bird species. Moreover, a recent study calculated the MAA of the chicken at different pure tones, and estimated the binaural cues experienced at those MAAs (Krumm et al., 2022). The results indicate that chickens might rely on ITD cues at low frequencies and on ILD cues at high frequencies (Krumm et al., 2022). However, a combination of ITD and ILD information within the same frequency regions as in owls (Kettler et al., 2017) cannot be excluded.

The ITD and ILD arriving at the ear drums are enhanced by the internally coupled middle ears of birds, which work as pressure difference receivers (Christensen-Dalsgaard, 2011). This effect might have a substantial influence on their localization accuracy. For instance, chicken's interaural cavities remarkably enhance the 'heard ITD' by a factor of up to 1.8 (Köppl, 2019). Thus, in the case of the closed-loop condition, the heard ITD at the MAA might become broader up to 101  $\mu$ s. Moreover, the



'heard ILD' is also significantly amplified in chickens (Köppl, 2019) and might also play an important role in azimuthal localization. However, the interaural canal effect varies across bird species: for instance, the interaural canal seems to play a role in the barn owl, especially at low frequencies (Kettler et al., 2016), but not in the starling (Klump and Larsen, 1992).

Chickens were better at localizing sounds in the closed-loop condition (long stimuli duration) compared to the open-closed condition (short stimuli duration). This phenomenon has also been observed in the starling (Feinkohl et al., 2013), but not in the barn owl (Knudsen et al., 1979) and the great horned owl (*Bubo virginianus*) (Beitel, 1991). In the closed-loop condition the chicken had enough time to actively move the head in order to increase the binaural cues coming to the ears, maximizing the localization acuity. In our case the head movement seems to be an anticipatory movement toward the response keys, rather than an orientation toward the sound source, as observed e.g., in the barn owl (Knudsen et al., 1979). Conversely, in the open-loop condition the sound source localization should rely exclusively on the binaural cues arriving at the ear drums when the head is in the standard position, i.e., frontally oriented. It is thought that the active head orientation is the main factor responsible for the better localization performance in closed-loop paradigms (Klump, 2000). However, the time duration might play a role in the localization accuracy simply due to the temporal constraints in processing brief sounds in the auditory system. Indeed, a study on humans with immobile heads showed that duration affects MAA along both azimuth and elevation (Strybel and Fujimoto, 2000). However, other studies conducted on humans did not report such an effect (Frens and van Opstal, 1995; Hofman and van Opstal, 1998). In order to disentangle the effect of motor response and auditory time integration in localization of brief sounds, future studies should be carried out e.g., where localization accuracy with freely orienting head is compared to the condition where the head is constrained in a fixed position.

In a final experiment, an attempt to measure the sound localization accuracy in elevation was made, but without success. The reason might be the restricted time window to train and test the roosters in the behavioral experiment, as the animals started to behave very erratically after reaching sexual maturity. Given the easier localization of sound sources along azimuth compared to elevation, the study started with a training in the azimuthal paradigm, followed by a switch to the elevational one. The paradigm change was accomplished by tilting the loudspeaker hoop of 30° through training sessions, up to the vertical position. However, the subjects lost interest and motivation in the task around the reach of the vertical position. Another option would have been training the chickens directly on the vertical position. However, given the low success rate in training roosters in the

azimuthal task, a training focused exclusively on the elevation task might have been even harder and time consuming for both the animal and the experimenter. On the other hand, in this study hens were not able to perform the final task, although they seem to be successful in a similar task but with a different paradigm (i.e., Go/NoGo paradigm, see Krumm et al., 2022).

Birds have evolved to mainly rely on vision for their survival. In chickens, there is behavioral evidence that the integration of visual and auditory stimuli is beneficial for signal detection (Verhaal and Luksch, 2016). However, even in the absence of visual stimuli, the chicken shows a significant accuracy in localizing frontal sound sources, which can be fundamental for its survival in critical conditions, for example to localize predators or conspecifics out of sight. However, there are still several open questions. For instance, given the fact that predators and possible threats may also come from above the animal, it would be interesting to measure the localization accuracy along elevation - maybe with a different paradigm than what I used - and compare it with the acoustic cues available to accomplish the task.

### 2.3.2 Head movements during localization

The purpose of the analysis of the 3D position and orientation of the chicken's head was to assess a possible behavioral strategy used to improve the sound localization accuracy during closed-loop stimuli. A study showed that, when the starling moves the head in a closed-loop sound localization task, the head movements increase the localization accuracy, even though this improvement is not related to the specific type of movement pattern (Feinkohl et al., 2013). However, starlings preferred to orient their beak toward the sound source, whereas towhees prefer to orient the head laterally (Nelson and Suthers, 2004). In our case, there was no clear head movement that could be linked to a sound localization behavior: the chicken did not orient the head as a function of the sound source location, but rather approached the response keys already while the target sound was played. This indicates that the reflexive orienting response to auditory stimuli, well studied in the barn owl (Knudsen et al., 1979) and also observed in the chicken (Adamo and Bennett, 1967) and the starling (Feinkohl et al., 2013), was not preserved during this task.

In principle, given the task paradigm, this behavior should have been avoided: the response was recorded – and for correct responses, the reward was delivered – only after the target sound presentation, thus an anticipated response peck would not increase the rewarding rate, but rather entail an additional energy cost; moreover, in order to reduce any confusion for the subject, the response period was indicated by the light of 2 LEDs next to each response key. Interestingly, this

response anticipation was also observed for the other subjects. Even though the chicken might have displayed this motor pattern primarily to get the reward faster, at the same time the change of head position during the sound presentation provided a change of the binaural cues reaching the ears, thus being potentially beneficial for sound localization. However, in our case the contribution of this behavior on the localization accuracy is hard to quantify.

Nonetheless, there are different ways to overcome such a problem for future behavioral experiments. For instance, by changing the response procedure, where the animal – instead of using the head to peck buttons – would hop on two different perches or move toward two different locations. This way the head movements would not be related to the response pattern, but solely to sound localization, which would largely improve the interpretation of the results. Moreover, the usage of IR markers pierced onto the comb and neck provided, on the one hand, the advantage of a quick and minimally invasive operation on the animal, but on the other hand, the disadvantage of an occasional instability of the markers that, especially after some weeks and during fast head startles, compromised the quality and accuracy of the 3D reconstruction. This technical problem can be solved by applying on the skull a rigid marker holder, which, in principle, would guarantee a more consistent mocap data acquisition.

## 3 Two Types of Auditory Spatial Receptive Fields in Different Parts of the Chicken's Midbrain

---

This chapter is modified from the Materials and Methods, Results and Discussion sections that correspond to the following publication:

“Two types of auditory spatial receptive fields in different parts of the chicken's midbrain” (Maldarelli et al., 2022a)

The article is published in *The Journal of Neuroscience*, which permits authors the reproduction of published articles for dissertations without charge or further license (see Figure A1).

---

### 3.1 Materials and Methods

#### 3.1.1 Animals

We collected data from 28 chickens (*Gallus gallus domesticus*, White Leghorn, 12 males and 16 females) aged between 58 and 114 d posthatch. We used adult chickens because their auditory system is fully developed in contrast to young chickens (Smith, 1981; Manley et al., 1991) and head-related transfer function (HRTF) data for a virtual stimulus presentation were available (Schnyder et al., 2014). Fertilized eggs were provided by the Department of Reproductive Biology, Technical University of Munich (TUM) School of Life Sciences, incubated at 37°C and 70% humidity and, after hatching, reared at the animal facility of the Chair of Zoology, TUM School of Life Sciences. The animals were kept in groups in cages with access to sand, perches, water, and food *ad libitum*. The bird housing facilities were artificially illuminated with UV-balanced light in a 12/12 h light/dark cycle. All experiments were performed according to the principles regarding the care and use of animals

adopted by the German Animal Welfare Law for the prevention of cruelty to animals. The study was approved by the Government of Upper Bavaria, Germany.

#### **3.1.2 Surgery**

All protocols and procedures were in accordance with the institutional guidelines of the authorities of Upper Bavaria, Germany (permit no. ROB-55-2-2532-Vet\_02-18-154). Animals were anaesthetized with an initial dose of ketamine (40mg/kg) and xylazine (12mg/kg) via intramuscular injection in the breast muscle. Anesthesia was maintained by a constant injection of anesthetic (ketamine: 13mg/kg/h; xylazine: 4mg/kg/h) via a syringe pump (LA-30, Landgraf Laborsysteme HLL GmbH). The heart rate was constantly monitored with two EKG electrodes placed in a chest muscle and in the contralateral leg. Cloacal temperature was monitored and maintained above 39.5°C using a homoeothermic blanket system (Harvard 50-7137, Scientific & Research Instruments Ltd.). The head was held in a fixed position by means of two ear bars connected to a surgery stereotaxic setup. The scalp was anaesthetized with xylocaine (AstraZeneca GmbH), the feathers were removed with forceps and the scalp was opened along the midline. A craniotomy was performed above the left midbrain and the meninges were opened to expose the brain surface for electrode penetration. An aluminum head holder was attached to the skull with dental cement (Paladur, Kulzer GmbH) to fix the head in the setup for the recording. During anesthesia a negative pressure may build up in the middle ear cavity, preventing the tympanic membrane from vibrating naturally (Larsen et al., 2016). However, in our case, the surgical opening was extended up to the trabecular bone, caudal in respect of the OT, connected to the bullae and interbullae passage described previously (Larsen et al., 2016), thus ensuring middle-ear ventilation. To reconstruct the anatomic position of the recordings, the electrode was coated with a fluorescent dye (DiO or DiI) before the first penetration, following a procedure described previously (DiCarlo et al., 1996). Briefly, a dye solution was prepared by dissolving dye crystals in ethanol (DiI: 50mg/ml, DiO: 42mg/ml). Then, the electrode tip was dipped into the solution, allowing it to dry in air for 5 s. The procedure was repeated 10 times. Afterwards, the electrode was placed on the surface of the brain by visual inspection and guided into the brain tissue by a microcontroller (Scientifica Ltd). At the end of the experiment the animals were euthanized with an intrapulmonary injection of sodium-pentobarbital (200mg/kg, Narcoren) and decapitated with poultry scissors.

### 3.1.3 Stimulus generation and recording

The recordings were performed in a sound-attenuating chamber (IAC, Niederkrüchten). Stimuli were either pure tones or broadband (BB) noise (100–5000Hz). Fresh noise stimuli were digitally generated for each single trial, so that the averaged neural response across trials cancels out the possible modulation of the neural activity in response to the amplitude envelope of the noise stimuli. The stimuli were generated by a custom-written script in MATLAB (MathWorks), converted to analog signals via an external sound card (Fireface 400, RME), and presented binaurally via earphones (ER4S, Etymotics) using the software AudioSpike (HörTech gGmbH). The earphones were not sealed to the animal's ear canals, hence preventing physical constraints in the air vibration in the inner ear. In order to obtain the aSRE, we presented sounds via earphones in a virtual auditory space (VAS) created by fresh BB noise filtered with HRTFs corresponding to specific locations in space. The HRTFs were not individualized; for all recordings we used the HRTF data obtained in a previous study (Schnyder et al., 2014). Since the HRTFs were measured via microphones placed at the position of the eardrums, all properties of the sound reaching the eardrum under natural conditions were fully captured. Furthermore, it has been previously shown that, in the barn owl, there is a good correspondence between the neural responses obtained by HRTF stimuli and free-field stimulation (Keller et al., 1998). Since the binaural cues in the HRTFs of different adult chickens do not change remarkably (see section 3.2.1) and the head size of the chicken used for the chosen HRTF database (interaural distance: 31 mm) was compatible with the head size of the chickens of our study (average interaural distance from four subjects:  $30 \pm 2$  mm), we used one HRTF dataset as stimuli for all the tested chickens. The neural activity was recorded using a tungsten electrode (impedance: 2 MX, WPI GmbH), preamplified (ExAmp-20KB, Kation Scientific), passed through a HumBug (Quest Scientific Instruments Inc.) to eliminate traces of power line noise and converted to a digital signal (Fireface 400, RME, sampling rate: 44,100Hz). We used the software AudioSpike (HörTech gGmbH) for bandpass filtering of the recorded signal (0.3–3 kHz) and visually monitoring the online signal. While advancing the electrode into the brain, a contralateral or bilateral BB noise stimulus was presented to elicit an auditory response. When a responsive unit was detected, the protocol consisted in determining the threshold level, followed by different series of stimuli to measure the following properties: spatial tuning, ITD tuning, ILD tuning, and frequency tuning (comparable to Aralla et al., 2018). Each set of stimuli was presented in a pseudo-randomized order. Each stimulus had a duration of 150ms, with an interstimulus interval (ISI) of 500ms. A cosine ramp function of 20ms was applied at the beginning and the end of the stimuli to avoid spectral splatter.

### 3.1.4 Stimuli presentation

The threshold was estimated by presenting binaural or monaural BB noise in a level range from 10 dB SPL up to 90 dB SPL. Each level was presented 10 times. The threshold was defined as the level at which the unit started responding to the stimuli. The threshold was estimated via visual inspection of the plot showing the mean spike rate as a function of the level. The VAS stimuli simulated 429 different positions. The azimuthal range was  $\pm 180^\circ$ , the elevational range was  $\pm 67.5^\circ$ . The average binaural level was 10–15 dB above threshold (the level refers to the RMS SPL of the stimulus at the frontal position:  $0^\circ$  azimuth,  $0^\circ$  elevation). Each spatial position was presented 10 times. The ITD stimuli were typically presented at 20 dB SPL above threshold, within a range of  $\pm 500$  ms and steps of 50 ms. Each condition was tested 20 times. The ILD stimuli were presented with an average binaural level of 20 dB SPL above threshold and an ILD range typically within  $\pm 40$  dB, with 4-dB steps. Each stimulus was presented 20 times. The monaural stimuli consisted in the presentation of BB noise at different sound pressure levels, in a range of 0–40 dB above threshold, with 2-dB steps and 20 repetitions for each level. For the frequency tuning we usually presented pure tones in a range between 0.1 and 4.85 kHz, at intervals of five steps per octave, at 20 dB above threshold. Each stimulus was presented 10 times.

### 3.1.5 Data analysis

#### Spike sorting and peristimulus time histogram (PSTH) time window selection

Evaluation of the unit type (multi or single) was conducted offline. A recording was labeled as single-unit if only one type of spike waveform was detected and if  $<10\%$  of the interspike intervals had a duration  $\leq 3$  ms. In all the other cases, defined as multi-unit, it was possible to isolate the response of single units using spike-sorting. Both unit labeling and spike sorting were conducted using Wave\_clus 3 (Chaure et al., 2018) in MATLAB. For each recording, a PSTH of the neuronal activity for all the repetitions was created. The PSTH contained a 50-ms prestimulus (Pre) window, 150ms of stimulus presentation (Stim) window and 300ms of poststimulus (Post) period. A response window was defined individually for each recording with the following procedure: a 20-ms window was moved in 1-ms steps over the Stim and Post recording windows, and the responses in this 20-ms window were compared with the first 20ms of the Pre window, which included only spontaneous activity, to identify response windows that were significantly different from spontaneous activity. The first consecutive windows with a significant difference in activity (Wilcoxon signed-rank test,  $p \leq 0.01$ )

were considered the start of the response window and the last two windows with significant activity were the end of the response window (window start: median = 53ms, range: 50–213ms; window end: median = 297 ms, range: 80–485ms). If there was no significant response, we ruled out the unit as unresponsive. The significant change in activity could indicate either an increase of activity (excitation) or a decrease (inhibition).

#### **Frequency tuning**

We first tested whether a unit was frequency tuned (see section 3.1.6). If the unit was tuned, we fitted a spline curve to the frequency response data (MATLAB 'spline' function). The best frequency (BF) was defined as the frequency which elicited the strongest neural response, and it was calculated as the frequency at the peak of the spline fit.

#### **Monaural response**

Monaural responses were recorded for ipsilateral and contralateral stimulation to test whether a unit was responsive to purely binaural or also monaural stimulation. If a significant difference was present in at least three consecutive levels, the unit was classified as excitatory (E) or inhibitory (I) according to an increase or decrease of activity, respectively. In all the other situations, it was classified as nonresponsive ("0").

#### **Spatial tuning**

Classification of the aSRF was based on its location in the VAS. aSRF could be located mainly within the contralateral hemifield (called "contra"), the ipsilateral hemifield (called "ipsi"), or broadly distributed on both sides (called "bilateral"). This classification was based on the distribution of the aSRF area with a spike rate >50% of the maximum response. If >75% of the resulting area was present on one hemifield, the aSRF was labeled as "contra" or "ipsi," according to the hemifield, otherwise it was labeled as "bilateral." For the units with contralateral response, we also calculated the centroid. In addition, the "contra" units were classified according to the aSRF shape. The two main aSRF shapes we determined were the "round" and the "annulus" type. An aSRF was classified as round if its peak was located near its centroid. Alternatively, a receptive field was classified as annulus if it had a ring-shape, with a decrease of activity at the centroid. The aSRF type classification was assessed from the azimuthal cross-section at 0° elevation of the normalized spike activity array (MATLAB curve fit: 'csaps' function, smoothing parameter: 0.0075; peaks detection: 'findpeak')



function, 'MinPeakProminence',0.05). If one main peak was detected around the centroid position, it was classified as "round." If it presented two local maxima with a local minimum around the centroid, it was classified as "annulus." aSRFs were defined "broad" if more than two local maxima were detected. This category includes aSRFs with a "patchy" shape, not presenting any clear pattern and broadly spread mostly within the contralateral hemifield. Unit classification was automated using a custom MATLAB script, and only 6 units (9%) required manual classification editing after visual inspection. For round and annulus aSRFs, some spatial features were measured for subsequent analysis. For both aSRF types, the "medial peak" was defined as the azimuthal position corresponding to the peak of neural activity close to the frontal location (i.e., 0° azimuth). The outer diameter was defined as the azimuthal distance between the two most distant points where the normalized spike rate is equal to 0.5. Regarding only the annular aSRFs, the local-maxima-diameter was defined as the azimuthal distance between the two local maxima. These measurements were based on the detection of local maxima from the fitted curve of the spike rate cross-section at 0° elevation (MATLAB curve fit: 'csaps' function, smoothing parameter: 0.0075; peaks detection: 'findpeak' function, 'MinPeakProminence',0.05). We organized the aSRF data in a two-dimensional azimuth-by-elevation-spike activity array. For ease of view the data were smoothed in azimuth and elevation with a standard MATLAB function (curve fit: 'csaps' function, smoothing parameter: 0.005). We plotted the data as contour plots (contour spacing of 11% of normalized spike rate).

#### **ITD tuning**

First, we tested whether a unit was ITD-sensitive or not (see 3.1.6). If it was ITD-sensitive, a curve was fitted to the ITD response data (MATLAB 'spline' function). Based on the ITD tuning curve, we measured the best ITD (ITD at maximum value of spline) and the ITD response width (ITD range with activity >50% of maximum). Positive ITD values indicate contralateral leading and negative values ipsilateral leading sounds.

#### **ILD tuning**

As for the ITD stimuli, we tested whether a unit showed ILD sensitivity or not. If it was ILD-sensitive, we applied a cubic smoothing spline to the ILD response data (MATLAB 'csaps' function, smoothing parameter: 0.03). Since the ILD tuning curves were typically sigmoidal, we calculated the maximum ILD, the 50% cutoff value (the ILD value at 50% of the maximum spike rate) and the ILD response

width (ILD range with activity >50% of maximum spike rate). Positive ILD values indicate a higher sound pressure level at the contralateral ear.

#### **Histology and anatomic reconstruction**

After the decapitation of the animal, the brain was removed from the skull and fixed in 4% PFA solution for at least 24 h at 6°C. Then, the brain was cryoprotected in 30% saccharose in phosphate buffer (PB; 0.1 M, pH 7.4) for at least 24 h and subsequently sectioned at 100  $\mu$ m on a microtome (Microm HM440E, GMI) along the sagittal plane, and collected into PB. Slices were mounted onto object slides coated with chromalum gelatin, then covered with DAPI-Propyl gallate (to identify brain structures) and a cover slip. Subsequently, we identified the fluorescent electrodes tracks using a fluorescence microscope (Olympus BX 63F). Since the electrode penetrations were mostly parallel to the sectioning plane (sagittal plane), the dye traces were easily detectable under the microscope. During the recordings, we measured the position of the recordings along the rostro-caudal (RC) and medio-lateral (ML) axes, parallel to the stereotaxic arms (resolution = 0.1 mm), as well as along the dorso-ventral (DV) axis, parallel to the microcontroller (resolution = 0.001 mm). If the microcontroller was tilted to a certain angle from the standard axes orientation to provide a perpendicular entrance of the electrode through the brain surface, the angle was taken into account in the calculations of the final coordinates. We also measured the reference point, defined by the coordinates of the zero plane along each axis, according to the measurement system in the atlas by Puelles (2007). More specifically, the zero coronal and horizontal planes were aligned to the ear bars, while the zero sagittal plane was aligned to the midline. Moreover, during the recordings, from the skull opening it was possible to expose the most external point of the OT, thus we could measure the total ML extent of the midbrain from the midline. For each subject, a ratio between the total ML distances measured from the atlas and from the brain was used as a shrinkage/expansion factor to compensate for offsets because of differences in individual brain sizes, and it was applied to the stereotaxic coordinates along all three axes. From these data, the position of the first penetration along the ML axis was defined as the compensated ML distance from the midline, and the assessment was supported by the dye track in the brain slides. Based on the stereotaxic information and the visual cue in the brain slides, it was possible to reconstruct the coordinates of the first penetration along the three axes, expressed as a distance from the reference point. The position of the other recording sites was estimated by the relative distance from the first one, applying the correction factor. Then we transferred the coordinates into the atlas coronal planes, where each recording site was assigned to the closest plane. This plane

was <0.12 mm away from the recording site along the RC coordinate, since the interplane distance in the atlas is 0.24 mm. Since the FRLx is not reported in the atlas, the contour of the FRLx was defined by using the boundaries shown by Niederleitner et al. (2017) (see their Fig. 4). Moreover, it was possible to estimate the OT layers from the depth of the electrode penetrations, typically orthogonal to the brain surface. We depicted the coordinates along the coronal views because it was necessary for projecting the OT recording sites onto the brain surface and because our brain area of interest was represented with higher resolution in the coronal view (i.e., smaller interplane distance) compared with the sagittal view. In some cases, before the coronal representation, the recordings were also mapped in the sagittal planes, to visually check whether there was a match between the position estimated from the stereotaxic coordinates and the position of the electrode dye track in the brain slide. This was only applied to those recordings distant  $\pm 0.2$  mm from the sagittal planes. In the other cases, the locations were not plotted onto the sagittal planes.

#### **Projection onto the OT surface**

Since previous studies showed that the avian OT has a topography of visual and/or auditory stimuli on the brain surface (e.g., in barn owl, Knudsen 1982; in pigeon, Clarke and Whitteridge 1976), we investigated whether a topography of the auditory space was also present along the chicken's OT surface. Therefore, we projected the location of the OT units onto the brain surface following a revised version of the procedure used in a previous study (Knudsen, 1982). From the atlas coronal view, we defined the projected location of each OT recording site as the surface point with the shortest distance from the unit coordinates. We measured the length of the OT surface for each atlas slide, we calculated the position of each projection along the OT surface, and the position of the most lateral point of the OT surface. Then, the OT surface sections were represented as a flattened line for the two-dimensional representation. The lateral point was used as reference point to align the flattened OT surfaces to each other along the same horizontal line in the RC axis.

#### **3.1.6 Statistical analysis**

For characterizing the monaural responses, we used a Mann–Whitney U test ( $p \leq 0.01$ ) to test the spike rate difference, at each level, between the neural response and the prestimulus spontaneous activity. The frequency, ITD and ILD tuning were assessed using a Kruskal–Wallis test ( $p \leq 0.01$ ) for comparison of the neural response spike rates across the tested values of the parameter. To test the ITD/ILD sensitivity within the physiological range, the same statistical test was performed on a

smaller range of tested stimuli (ITD:  $\pm 200$  ms, ILD:  $\pm 8$  dB). The discrepancy between the measured physiological range of ITDs and ILDs ( $\pm 173$  ms,  $\pm 5.9$  dB, respectively; see section 3.2) and the tested range is given by the step size of the ITD and ILD stimuli (50 ms and 4 dB steps, respectively). If we had tested only in the  $\pm 150$  ms ITD range and  $\pm 4$  dB ILD range, we would have disregarded the neural response at most external values. The significant difference in diameter and best ITD between annulus and round aSRFs was tested using a Wilcoxon rank-sum test,  $p \leq 0.01$ . For the analysis of topographic maps, the correlation between specific tuning properties (i.e., aSRF medial peak location, best ITD) and the position of the corresponding recording sites along each anatomic axis was conducted using the Spearman's correlation coefficient.

## 3.2 Results

### 3.2.1 VAS stimuli

For the VAS stimuli presentation, we chose one of the four available chicken HRTFs from the database recorded by Schnyder et al. (2014). The ITDs were concentrically aligned with the interaural axis (range =  $\pm 173$  ms; Fig 3.1A), and interestingly, the ILDs modulated along the elevational axis (range =  $\pm 5.9$  dB; Fig 3.1B). The physiological range of ITDs was greater at low frequencies (0.1 – 2.5 kHz; range:  $\pm 182$  ms) than at high frequencies (2.5 – 5 kHz; range:  $\pm 163$  ms), whereas the ILDs had a wider range at high frequencies (low frequency range:  $\pm 3.1$  dB; high frequency range:  $\pm 9.3$  dB). These results are in line with the duplex theory, suggesting that ITDs can be used as localization cues at low frequencies, whereas ILDs at high frequencies (Rayleigh, 1907). The averaged ranges of ITDs and ILDs among the available HRTF datasets were slightly bigger than those from the HRTF used for the VAS stimuli (ITD range:  $\pm 196$  ms, ILD range:  $\pm 7.0$  dB). The ILD variance among HRTF datasets was larger than the ITD variance, but both were relatively small if compared with the total range (ITD: SD/total range = 7%; ILD: SD/total range = 14%), suggesting that the ITDs and ILDs do not change remarkably across subjects and justifying the usage of one database of VAS stimuli for all subjects (Fig. 3.1C–F).

### 3.2.2 Basic properties

We recorded auditory neural responses from 69 single units from either the OT or the FRLx. A total of 42 units (61%) were located in the OT, while 27 units (39%) were in the FRLx. All 69 units responded to binaural BB noise (see example responses in Fig. 3.2A,B). The typical PSTH profile in FRLx and OT

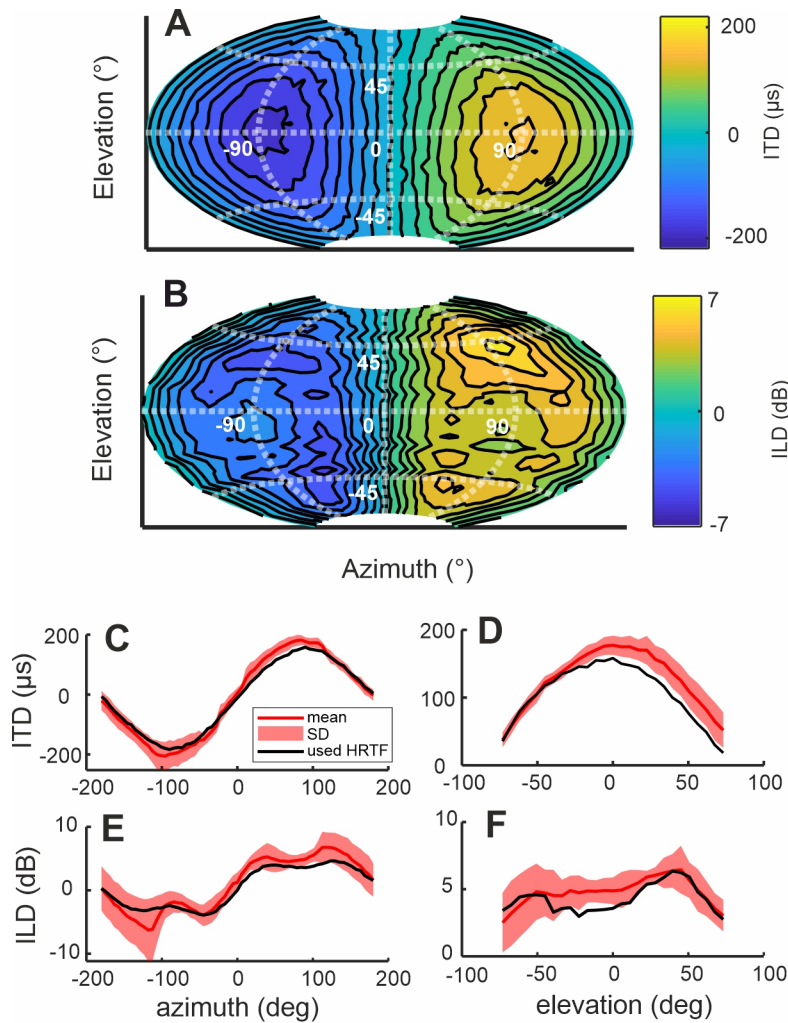


**Figure 3.1** ITDs and ILDs of the VAS stimuli. A-B) Hammer projection of the distribution of (A) ITDs and (B) ILDs of the VAS stimuli, within the broadband frequency range (0.1-5 kHz). C-F) Mean and standard deviation of (C, D) the ITD-cross-section and (E, F) the ILD-cross-section across 4 HRTFs of adult chickens, along azimuth at elevation  $0^{\circ}$  and along elevation at azimuth  $+90^{\circ}$ . The black line represents the ITDs/ILDs of the HRTF used in this study.

units had an onset peak followed by a sustained or build-up profile, and with a latency around 14ms after stimulus onset (FRLx: median = 13ms, range: 10–98ms; OT: median = 15ms, range: 10–174ms; Fig. 3.2C,D). Only a minority of units were frequency tuned, i.e., responded to pure tones [OT: 4 units (10%); FRLx: 10 units (37%); Fig. 3.2E]. BFs ranged between 0.1 and 4.9 kHz. Moreover, we found that most of the BFs were in the low frequency range (2 kHz; OT: 3 units (75%); FRLx: 6 units (60%)).

### 3.2.3 Monaural responses

We measured the monaural response of 57 units (FRLx: 22 units; OT: 35 units) for both ipsilateral and contralateral BB noise. We found that, for both FRLx and OT units, the most frequently observed monaural response type was responsive only to contralateral stimulation [“0E”; OT: 17 units (48%);

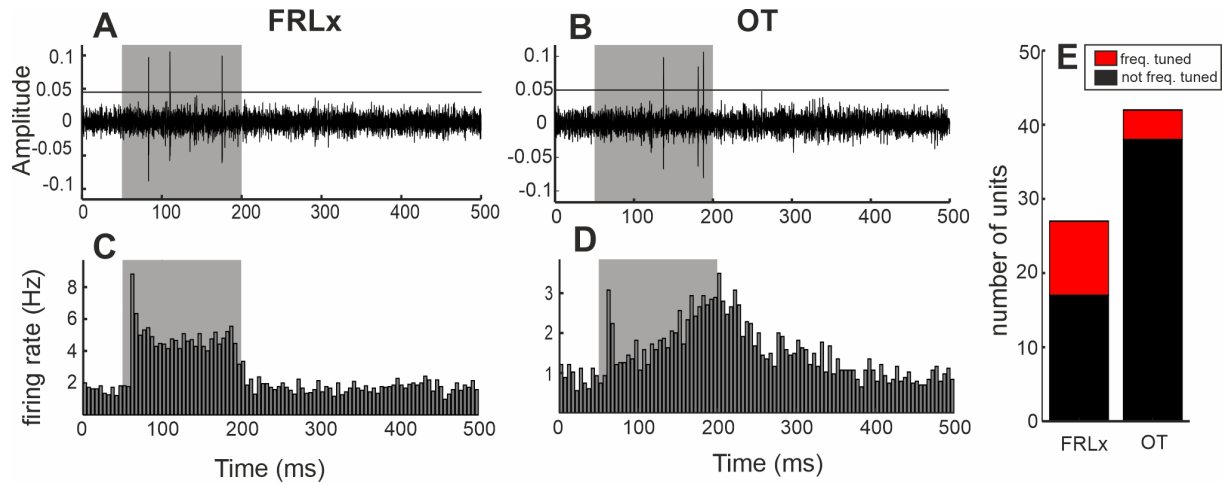


**Figure 3.2** Neural responses to auditory stimulation in FRLx and OT. A-B) Examples of a raw data trace aligned to the presentation protocol of virtual auditory space stimuli from a unit in A) FRLx and B) OT. The shaded area indicates the time window of stimulus presentation. The horizontal line indicates the threshold for spike detection. C-D) Example of PSTH of one unit, after spike sorting, obtained from the recording shown in A and B recorded from (C) FRLx and (D) OT. The bin width is 5 ms. E) Only a minority of units in FRLx and OT showed frequency tuning to pure tones.

FRLx: 17 units (77%)]. A high percentage of OT units were not responsive to either ipsilateral or contralateral stimulation [“00”; OT: 15 (43%); FRLx: 4 units (18%)]. Only a minority showed ipsilateral excitation (“EE,” “E0”) or ipsilateral inhibition (“IE”; Tables 3.1, 3.2).

**Table 3.1** Count and percentage of units in the OT classified by the combination of monaural response types.

|      |   | Contra  |   |          |
|------|---|---------|---|----------|
|      |   | E       | I | O        |
| Ipsi | E | 1 (3%)  | 0 | 1 (3%)   |
|      | I | 1 (3%)  | 0 | 0        |
|      | O | 17(48%) | 0 | 15 (43%) |

**Table 3.2** Count and percentage of units in the FRLx classified by the combination of monaural response types.

|      |   | Contra   |   |         |
|------|---|----------|---|---------|
|      |   | E        | I | O       |
| Ipsi | E | 1 (5%)   | 0 | 0       |
|      | I | 0        | 0 | 0       |
|      | O | 17 (77%) | 0 | 4 (18%) |

### 3.2.4 aSRFs

Most of the units had an annular aSRF (24 units, 35%; Fig. 3.3A) or round aSRF (27 units, 39%; Fig. 3.3B), whereas a minority presented a broad aSRF (8 units, 12%; Fig. 3.3C) or bilateral aSRF (10 units, 14%; Fig. 3.3D). Except for the bilateral units, all the remaining units responded to the contralateral hemifield of the VAS (59 units, 86%). Three units (4%) showed inhibitory response and

were excluded from subsequent analysis. The round and annular aSRFs had the centroid placed at  $90 \pm 15^\circ$  in azimuth and  $0 \pm 8^\circ$  in elevation. The mean position of the centroids was at  $91^\circ$  azimuth and  $-2^\circ$  elevation [annulus:  $94^\circ$  azimuth,  $-1^\circ$  elevation (Fig. 3.3E); round:  $90^\circ$  azimuth,  $-2^\circ$  elevation (Fig. 3.3F)]. For 4 units with annular aSRF, the centroid could not be determined because of their irregular shape and were not included in the subsequent analysis. The azimuthal diameter of the outer border of the annular aSRFs ranged from  $127^\circ$  to  $212^\circ$  (mean  $162^\circ$ ), whereas the diameter of the round aSRF ranged from  $64^\circ$  to  $181^\circ$  (mean  $119^\circ$ ). The mean diameter of the outer border of the annular aSRF was significantly larger than the mean diameter of the round type (Wilcoxon rank-sum test,  $p < 0.001$ ; Fig. 3.3G). Taken together, these data suggest that the round and annular aSRFs are placed in a concentric manner around the aural-visual axis, where the smaller round aSRFs are surrounded by the annular aSRFs.

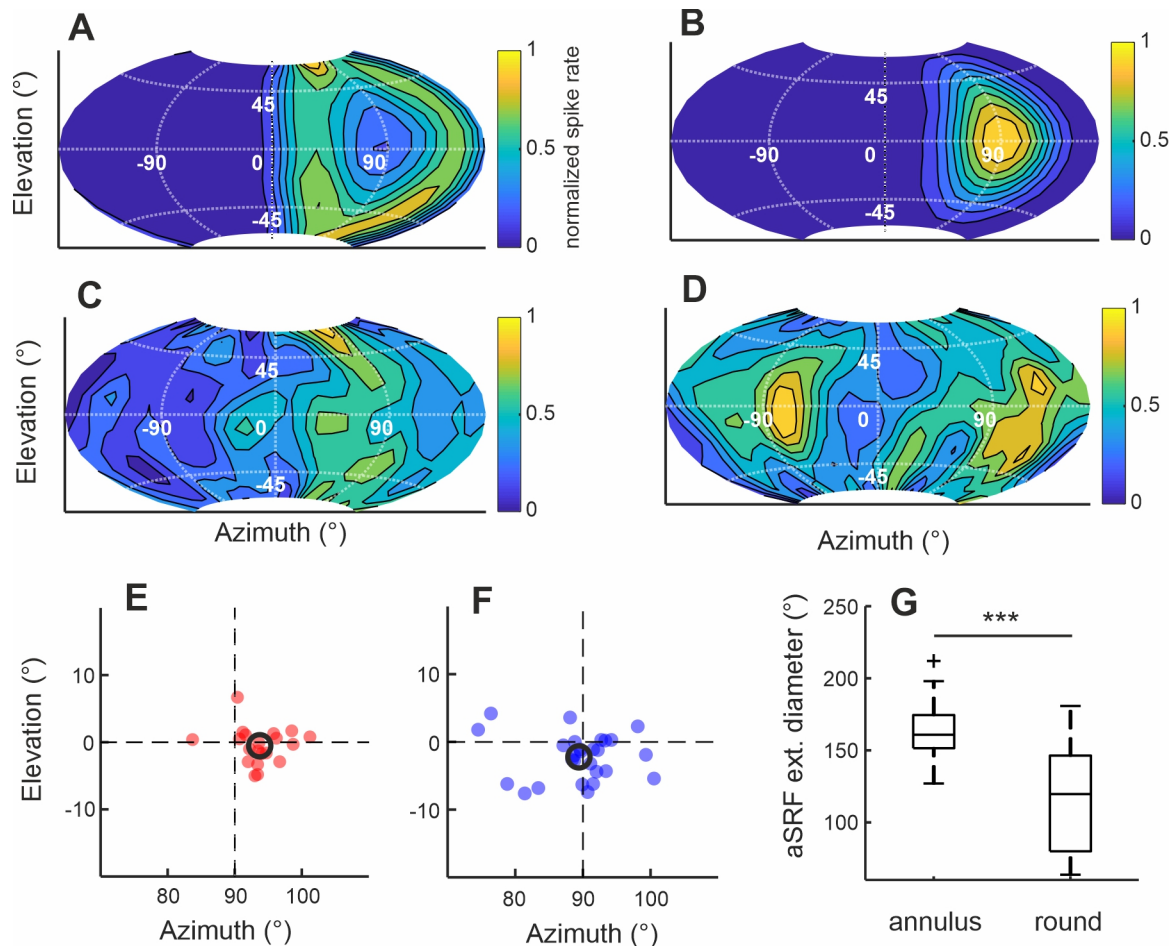


**Figure 3.3** Properties of the auditory spatial receptive fields. Examples of aSRF types for the A) annular, B) round, C) broad and D) bilateral types. The spike-maps are smoothed and represented in the Hammer projection. The colormap shows the normalized spike rate range. The step size of the isolines is 11% of the normalized spike rate. E-F) The position of the centroids of (E) annular aSRFs and (F) round aSRFs are centered around the lateral axis of the VAS. The black circle indicates the averaged centroid. G) The outer diameter of the annular aSRFs is significantly wider than the round aSRF diameter (Wilcoxon rank-sum test,  $p < 0.001$ ).

### 3.2.5 ITD and ILD tuning properties

We investigated whether the ITD and ILD tuning could explain the shape and location of the round and annular aSRFs. The distribution of the ITDs in the VAS stimuli has two main features. First, there is a gradient along the azimuthal axis, ranging between positions at  $-90^\circ$  and  $+90^\circ$  in azimuth. Second, the ITDs are arranged concentrically around the interaural axis, forming a cone of confusion (Fig. 3.1A). These features already suggest that neurons with longer best ITDs might possess a round aSRF, whereas smaller best ITDs would generate an annulus shaped aSRF. On the other hand, although the ILDs lack such a concentric configuration, they present two main peaks at around  $+50^\circ$  and  $-50^\circ$  elevation and a notch at the interaural axis (Fig. 3.1B). These ILD cues are the result of the head-induced monaural gain cues (Schnyder et al., 2014), which might be used by the chicken for elevational localization. Thus, we investigated whether they also play a role in the formation of the aSRFs. We tested the ITD tuning in 68 units. ITD tuning curves usually exhibited a sharp peak (Fig. 3.4A) and in 98% of the cases had contralaterally leading best ITDs. Half of the round aSRF units were tuned to ITD (15 units; 52%) and the majority of annular aSRF units (16 units; 71%) had best ITDs within the physiological range. No broad and bilateral aSRF unit was tuned to ITD (Fig. 3.4B). The best ITDs of the annulus units were significantly smaller than those of the round units (round: range from 105 to 287 ms, mean = 198 ms; annulus: range from -9 to 152 ms, mean = 86 ms; Wilcoxon rank-sum test:  $p < 0.001$ ; Fig. 3.4C,D). Moreover, the local-maxima-diameter of annular aSRFs and the outer diameter of round aSRFs correlated with the best ITDs [round: Pearson's  $r = -0.74$ ,  $p = 0.002$  (Fig. 3.4E); annulus: Pearson's  $r = -0.81$ ,  $p < 0.001$  (Fig. 3.4F)]. These results suggest that the best ITDs are mainly used by units exhibiting well defined contralateral aSRFs (i.e., annulus and round shape), where the ITDs are informative in defining the aSRF diameter. Furthermore, the ITD tuning width was relatively narrow in both FRLx and OT units (FRLx: median = 112 ms, range = 66–417 ms; OT: median = 132 ms, range = 69–296 ms).

We tested the ILD tuning in 57 units. The ILD response curves typically had a sigmoidal shape (Fig. 3.5A). Most of the round and annulus units were tuned to ILD (round: 17 units, 74%; annulus: 15 units, 83%). However, only a smaller portion of the round aSRF units was responsive within the physiological range (round: 8 units, 35%; annulus: 12 units, 67%; Fig. 3.5B). 94% of the ILD-tuned units responded to contralateral values (Fig. 3.5C). We investigated whether also the ILD tuning plays a role in the formation of aSRFs. If considering all the ILD-tuned units, the 50% ILD cutoff values correlate to the diameter of the round and annular units [round: Pearson's  $r = -0.72$ ,  $p = 0.002$  (Fig. 3.5D); annulus: Pearson's  $r = -0.57$ ,  $p = 0.027$  (Fig. 3.5E)]. These results suggest that round



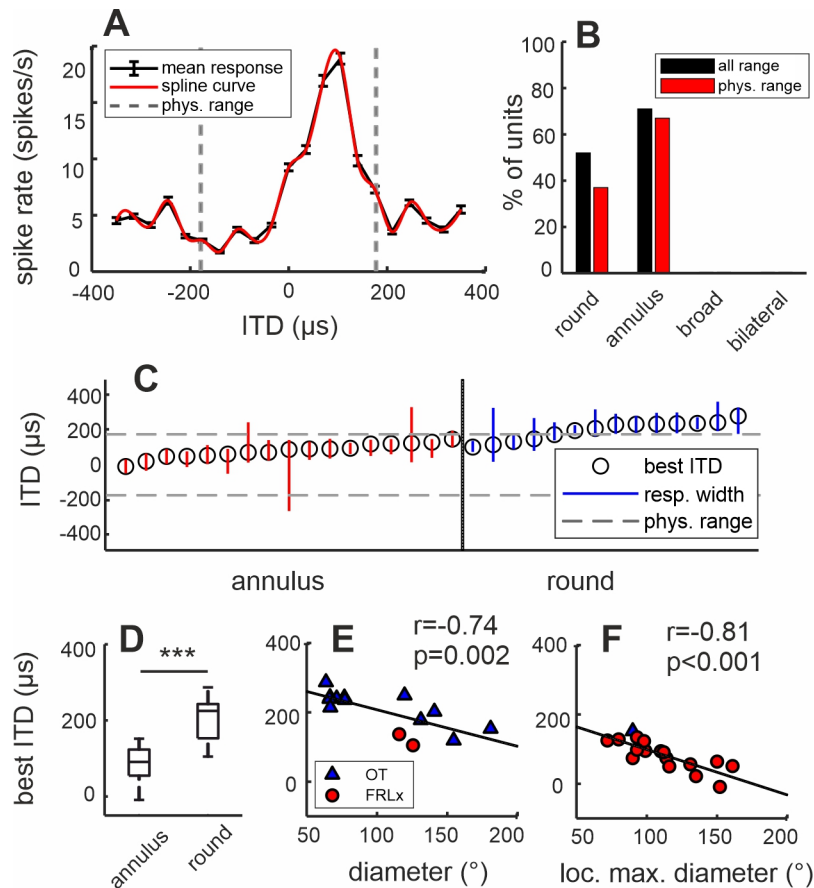


**Figure 3.4** ITD tuning properties. A) Example of ITD tuning curve recorded from FRLx. Note the sharp response peak. The error bars indicate the standard error of the mean. Positive ITD values indicate contralateral leading and negative values ipsilateral leading sounds. The dashed lines indicate the physiological range measured from the VAS stimuli. B) Count of units classified as ITD tuned, within the physiological range or beyond. C) Representation of all the ITD-tuned units showing the best ITD and the ITD response width. The dashed lines indicate the physiological range measured from the VAS stimuli. D) The best ITDs in the annulus aSRFs are significantly smaller than in the round aSRFs. (Wilcoxon rank-sum test,  $p < 0.001$ ). E-F) The best ITD is correlated with (E) the outer diameter of the round and (F) the local-maxima-diameter of the annular aSRFs (round: Pearson's  $r = -0.74$ ,  $p = 0.002$ ; annulus: Pearson's  $r = -0.81$ ,  $p < 0.001$ ).

and annular aSRFs might be created by converging ITD and ILD information. Indeed, a consistent percentage of annular and round units were selective to both ITD and ILD cues (annulus: 13 units, 72% of tested units; round: 11 units, 48% of tested units, broad and bilateral: 0 units), and they were responsive to ITD and ILD values related to the contralateral hemifield (i.e., contralateral leading sounds for ITDs, and louder contralateral sounds for ILDs). Furthermore, we investigated whether the properties of the ILD tuning curves vary between FRLx and OT. The median position of the 50% ILD cutoff was close to the physiological range for both FRLx and OT units, but the variability in the neural population was relatively high (FRLx: median = 7 dB, range = -35 – 14 dB; OT: median = 7 dB, range = -35 – 37 dB). In contrast to what was observed for the ITD tuning, this result shows that units in FRLx and OT were sensitive to a broader range of ILD values.

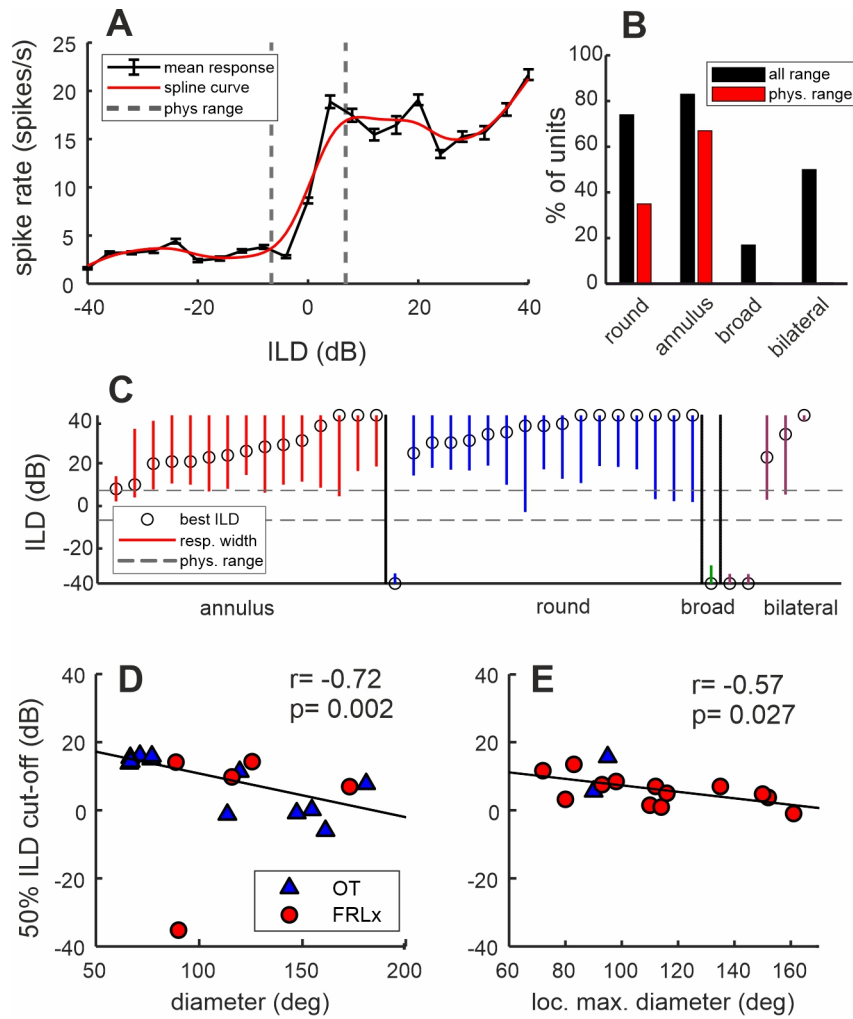


**Figure 3.5** ILD tuning properties. A) Example of ILD tuning curve recorded from the FRLx. Note the sigmoid shape. The error bars indicate the standard error of the mean. The dashed lines indicate the physiological range measured from the VAS stimuli. B) Count of units classified as ILD tuned, within the physiological range or beyond. C) Representation of all the ILD-tuned units showing the max ILD and the ILD response width. The dashed lines indicate the physiological range measured from the VAS stimuli. D-E) 50% cut-off of the ILD response of (D) round and (E) annular aSRFs, plotted as a function of the aSRF diameter. Both round and annular units show linear correlation (round (without outlier at -35 dB): Pearson's  $r = -0.72$ ,  $p = 0.002$ ; annulus: Pearson's  $r = -0.57$ ,  $p = 0.027$ ).

### 3.2.6 The units in FRLx and OT show different aSRFs

Most of the round aSRF units were located in the deep layers (layers 13–14) of the OT (20 units, 71%) and most of the annulus aSRF units were located in the FRLx (20 units, 84%). Any broad and bilateral aSRF units were located in the OT (Fig. 3.6A). It was not possible to determine the exact position of 8 units, because of lack of fluorescence tracing. However, it was possible to determine that these units were located in the layers of the OT and not in other midbrain structures, by using the stereotaxic information. The location of these units was not used in the calculation of the topographic maps (see next paragraph). In the OT, directions around the audiovisual axis were overrepresented, as seen by the normalized average of the aSRFs obtained from neurons in the OT (Fig. 3.6B). The same average

for the FRLx neuron, on the other hand, revealed uniform representation of locations around but also excluding 90° azimuth (Fig. 3.6C). These results show different spatial tuning properties of FRLx and OT in responding to specific areas of the auditory space.

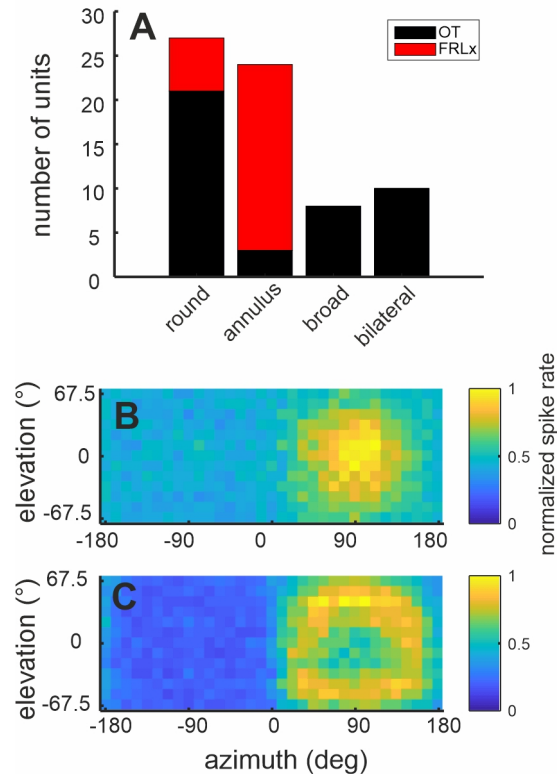


**Figure 3.6** Distribution of aSRFs in FRLx and OT. A) Histogram showing the number of units for each aSRF type and their location in the midbrain structures. The annular aSRFs units are predominantly located in the FRLx, while the other types are in the OT. B) The average of the aSRFs from OT units shows the over-representation of the spatial area at the interaural axis. C) The average of the aSRFs from FRLx units shows the overall neural response to the circular area around the interaural axis.

### 3.2.7 Topographic map in FRLx and OT

Thanks to fluorescence tracing and stereotaxic reconstruction (Fig. 3.7A), it was possible to reconstruct the position of the recording sites in the atlas coronal view (Fig. 3.7B). Given the aSRF selectivity of FRLx and OT at the neural population level, we investigated the presence of a topographic map related to the aSRF for each brain area. There was a significant correlation among the FRLx neurons between the annular aSRFs medial peak and the round aSRF central peak, and the location along both the RC (Spearman's  $r = -0.51$ ,  $p = 0.0067$ ; Fig. 3.7C) and DV axes (Spearman's  $r = 0.57$ ,  $p = 0.0020$ ; Fig. 3.7D), but not along the ML axis (Fig. 3.7E). However, when analyzing individual aSRF types, we found that the medial peak of annular aSRFs correlates with the location along both RC (Spearman's  $r = -0.62$ ,  $p = 0.0028$ ) and DV (Spearman's  $r = 0.73$ ,  $p = 0.0002$ ) axes, while the round aSRFs are only significantly organized along the RC axis (RC: Spearman's  $r = -0.84$ ,  $p = 0.0444$ ; DV: Spearman's  $r$

=0.41,  $p = 0.4333$ ), probably because of the low number of round aSRF units. This result suggests that there is an aSRF map arranged in a concentric manner, where smaller annular aSRFs are computed at the dorsal and caudal edge, whereas the diameter progressively increases toward the ventral and rostral edge (Fig. 3.7F). In the same way, the best azimuth of round aSRFs shifts from locations at the back of the animal head (azimuth range  $>90^\circ$ ) toward locations in the frontal field (azimuth  $<90^\circ$ ). Thus, to verify whether such an aSRF map reflects a possible ITD map in the FRLx, we compared the best ITD, calculated from the ITD tuning curve, of both annular and round aSRF units as function of the recording site, finding a significant correlation along both RC axis (Spearman's  $r = 0.50$ ,  $p = 0.034$ ; Fig. 3.7G) and DV axis (Spearman's  $r = -0.49$ ,  $p = 0.039$ ; Fig. 3.7H), but not along the ML axis (Fig. 3.7I). The correlation was preserved when the best ITDs of only annular units are considered (RC: Spearman's  $r = -0.55$ ,  $p = 0.0258$ , DV: Spearman's  $r = 0.58$ ,  $p = 0.0191$ ). Only 2 round aSRF units showed a best ITD in the FRLx, thus the correlation coefficient was not calculated for those units alone. These results indicate the presence of an ITD map aligned with the aSRF map: smaller annular aSRFs and longer ITDs are computed at more caudal and dorsal positions in the FRLx, whereas bigger annular aSRFs and smaller ITDs are generated at more rostral and ventral locations (compare Fig. 3.7F,J).

We also investigated whether a topographic map of aSRFs is present in the deep layers of the OT. We did not find a significant correlation between the medial peak of both round and annular aSRFs and the projection of the units along the RC axis (Spearman's  $r = 0.17$ ,  $p = 0.4682$ ; Fig. 3.8A) or DV axis (Spearman's  $r = -0.30$ ,  $p = 0.1979$ ; Fig. 3.8B). No significant correlation was detected considering the medial peak of the round aSRFs alone (RC axis: Spearman's  $r = 0.16$ ,  $p = 0.5330$ ; DV axis: Spearman's  $r = -0.32$ ,  $p = 0.1973$ ), suggesting that the round aSRFs are not topographically represented in the OT (Fig. 3.8C).

### 3.3 Discussion

Our study aimed at characterizing the auditory spatial properties of neurons in two midbrain areas, the OT and the FRLx, and the role of ITD and ILD tuning in shaping the aSRFs. We showed that most of the aSRFs in the FRLx and in the OT of the chicken are confined in both azimuth and elevation; the FRLx units mainly displayed ring-shaped "annular" aSRFs, while the OT units showed round aSRFs (Fig. 3.9). The role of ITD/ILD tuning in aSRF formation, the implications for auditory processing in the avian midbrain and for multimodal integration in OT are discussed.

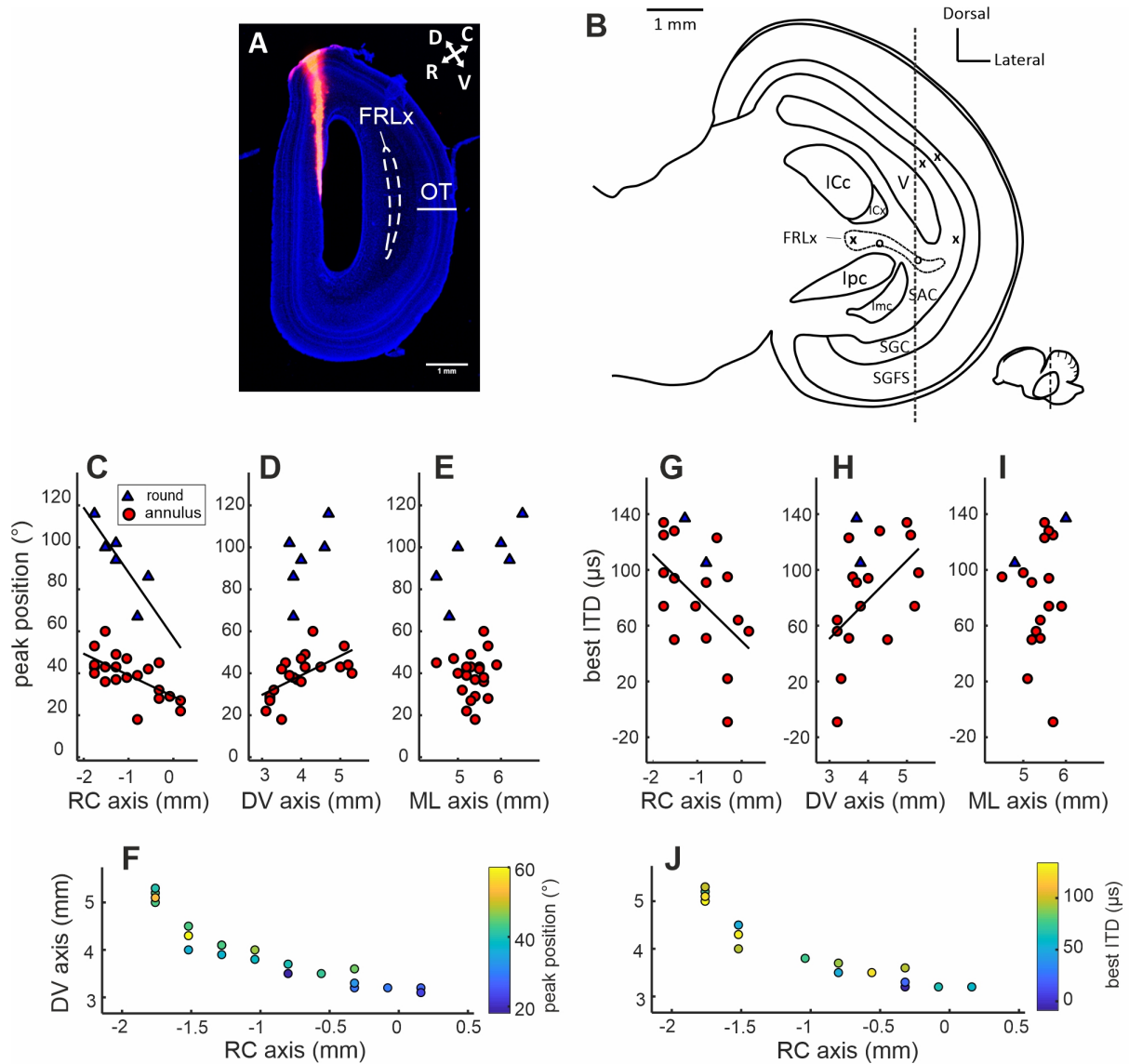


**Figure 3.7** Anatomical reconstruction of recoding sites and topographic map of the annular aSRFs in the FRLx. A) Example of histological slide. Sagittal section of the left midbrain. Note the trace of the electrode penetration (orange, DiI) and the midbrain structures (blue, DAPI), especially the layers of the OT. The location of the FRLx has been estimated based on the reconstruction in Niederleitner et al. (2017). No unit was recorded along the visible electrode track. V=ventral, D=dorsal, R=rostral, C=caudal. B) Example of recording sites in OT and FRLx in coronal view. Different symbols indicate different aSRF shapes (x=round, o=annulus). The dashed line represents the estimated position of the slide shown in (A). FRLx = formatio reticularis lateralis pars externa; SAC= stratum album centrale; SGC= stratum griseum centrale; ICc= central nucleus of the inferior colliculus; ICx= external nucleus of the inferior colliculus; Ipc= nucleus isthmi pars parvocellularis; Imc= nucleus isthmi pars magnocellularis; V= ventriculus; SGFS= stratum griseum et fibrosum superficiale of the tectum. C-E) Scatter plots of the medial peak of the aSRFs as function of the position of the recording sites along (C) rostro-caudal (RC) axis, (D) dorso-ventral (DV) axis and (E) medio-lateral (ML) axis. The medial peak of annular aSRFs correlated along both RC and DV axes (RC: Spearman's rho=-0.62, p=0.0028; DV: Spearman's rho=0.73, p=0.0002), while the round aSRFs correlated only along the RC axis (Spearman's rho=-0.84, p=0.0444). F) Position of the medial peak of annular aSRF units in the FRLx, according to the atlas coordinates, along the RC and DV axes. Note the gradient along the axes. G-I) Scatter plots of the best ITD in function of the position of the recording sites along (G) RC axis, (H) DV axis and (I) ML axis. The best ITD of the annular aSRFs correlates along both RC and DV axes (RC: Spearman's rho=-0.55, p=0.0258; DV: Spearman's rho=0.58, p=0.0191). J) Best ITD of annular aSRF units in the FRLx, according to the atlas coordinates, along the RC and DV axes. Note the gradient along the axes.

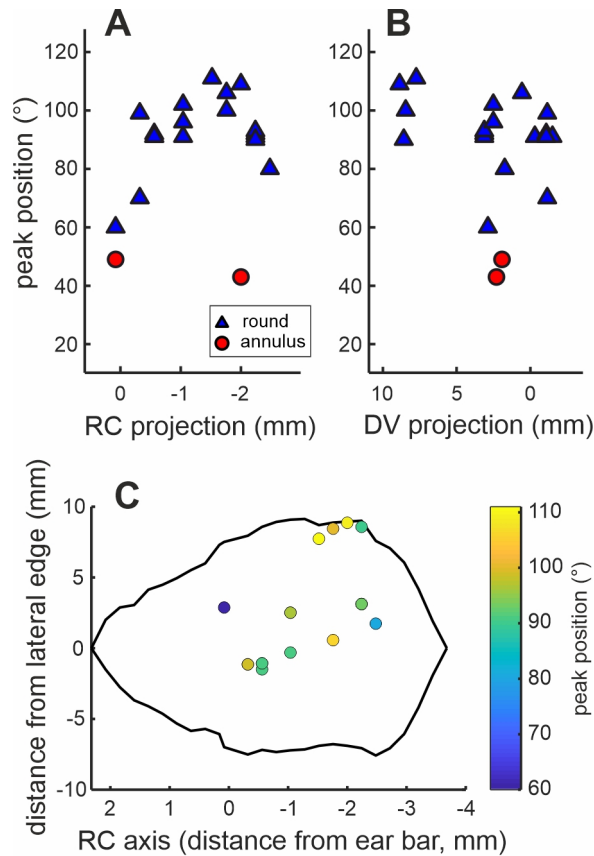


**Figure 3.8** Projection of aSRFs onto the OT surface. A-B) Plots of medial peak of annular and round aSRFs as function of the projected location along (A) rostro-caudal (RC) and (B) dorso-ventral (DV) axes. The round aSRFs were not topographically organized along the two axes (RC axis: Spearman's  $\rho=0.31$ ,  $p=0.1677$ ; DV axis: Spearman's  $\rho=-0.32$ ,  $p=0.1973$ ). C) Representation of the round aSRF units projected onto the surface of the OT, with the color-coding of the medial peak position. The black line indicates the borders of the OT surface.

### 3.3.1 Role of ITD and ILD tuning in aSRF formation

Our data suggest that annular and round aSRFs in OT and FRLx are mainly generated through a unit's tuning to ITD and ILD, which could allow generalist bird's midbrain neurons to encode for specific positions in elevation. This evidence stands in contrast with the hypothesis that generalist birds can only discriminate sound sources along azimuth (Klump, 2000). Electrophysiological studies showed that aSRFs in the ICx of birds with symmetrical ears are only limited in azimuth, not in elevation (Calford et al., 1985; Volman and Konishi, 1989, 1990). However, in our study the VAS range (azimuth:  $\pm 180^\circ$ , elevation:  $\pm 67.5^\circ$ ) was considerably wider than in the other studies, where it was limited to the frontal area of the auditory space. This limitation might have not permitted to reconstruct the entire shape of round and annular aSRFs, which may have appeared as vertical stripes (Volman and Konishi, 1989; see their Figs. 3, 6), or other uncompleted shapes (Calford et al., 1985; see their Fig. 2B,C). In the barn owl, ITDs are exclusively informative for horizontal location of a sound source and ILDs mainly for vertical directions (Moiseff (1989b); Takahashi et al. (2003), and the multiplicative computation of

### 3 Two Types of Auditory Spatial Receptive Fields in Different Parts of the Chicken's Midbrain

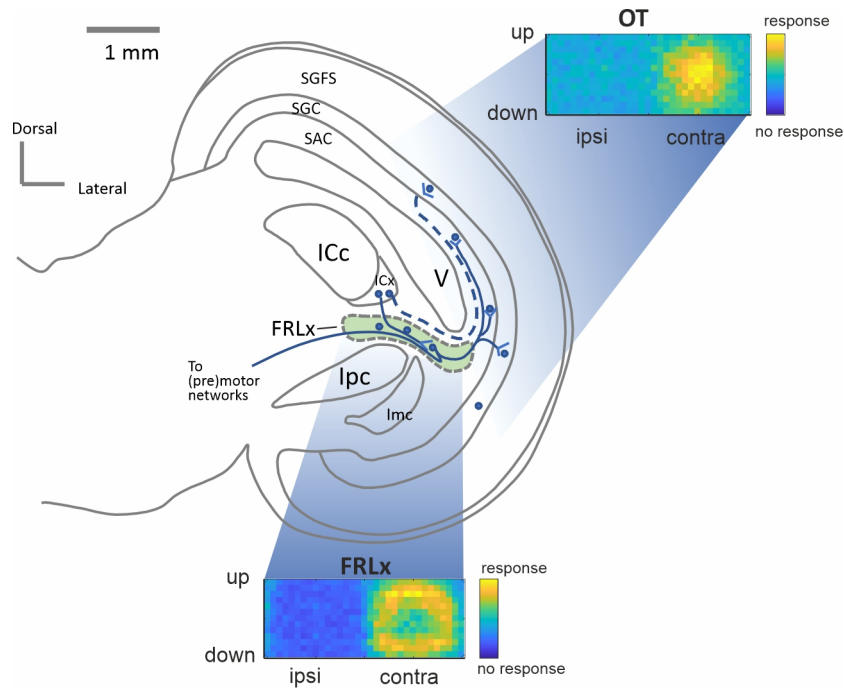


**Figure 3.9** Schematic of the representation of the auditory space in FRLx and OT. The neurons in the FRLx, which have annular aSRFs, receive input from the ICx and broadly project to the neurons in the OT deep layers, which are sensitive to auditory locations around the lateral axis. Beside this pathway, some ICx neurons directly project to the OT. [FRLx = formatio reticularis lateralis pars externa; SAC= stratum album centrale; SGC= stratum griseum centrale; ICc= central nucleus of the inferior colliculus; ICx= external nucleus of the inferior colliculus; Ipc= nucleus isthmi pars parvocellularis; Imc= nucleus isthmi pars magnocellularis; V= ventriculus; SGFS= stratum griseum et fibrosum superficiale of the tectum].

these two cues in the ICx provides narrowly tuned aSRFs (Peña and Konishi, 2001; Fischer et al., 2007). In generalist birds the main cue for spatial tuning might be provided by the ITDs: the aSRF may be round for preferred ITDs close to those occurring at 190° in azimuth or lead to increased response at a ring-shaped cone of confusion. However, also the BB ILDs seem to be informative for spatial sensitivity, especially for the round aSRFs. We could not investigate the role of spectral ILDs, as well as the role of low and high frequency ranges for binaural cues processing. Future studies are needed to investigate the aspects of ITD/ILD processing in FRLx and OT. When compared with other chicken auditory nuclei, the ITD tuning responses in FRLx and OT are narrower than in more peripheral processing levels, such as the chicken nucleus laminaris (Köppl and Carr, 2008) and IC (Aralla et al., 2018). The ILD tuning responses were sigmoidal, as observed in the chicken lateral lemniscal nucleus (LLD; Sato et al., 2010), however in FRLx and OT the steep part of the ILD curves spans across a broader range than what observed in LLD. The ILD tuning in FRLx and OT is mainly comparable to the “contra-dominated” type of the chicken’s IC described previously (Aralla et al., 2018).



### 3.3.2 Auditory spatial tuning along the pathway ICx–FRLx–OT

Birds have internally coupled ears (ICE) which increase both ITDs and ILDs that reach the ear drums. This effect may increase spatial resolution and it is particularly beneficial for small sized birds, which otherwise would experience small ITDs and ILDs. In the chicken, the enhancement of the presented ITDs and the ITD-dependent amplitude modulation can reach a factor of up to 1.8 and 2.22, respectively (Köppl, 2019). Thus, according to our HRTF measurements, the “heard” ITD and ILD ranges might broaden up to  $\pm 353$  ms and  $\pm 15.5$  dB, respectively. These cues are then processed along the auditory pathway up to the midbrain nuclei, such as the IC, the FRLx and the OT. The FRLx receives input from ICx and projects to the OT, and it is discussed as the plesiomorphic connection between these two nuclei (Niederleitner et al., 2017). As far as we know, our study is the first in which aSRFs in the FRLx were recorded *in vivo*. Our main finding is a predominance of annular aSRFs which are arranged in a topographic map. In the barn owl, the ICx has a 2D-auditory space map which is projected to the OT, preserving spatial tuning in ICx (Knudsen and Konishi, 1978; Knudsen and Knudsen, 1983). The ICx of symmetrically eared owls contains a topographic map of the best azimuth, where lateral locations are represented at the posterior part of the ICx, and increasingly frontal best azimuths are at more anterior positions (Volman and Konishi, 1989, 1990). Likewise, in our study the smaller annular aSRFs were located at the posterior FRLx area, and progressively larger aSRFs (responsive to more frontal azimuths) were present at more anterior locations. Spatial tuning and medial preferred directions might be projected from ICx onto FRLx. The physiological function of the annular aSRFs in the FRLx might be to encode the offset of the auditory stimulus from the lateral axis, yielding an “error signal”, where the neural response along the aSRF ring defines the angular distance of the stimulus from the visual axis. This information might be transferred to the (pre) motor networks (Niederleitner et al., 2017) to provide a quick response to a stimulus, or to trigger saccadic head movements to align the stimulus to the visual axis. Spatial tuning in the OT was dominated by round aSRFs, encoding lateral locations and not organized in a topographic map. Similar tuning was found in the pigeon OT (Lewald and Dörrscheidt, 1998), indicating that the auditory resolution in generalist birds’ OT is much lower than in the barn owl, where neurons are narrowly tuned to specific locations in space creating a place code of the auditory space (Knudsen, 1982). The lack of ring shaped aSRFs in the OT implies that FRLx neurons that project onto the OT may create a source for lateral inhibition and shape the tuning in OT. An alternative explanation is that the place coding of space in FRLx is converted to a rate code in OT. Such a mechanism has been observed in the barn owl, where ICx and OT, which have a map of auditory space based on place



coding, project to the midbrain tegmentum, involved in eye gaze orientation, which operates as a rate code nucleus (Cazettes et al., 2018; Peña et al., 2019). However, rate code would generate ambiguities in a 2D environment, thus it would only be useful for coding sound directions along the azimuthal or elevational plane.

### 3.3.3 Implications for auditory localization and multimodal integration

The OT, like the superior colliculus, is an important computational hub for multimodal integration (Stein and Meredith, 1993; Knudsen and Brainard, 1995). Both visual and auditory stimuli are processed in the chicken OT (Cotter, 1976), and young chicks show audiovisual integration (Verhaal and Luksch, 2016). In contrast to the barn owl, which possesses auditory specializations and frontally oriented eyes as adaptations for nocturnal hunting (Harmening and Wagner, 2011; Wagner et al., 2013), generalist birds mainly rely on vision and have laterally oriented eyes to monitor the surroundings (Iwaniuk et al., 2008). Thus, the lateral visual axis strongly overlaps with the interaural axis (Schnyder et al., 2014). This implies that the over-representation of the auditory space around the lateral axis in the OT might correspond to the visual segment inspected by the area centralis. However, the size of the auditory and visual RFs is remarkably different: if the aSRFs have a mean diameter of  $120^\circ$ , the visual RFs are not bigger than  $25^\circ$  (Verhaal and Luksch, 2013). This discrepancy might be explained by the law of inverse effectiveness, as part of the neural computational rules underlying multimodal integration (Stanford and Stein, 2007). It states that multimodal integration is strongest for stimuli that, when presented alone, are minimally effective in eliciting a neuronal response. When sound and image are faint, even a receptive field as large as the aSRFs that we found can be beneficial, as it increases the likelihood that weak stimuli will reach the detection threshold. From an evolutionary perspective, the sensory organs have evolved to ensure an animal's survival. If the sensory periphery, for physical reasons, does not allow the precise location of a stimulus, it is nevertheless beneficial to exploit the information by orienting another, more precise distance sense. Because of the diurnal lifestyle of early vertebrates, the visual system had been dominant in most taxa; however, mammalian (especially therian) evolution went through a nocturnal niche which strongly altered the sensory layout and tuned the auditory system toward high precision. Thus, our findings in the chicken might represent the ancestral situation for vertebrates. It will be interesting to see whether other amniotes such as lizards process auditory stimuli in a similar fashion.

## 4 General Discussion and Outlook

This thesis focuses on behavioral and neurophysiological aspects of sound localization in the chicken (*Gallus gallus*). Precisely, it is divided into two studies: one regards the behavioral aspects of sound localization in azimuth – i.e., the degree of accuracy and the head movement patterns during localization -; the second one investigated the neural representation of auditory space in specific areas of the midbrain. However, before discussing the impact of my results in a broader context and with an evolutionary perspective, it is necessary to provide a short overview of the evolution of hearing capabilities in vertebrates.

The auditory system is a sense that allows the identification of environmental energy patterns, in this case particle waves, over a distance. Orienting in the environment is critical to approach or avoid a given stimulus, for example in the context of food search or predator avoidance, and thus distance senses are widespread in the animal kingdom. However, while visual systems were developed early on, and eyes to analyze light patterns are found in numerous taxa, auditory systems were only developed in insects on one hand, and in vertebrates on the other hand. The earliest vertebrates already showed a rich variation of mechanosensory elements to detect particle waves as well as gravitational and dynamic forces, i.e., they had lateral line systems and inner ear structures (Pombal and Megías, 2020). From the inner ear hair cell maculae of these early forms, the auditory maculae of later taxa evolved. However, even though the neuronal computation of sound direction is much more difficult in water due to the higher propagation speed, fish developed hearing apparatuses that allowed them to locate sound (for a review see Popper and Fay, 1993; Putland et al., 2019). The inner ear of fish consists of three semicircular canals, used for equilibrium orientation in the three-dimensional space, and the real auditory organ, which contain hair cells and otoliths. As fish have a density roughly equal to the surrounding water, the fish body moves together with the displacement of the water mass. However, the denser otoliths move with a different acceleration, deforming the hair cells and providing a sensory input. Since the hair cells are inherently directional because of their cilia orientation, hearing directionality and sound source localization are already encoded at

this peripheral stage. This otolith-based mechanism allows detection of particle motion, but other fish species evolved other organs for sound pressure processing by exaptation of the swim bladder. For example, the lungfish has a gas bubble in the head, next to the middle ears. This bubble amplifies the underwater vibrations, which are then transmitted to the hearing organs (Christensen-Dalsgaard et al., 2011).

A critical event in natural history – and, consequently, in the evolution of hearing – is the emergence of vertebrates from water onto land and the spread of terrestrial four-limbed animals, called tetrapods. The first tetrapods had an amphibian-like semiaquatic lifestyle and had inner ears internally coupled through the mouth cavity, providing directionality and acting as pressure difference receivers (for a review see Christensen-Dalsgaard, 2011). However, they did not possess any tympanic middle ear, thus sounds were transmitted through the skull. Among the recent amphibians, only the anurans evolved a tympanic middle ear during the Triassic, the same period when this anatomical structure independently appeared in the main amniote groups (see below). Even in the consistent number of anuran species which have secondarily lost their middle ear, there is a sensitivity reduction only at high frequencies, whereas for low frequencies (below 400 Hz) the sensitivity is only partially impaired (Smotherman and Narins, 2004). This indicates that the early atympanate tetrapods might have had significant low-frequency hearing capability, including directional hearing through bone transmission. The evolution of an amniotic egg emancipated these animal species from water and made the spread on land possible. The amniotic egg evolved a rigid shell as protection from the air. In order to cope with air-borne sounds, auditory specializations in amniotes increased the frequency range of hearing and also its sensitivity. The amniote hearing organ – the basilar papilla – was a cluster of hair cells supported on a free basilar membrane and was the basis for the subsequent middle ear evolution in the other taxa. Around 320 Million years ago the stem reptiles broke up into several groups (Carroll, 1988): the mammal-like reptiles (or Synapsida) which later evolved into the true mammals; the Lepidosauria, which includes the squamates, such as lizards and snakes -; the Archosauria, including dinosaurs, Crocodilia and birds. From this time point on, parallel evolutionary paths of the auditory system took place (for a review see Manley, 2017). As mentioned above, during the Triassic, middle ears evolved independently among all amniote groups (Clack, 2002). These independent events might be convergent evolution due to the biological relevance of detection of airborne vibrations. Indeed, during this period also sound-producing insects appeared (Hoy, 1992). This novel middle ear structure consisted of an eardrum interfacing to the environmental air and a bone structure transmitting the vibrations to the inner ear. The presence of two ears, which

might seem simply a side product of the developmental constraints of symmetrical bodies, turned out to be fundamental for sound localization through the computation of binaural cues (Schnupp and Carr, 2009).

Mammalian ancestors evolved a three-ossicles middle ear (review in Manley, 2010). This structure evolved at least twice, i.e., among the ancestors of therian mammals and those of monotremes. Other auditory specializations appeared, such as the mammalian cochlea with the organ of Corti. The therian cochlea expanded remarkably by coiling, with a resulting great extension of frequency range, especially at high frequencies. In mammals the de-coupling of the ears is a derived condition that might have provided an improvement of low-frequency processing but, on the other hand, it required additional neural computation for directionality in the auditory system. Lastly, the evolution of external structures around the ear canals, called pinnae, had a huge impact in increase of sound sensitivity up to 20 dB – by funneling sound to the eardrum (Manley, 2017) – and of sound localization – by generating elevation-dependent monaural cues (Grothe et al., 2010). These specializations, leading to exquisite high-frequency hearing and localization capabilities, were in part driven by the nocturnality of mammalian ancestors which stressed auditory orientation at the expense of the visual system (Kaas, 2013). In Lepidosaurs and Archosaurs a bone used by the fish ancestor as a gill support – called columella – moved rostrally and became a connector between the inner ear and, through a cartilaginous formation called extracolumella, a thin membrane, the eardrum. This structure tremendously improved the vibration transmission from air to the liquid-filled cavities of the inner ear. Like in mammals, also in Archosaurs the appearance of a tympanic middle ear was accompanied by an elongation of the basilar papilla, with a consequent expansion of the hearing frequency range. Another feature of non-mammalian amniotes, preserved in birds, are the internally coupled ears (ICE). In birds the middle ears are connected through a complex system of trabeculae (Larsen et al., 2016) and there is evidence of its impact in the enhancement of the perceived binaural cues (ITDs and ILDs) compared to the presented ones (e.g., in barn owl: Moiseff and Konishi, 1981; Kettler et al., 2016; and chicken: Hyson et al., 1994; Köppl, 2019). These modulations of the auditory binaural cues are particularly important for the enhancement of sound localization in small birds.

Experiments have been conducted in the last decades in order to understand sound localization in birds (for a review, see Klump, 2000) and their related neural substrates, e.g., the representation of auditory space in the midbrain (Calford et al., 1985; Volman and Konishi, 1990; Grothe, 2018; Aralla et al., 2018). The avian species studied best in this regard is the barn owl, a nocturnal bird of prey with remarkable abilities to hunt in total darkness, exclusively driven by prey sounds (Payne,

1971; Konishi, 1973). As it has been shown by numerous studies, this performance is achieved by a variety of anatomical features in the periphery, as well as hypertrophied brain circuits and physiological adaptations (for a review, see Grothe, 2018). Most notably from the exterior is the asymmetric positioning of the outer ear openings, a feature that allows to use ITD cues for azimuthal localization and ILD cues for elevational localization (Moiseff, 1989b,a). However, most avian species - called generalist birds - have symmetrical ears and lack any auditory specialization to improve sound localization, and it is still debated and poorly understood how these animals can accurately locate sounds along elevation and what is the underlying neural computation. To our knowledge, only a few studies measured the sound localization accuracy in auditory generalist species (Rice, 1982; Klump et al., 1986; Park and Dooling, 1991; Feinkohl and Klump, 2013; Krumm et al., 2022), and electrophysiological studies in their auditory midbrain mainly focused on the IC (Calford et al., 1985; Volman and Konishi, 1989, 1990) and neglected higher-order midbrain areas, such as the OT, which has a role in integrating the auditory information from the IC with other senses, such as vision. Among the auditory generalist birds, the chicken is a well suited representative of this avian group, since several aspects of its auditory system – such as the anatomy, physiology, evolution and development – have already been studied in the last decades (for reviews: Rubel and Parks, 1988; Gleich et al., 2004). Moreover, it has already been used as a model for the plesiomorphic condition of the avian auditory system and compared to the auditory-specialist barn owl (Kubke and Carr, 2000; Takahashi et al., 2021)

In the first study, I conducted a behavioral experiment where 3 roosters performed a sound localization task with broad-band noise, using a 2-alternative forced choice paradigm. I determined the minimum audible angle (MAA) as measure for localization acuity in azimuth. In general, the results are comparable to previous MAA measurements with hens in Go/NoGo tasks (Krumm et al., 2022), showing a better localization acuity compared to other auditory generalist bird species tested so far. We found that chickens were better at localizing broadband noise with long duration (1 s; MAA=16°) compared to brief duration (0.1 s; MAA=26°). Moreover, the ITD and ILD at these MAAs are comparable to what measured in other non-auditory specialist bird species, indicating that they might be sufficiently broad to be informative for azimuthal sound localization. Additionally, for one subject the head movements during localization were tracked, and the results showed remarkable head turns during sounds with long duration towards the response keys, rather than towards the sound source, as observed in other species (Knudsen et al., 1979; Feinkohl et al., 2013). This correlation between head orientation and improved sound localization has been observed also in other avian species, such

as the barn owl (Knudsen et al., 1979) and the starling (Feinkohl et al., 2013). Rather than orienting the head in respect to the sound source, e.g., to maximize the binaural cues in a lateral position or using the frontal field where the resolution is highest, the simple change of binaural cues when aiming to the response keys might be sufficient to improve sound localization. A similar effect of head turns not aimed to sound sources has been observed in the starling (Feinkohl et al., 2013).

In a final experiment, an attempt to measure the sound localization accuracy in elevation was made, but without clear results. The reason is the restricted time window to train and test the roosters in the behavioral experiment, as at the time of the elevational task the animals reached sexual maturity and started to behave very erratically. In the future other attempts should be carried out, for example by training the chickens directly to the vertical localization task. This has already been done in auditory specialist animals, but it is less likely to be successful for a generalist bird, as the elevation task would be much harder to accomplish. In the barn owl, the most used paradigm to measure sound accuracy is tracking the spontaneous head orientation reflex towards sound sources (e.g., see Knudsen et al., 1979; Kettler and Wagner, 2014). Since this is an innate behavior, training is not required and it allows a relatively easy measurement of the localization also in elevation. In mammals, some studies measured the elevation localization accuracy with Go/NoGo or 2AFC paradigms (Heffner et al., 1996; Huang and May, 1996; Parsons et al., 1999). These studies did not report similar problems during the training, and most subjects were directly trained on the vertical setup, without a transition from the horizontal one.

The behavioral aspects observed with this study in the domestic chicken are likely inherited from the undomesticated ancestor, the red junglefowl (Lawal et al., 2020). The natural habitats of the red junglefowl are the tropical forests of Southeast Asia and South Asia. It takes shelter on trees especially to escape from terrestrial predation, and usually eats seeds and fallen ripe fruits on the ground, but occasionally also feeds on hanging fruit, perching on tree branches (Collias and Collias, 1967). This habitat likely hosts a high variety of possible predators, both terrestrial and aerial, that can easily hide in the dense vegetation. This context indicates that the red junglefowl requires a proper 3D sound localization ability for its survival. Even though the red junglefowl has been domesticated for the last 8 thousand years (Lawal et al., 2020), this period is relatively short in evolutionary terms. To my knowledge, there is no evidence of a side effect on the auditory system given by the artificial selection for meat and egg production in white leghorn chicken. However, given a likely reduction in predation pressure in the domesticated environment, a reduced auditory performance would not affect the fitness of the species and thus might spread through generations. Thus, it would be

interesting to investigate the sound localization behavior on the extant red junglefowl or other close undomesticated species (within genus *Gallus*) and compare it with the results of my study.

In the second study, I conducted *in vivo* extracellular recordings of single neurons in the OT and in the external portion of the *formatio reticularis lateralis* (FRLx), a brain structure located between the inferior colliculus (IC) and the OT, in anaesthetized chickens of either sex. I found that most of the auditory spatial receptive fields (aSRFs) were spatially confined both in azimuth and elevation, divided into two main classes: round aSRFs, mainly present in the OT, and annular aSRFs, with a ring-like shape around the interaural axis, mainly present in the FRLx and arranged in a topographic map. The data further indicate that ITD and ILD play a role in the formation of both aSRF classes. These results suggest that, unlike mammals and owls which have a congruent representation of visual and auditory space in the OT, generalist birds separate the computation of auditory space in two different midbrain structures. The hypothesis is that the FRLx-annular aSRFs define the distance of a sound source from the visual-auditory axis (in an “error signal” fashion), whereas the OT-round aSRFs are involved in multimodal integration of the stimulus around the lateral fovea. This peculiar neural processing of the auditory space is consistent with the concentric arrangement of the ITD/ILD cues reaching the eardrums (Maldarelli et al., 2022a) as well as the monaural cues available in elevation (Schnyder et al., 2014). Moreover, these findings seem to be related to the typical alignment of vision and hearing in generalist birds: in contrast to the barn owl, which possesses auditory specializations and frontally oriented eyes as adaptations for nocturnal hunting (Harmening and Wagner, 2011; Wagner et al., 2013), generalist birds mainly rely on vision and have laterally oriented eyes to monitor the surroundings (Iwaniuk et al., 2008). Thus, the lateral visual axis – approximately at the lateral fovea – strongly overlaps with the interaural axis (Schnyder et al., 2014). These findings raise hypotheses on the behavior that would maximize the localization and recognition of salient stimuli in the naturalistic environment. My hypothesis is that the chicken – and auditory generalist birds in general – would use saccadic head movements to estimate the distance of the target object from the lateral axis and adjust the head orientation until reaching the alignment with the lateral axis. At that point a better multimodal integration of the object and a subsequent recognition would be accomplished. In support of this hypothesis, there is evidence of lateral orientation of generalist birds’ head for visual inspection and auditory localization. Chickens visually inspect distant objects laterally, while close objects (at a distance below 0.3 m) are seen frontally and binocularly (Dawkins, 2002). A similar lateral orientation has also been observed during sound source localization by the towhee, an auditory generalist bird (Nelson and Suthers, 2004). Therefore, the lateralized inspection might be evolved as a mechanism

for audio-visual integration of salient distant objects. Furthermore, there is a vast body of literature showing visual lateralization in birds and the influence of experience during development. Indeed, in both chicken and pigeon there is neural and behavioral asymmetry related to vision (e.g., for a review see Halpern et al., 2005). In particular, because of the head position in the egg, the right eye of the embryo is exposed to light while the left one is occluded by the body. This condition is responsible for the asymmetry in the neural pathway in the chicken and pigeon, with consequent dominance of each eye for specific visual tasks (Rogers and Sink, 1988; Skiba et al., 2002). Moreover, there is evidence of the role of sexual and stress hormones and in the asymmetry development (Schwarz and Rogers, 1992; Rogers and Rajendra, 1993; Rogers and Deng, 2005). Thus, for the chicken – and auditory generalist birds in general – the lateralized inspection might be beneficial for both a better visual detection and a better audio-visual integration of the stimulus: in case of a salient biological agent (e.g., predator), the chicken might orient the best eye to maximize the categorization / detection ability of the visual stimulus (e.g., the image of the hiding predator) and at the same time efficiently integrating it with the auditory stimulus (e.g., the noise made by the predator while approaching).

In summary, two types of behavior for sound localization might be used by generalist birds according to the task and situation in the surroundings. The first one regards a ‘rough’ azimuthal localization – mainly along azimuth –, while the second one regards a ‘fine’ localization – especially along elevation – and subsequent stimulus recognition. The first type of localization might be used, for instance, for a first and quick orientation towards sounds emanating from, e.g., predators or conspecifics, which would mostly come from different azimuthal directions but at the same height of the animal. According to the behavioral results from my first study, in this case the chicken would not need to orient the head laterally, but generic head movements would already increase the accuracy of the localization, especially for long duration sounds, such as animal calls. This behavior would allow the animal to estimate at least from which side the target is present. In a putative second phase, a more precise localization of the target could be achieved, building on the rough estimation mentioned above – especially to detect stimuli along elevation. Examples in a naturalistic context might be the recognition of the potential conspecific / predator previously heard, or the proper localization of a flying predator, such as a hawk. Based on the neurophysiological findings of my second study, an alignment of the lateral head axis with the target stimulus using saccadic head movements might be used for localization and audio-visual integration. These conditions might apply also to other generalist birds, which are mainly flying species and where a proper 3D representation of the auditory space might be even more crucial for their survival and reproduction. In conclusion, several questions



arise from these results which should be investigated in the future, e.g., finding an effective paradigm to measure the sound localization accuracy also in elevation and investigate what is the behavioral strategy used for it; moreover, given the apparent mismatch between visual and auditory maps in the OT, another important research question is how the neural integration of visual and auditory stimuli is encoded in the avian midbrain.

Although generalist birds' brain has an accurate topographic map of visual space (Clarke and Whitteridge, 1976), from my studies it seems that this is not valid for the neural map of auditory space. This is in contrast with the canonical topographic representation of auditory space observed in mammals (Palmer and King, 1982) and avian specialists (Knudsen, 1982). These differences among animal taxa make evolutionary sense: during the rule of the dinosaurs, mammals were forced by predation pressure to adapt to a more nocturnal lifestyle. For this reason, mammals underwent a tremendous re-organization of the auditory system (towards high-frequency hearing, three middle ear bones, etc.; for a review, see Grothe et al., 2010) in order to mainly rely on hearing for their survival and reproduction in the dark environment. On the contrary, the plesiomorphic condition in sauropsids might be much close to what I found in the chicken, where an high-resolution neural representation of the main sense, i.e., vision, is supported by a more crude representation of an auxiliary sense as hearing. In the case of the barn owl, the auditory acuity evolved again as adaptation to nocturnal hunting lifestyle. To prove this hypothesis, further experiments would be needed in reptiles to see whether they share a similar neural computation of auditory stimuli with generalist birds. After a long period of neuroscientific research dominated by the mammalian and barn owl auditory system as the main neural model, these and future findings in avian species might show the peculiarity of other animal taxa in solving a common sensory challenge.

## Bibliography

- Adamo, N. J. and Bennett, T. L. (1967). The effect of hyperstriatal lesions on head orientation to a sound stimulus in chickens. *Experimental Neurology*, 19(2):166–175.
- Aralla, R., Ashida, G., and Köppl, C. (2018). Binaural responses in the auditory midbrain of chicken (*gallus gallus*). *The European journal of neuroscience*, 51(5):1290–1304.
- Bala, A. D. and Takahashi, T. T. (2000). Pupillary dilation response as an indicator of auditory discrimination in the barn owl. *Journal of Comparative Physiology A*, 186(5):425–434.
- Bala, A. D. S., Spitzer, M. W., and Takahashi, T. T. (2003). Prediction of auditory spatial acuity from neural images on the owl's auditory space map. *Nature*, 424(6950):771–774.
- Beitel, R. E. (1991). Localization of azimuthal sound direction by the great horned owl. *The Journal of the Acoustical Society of America*, 90(5):2843–2846.
- Bregman, A. S. (1990). *Auditory scene analysis: The perceptual organization of sound* / Albert S. Bregman. MIT Press, Cambridge, Mass. and London.
- Brinkløv, S., Fenton, M. B., and Ratcliffe, J. M. (2013). Echolocation in oilbirds and swiftlets. *Frontiers in physiology*, 4:123.
- Calford, M. B., Wise, L. Z., and Pettigrew, J. D. (1985). Coding of sound location and frequency in the auditory midbrain of diurnal birds of prey, families accipitridae and falconidae. *Journal of Comparative Physiology ? A*, 157(2):149–160.
- Carr, C. E. and Friedman, M. A. (1999). Evolution of time coding systems. *Neural computation*, 11(1):1–20.
- Carr, C. E. and Konishi, M. (1988). Axonal delay lines for time measurement in the owl's brainstem. *Proceedings of the National Academy of Sciences of the United States of America*, 85(21):8311–8315.

- Carr, C. E. and Konishi, M. (1990). A circuit for detection of interaural time differences in the brain stem of the barn owl. *Journal of Neuroscience*, 10(10):3227–3246.
- Carroll, R. L. (1988). *Vertebrate paleontology and evolution*. Freeman, New York.
- Catania, K. C. (2013). Stereo and serial sniffing guide navigation to an odour source in a mammal. *Nature Communications*, 4(1):1441.
- Cazettes, F., Fischer, B. J., Beckert, M. V., and Pena, J. L. (2018). Emergence of an adaptive command for orienting behavior in premotor brainstem neurons of barn owls. *Journal of Neuroscience*, 38(33):7270–7279.
- Chaure, F. J., Rey, H. G., and Quian Quiroga, R. (2018). A novel and fully automatic spike-sorting implementation with variable number of features. *Journal of neurophysiology*, 120(4):1859–1871.
- Christensen-Dalsgaard, J. (2011). Vertebrate pressure-gradient receivers. *Hearing Research*, 273(1-2):37–45.
- Christensen-Dalsgaard, J., Brandt, C., Wilson, M., Wahlberg, M., and Madsen, P. T. (2011). Hearing in the african lungfish (protoperus annectens): pre-adaptation to pressure hearing in tetrapods? *Biology Letters*, 7(1):139–141.
- Clack, J. A. (2002). Patterns and processes in the early evolution of the tetrapod ear. *Journal of neurobiology*, 53(2):251–264.
- Clarke, P. G. and Whitteridge, D. (1976). The projection of the retina, including the 'red area' on to the optic tectum of the pigeon. *Quarterly Journal of Experimental Physiology and Cognate Medical Sciences*, 61(4):351–358.
- Collias, N. E. and Collias, E. C. (1967). A field study of the red jungle fowl in north-central india. *The Condor*, 69(4):360–386.
- Cotter, J. R. (1976). Visual and nonvisual units recorded from the optic tectum of gallus domesticus. *Brain, behavior and evolution*, 13(1):1–21.
- Dawkins, M. S. (2002). What are birds looking at? head movements and eye use in chickens. *Animal behaviour*, 63(5):991–998.
- DiCarlo, J. J., Lane, J. W., Hsiao, S. S., and Johnson, K. O. (1996). Marking microelectrode penetrations with fluorescent dyes. *Journal of Neuroscience Methods*, 64(1):75–81.

- Feinkohl, A., Borzeszkowski, K. M., and Klump, G. M. (2013). Effect of head turns on the localization accuracy of sounds in the european starling (*sturnus vulgaris*). *Behavioural brain research*, 256:669–676.
- Feinkohl, A. and Klump, G. M. (2013). Azimuthal sound localization in the european starling (*sturnus vulgaris*): II. psychophysical results. *Journal of comparative physiology. A, Neuroethology, sensory, neural, and behavioral physiology*, 199(2):127–138.
- Fischer, B. J., Peña, J. L., and Konishi, M. (2007). Emergence of multiplicative auditory responses in the midbrain of the barn owl. *Journal of neurophysiology*, 98(3):1181–1193.
- Frens, M. A. and van Opstal, A. J. (1995). A quantitative study of auditory-evoked saccadic eye movements in two dimensions. *Experimental Brain Research*, 107(1):103–117.
- Gatehouse, R. W. and Shelton, B. R. (1978). Sound localization in bobwhite quail (*colinus virginianus*). *Behavioral Biology*, 22(4):533–540.
- Gleich, O., Fischer, F. P., Köppl, C., and Manley, G. A. (2004). Hearing organ evolution and specialization: Archosaurs. In Manley, G. A., Fay, R. R., and Popper, A. N., editors, *Evolution of the Vertebrate Auditory System*, pages 224–255. Springer New York, New York, NY.
- Griffin, D. R. (1953). Acoustic orientation in the oil bird, *steatornis*. *Proceedings of the National Academy of Sciences of the United States of America*, 39(8):884–893.
- Grothe, B. (2018). How the barn owl computes auditory space. *Trends in neurosciences*, 41(3):115–117.
- Grothe, B., Pecka, M., and McAlpine, D. (2010). Mechanisms of sound localization in mammals. *Physiological reviews*, 90(3):983–1012.
- Halpern, M. E., Güntürkün, O., Hopkins, W. D., and Rogers, L. J. (2005). Lateralization of the vertebrate brain: taking the side of model systems. *Journal of Neuroscience*, 25(45):10351–10357.
- Harmening, W. M. and Wagner, H. (2011). From optics to attention: visual perception in barn owls. *Journal of Comparative Physiology A*, 197(11):1031–1042.
- Heffner, R. S. and Heffner, H. E. (1988). Sound localization acuity in the cat: Effect of azimuth, signal duration, and test procedure. *Hearing Research*, 36(2-3):221–232.
- Heffner, R. S., Koay, G., and Heffner, H. E. (1996). Sound localization in chinchillas III: Effect of pinna removal. *Hearing Research*, 99(1-2):13–21.

- Heiligenberg, W. (1991). *Neural nets in electric fish*. Computational neuroscience series. MIT Press, Cambridge, Mass and London.
- Hill, E. M., Koay, G., Heffner, R. S., and Heffner, H. E. (2014). Audiogram of the chicken (*Gallus gallus domesticus*) from 2 Hz to 9 kHz. *Journal of comparative physiology. A, Neuroethology, sensory, neural, and behavioral physiology*, 200(10):863–870.
- Hofman, P. M. and van Opstal, A. J. (1998). Spectro-temporal factors in two-dimensional human sound localization. *The Journal of the Acoustical Society of America*, 103(5 Pt 1):2634–2648.
- Hofman, P. M., van Riswick, J. G., and van Opstal, A. J. (1998). Relearning sound localization with new ears. *Nature Neuroscience*, 1(5):417–421.
- Hoy, R. R. (1992). The evolution of hearing in insects as an adaptation to predation from bats. In Webster, D. B., Fay, R. R., and Popper, A. N., editors, *The Evolutionary biology of hearing*, pages 115–129. Springer-Verlag, New York.
- Huang, A. Y. and May, B. J. (1996). Spectral cues for sound localization in cats: effects of frequency domain on minimum audible angles in the median and horizontal planes. *The Journal of the Acoustical Society of America*, 100(4 Pt 1):2341–2348.
- Hyson, R. L., Overholt, E. M., and Lippe, W. R. (1994). Cochlear microphonic measurements of interaural time differences in the chick. *Hearing Research*, 81(1-2):109–118.
- Iwaniuk, A. N., Heesy, C. P., Hall, M. I., and Wylie, D. R. W. (2008). Relative wulst volume is correlated with orbit orientation and binocular visual field in birds. *Journal of comparative physiology. A, Neuroethology, sensory, neural, and behavioral physiology*, 194(3):267–282.
- Jeffress, L. A. (1948). *A place theory of sound localization*, volume 41.
- Kaas, J. H. (2013). The evolution of brains from early mammals to humans. *Wiley interdisciplinary reviews. Cognitive science*, 4(1):33–45.
- Keller, C. H., Hartung, K., and Takahashi, T. T. (1998). Head-related transfer functions of the barn owl: measurement and neural responses. *Hearing Research*, 118(1-2):13–34.
- Kettler, L., Christensen-Dalsgaard, J., Larsen, O. N., and Wagner, H. (2016). Low frequency eardrum directionality in the barn owl induced by sound transmission through the interaural canal. *Biological Cybernetics*, 110(4-5):333–343.

- Kettler, L., Griebel, H., Ferger, R., and Wagner, H. (2017). Combination of interaural level and time difference in azimuthal sound localization in owls. *eNeuro*, 4(6).
- Kettler, L. and Wagner, H. (2014). Influence of double stimulation on sound-localization behavior in barn owls. *Journal of comparative physiology. A, Neuroethology, sensory, neural, and behavioral physiology*, 200(12):1033–1044.
- Klump, G. M. (2000). Sound localization in birds. In *Comparative Hearing: Birds and Reptiles*, pages 249–307. Springer, New York, NY.
- Klump, G. M. and Larsen, O. N. (1992). Azimuthal sound localization in the european starling (*sturnus vulgaris*): I. physical binaural cues. *Journal of Comparative Physiology A*, 170(2):243–251.
- Klump, G. M. and Shalter, M. D. (1984). Acoustic behaviour of birds and mammals in the predator context; i. factors affecting the structure of alarm signals. ii. the functional significance and evolution of alarm signals. *Zeitschrift für Tierpsychologie*, 66(3):189–226.
- Klump, G. M., Windt, W., and Curio, E. (1986). The great tit's (*parus major*) auditory resolution in azimuth. *Journal of Comparative Physiology A*, 158(3):383–390.
- Knudsen, E. I. (1982). Auditory and visual maps of space in the optic tectum of the owl. *Journal of Neuroscience*, 2(9):1177–1194.
- Knudsen, E. I., Blasdel, G. G., and Konishi, M. (1979). Sound localization by the barn owl (*tyto alba*) measured with the search coil technique. *Journal of Comparative Physiology ? A*, 133(1):1–11.
- Knudsen, E. I. and Brainard, M. S. (1995). Creating a unified representation of visual and auditory space in the brain. *Annual Review of Neuroscience*, 18(1):19–43.
- Knudsen, E. I. and Knudsen, P. F. (1983). Space-mapped auditory projections from the inferior colliculus to the optic tectum in the barn owl (*tyto alba*). *Journal of Comparative Neurology*, 218(2):187–196.
- Knudsen, E. I. and Konishi, M. (1978). A neural map of auditory space in the owl. *Science (New York, N.Y.)*, 200(4343):795–797.
- Knudsen, E. I. and Konishi, M. (1979). Mechanisms of sound localization in the barn owl (*tyto alba*). *Journal of comparative physiology*, 133(1):13–21.

- Koch, U. R. and Wagner, H. (2002). Morphometry of auricular feathers of barn owls (*tyto alba*). *European Journal of Morphology*, 40(1):15–21.
- Konishi, M. (1973). How the owl tracks its prey: Experiments with trained barn owls reveal how their acute sense of hearing enables them to catch prey in the dark. *American Scientist*, 61(4):414–424.
- Konishi, M. and Knudsen, E. I. (1979). The oilbird: hearing and echolocation. *Science (New York, N.Y.)*, 204(4391):425–427.
- Köppl, C. (1997). Phase locking to high frequencies in the auditory nerve and cochlear nucleus magnocellularis of the barn owl, *tyto alba*. *Journal of Neuroscience*, 17(9):3312–3321.
- Köppl, C. (2019). Internally coupled middle ears enhance the range of interaural time differences heard by the chicken. *Journal of Experimental Biology*, 222(Pt 12).
- Köppl, C. and Carr, C. E. (2008). Maps of interaural time difference in the chicken's brainstem nucleus laminaris. *Biological Cybernetics*, 98(6):541–559.
- Köppl, C., Gleich, O., and Manley, G. A. (1993). An auditory fovea in the barn owl cochlea. *Journal of Comparative Physiology A*, 171(6):695–704.
- Krumm, B., Klump, G. M., Köppl, C., Beutelmann, R., and Langemann, U. (2022). Chickens have excellent sound localization ability. *Journal of Experimental Biology*, 225(5).
- Krumm, B., Klump, G. M., Köppl, C., and Langemann, U. (2019). The barn owls' minimum audible angle. *PloS one*, 14(8):e0220652.
- Kubke, M. and Carr, C. E. (2000). Development of the auditory brainstem of birds: comparison between barn owls and chickens. *Hearing Research*, 147(1-2):1–20.
- Kuhn, G. F. (1977). Model for the interaural time differences in the azimuthal plane. *The Journal of the Acoustical Society of America*, 62(1):157–167.
- Larsen, O. N., Christensen-Dalsgaard, J., and Jensen, K. K. (2016). Role of intracranial cavities in avian directional hearing. *Biological Cybernetics*, 110(4-5):319–331.
- Lawal, R. A., Martin, S. H., Vanmechelen, K., Vereijken, A., Silva, P., Al-Atiyat, R. M., Aljumaah, R. S., Mwacharo, J. M., Wu, D.-D., Zhang, Y.-P., Hocking, P. M., Smith, J., Wragg, D., and Hanotte, O. (2020). The wild species genome ancestry of domestic chickens. *BMC biology*, 18(1):13.

- Lewald, J. and Dörrscheidt, G. J. (1998). Spatial-tuning properties of auditory neurons in the optic tectum of the pigeon. *Brain Research*, 790(1-2):339–342.
- Luksch, H. (2003). Cytoarchitecture of the avian optic tectum: neuronal substrate for cellular computation. *Reviews in the Neurosciences*, 14(1-2):85–106.
- Maldarelli, G., Firzlaff, U., Kettler, L., Ondracek, J. M., and Luksch, H. (2022a). Two types of auditory spatial receptive fields in different parts of the chicken's midbrain. *Journal of Neuroscience*.
- Maldarelli, G., Firzlaff, U., and Luksch, H. (2022b). Azimuthal sound localization in the chicken. *PLOS ONE*, 17(11):e0277190.
- Manley, G. A. (2010). An evolutionary perspective on middle ears. *Hearing Research*, 263(1-2):3–8.
- Manley, G. A. (2017). Comparative auditory neuroscience: Understanding the evolution and function of ears. *Journal of the Association for Research in Otolaryngology : JARO*, 18(1):1–24.
- Manley, G. A., Kaiser, A., Brix, J., and Gleich, O. (1991). Activity patterns of primary auditory-nerve fibres in chickens: Development of fundamental properties. *Hearing Research*, 57(1):1–15.
- Marler, P. (1955). Characteristics of some animal calls. *Nature*, 176(4470):6–8.
- Mills, A. W. (1958). On the minimum audible angle. *The Journal of the Acoustical Society of America*, 30(4):237–246.
- Moiseff, A. (1989a). Bi-coordinate sound localization by the barn owl. *Journal of Comparative Physiology A*, 164(5):637–644.
- Moiseff, A. (1989b). Binaural disparity cues available to the barn owl for sound localization. *Journal of Comparative Physiology A*, 164(5):629–636.
- Moiseff, A. and Konishi, M. (1981). Neuronal and behavioral sensitivity to binaural time differences in the owl. *Journal of Neuroscience*, 1(1):40–48.
- Moore, D. R. and King, A. J. (1999). Auditory perception: The near and far of sound localization. *Current Biology*, 9(10):R361–R363.
- Nelson and Stoddard (1998). Accuracy of auditory distance and azimuth perception by a passerine bird in natural habitat. *Animal behaviour*, 56(2):467–477.



- Nelson, B. S. and Suthers, R. A. (2004). Sound localization in a small passerine bird: discrimination of azimuth as a function of head orientation and sound frequency. *Journal of Experimental Biology*, 207(23):4121–4133.
- Niederleitner, B., Gutierrez-Ibanez, C., Krabichler, Q., Weigel, S., and Luksch, H. (2017). A novel relay nucleus between the inferior colliculus and the optic tectum in the chicken ( *gallus gallus* ). *Journal of Comparative Neurology*, 525(3):513–534.
- Novick, A. (1959). Acoustic orientation in the cave swiftlet. *The Biological Bulletin*, 117(3):497–503.
- Overholt, E. M., Rubel, E. W., and Hyson, R. L. (1992). A circuit for coding interaural time differences in the chick brainstem. *Journal of Neuroscience*, 12(5):1698–1708.
- Palmer, A. R. and King, A. J. (1982). The representation of auditory space in the mammalian superior colliculus. *Nature*, 299(5880):248–249.
- Park, T. J. and Dooling, R. J. (1991). Sound localization in small birds: absolute localization in azimuth. *Journal of comparative psychology (Washington, D.C. : 1983)*, 105(2):125–133.
- Parks, T. N. and Rubel, E. W. (1975). Organization and development of brain stem auditory nuclei of the chicken: organization of projections from n. magnocellularis to n. laminaris. *Journal of Comparative Neurology*, 164(4):435–448.
- Parsons, C. H., Lanyon, R. G., Schnupp, J. W., and King, A. J. (1999). Effects of altering spectral cues in infancy on horizontal and vertical sound localization by adult ferrets. *Journal of neurophysiology*, 82(5):2294–2309.
- Patterson, R. and Martin, W. L. (1992). Human stereopsis. *Human factors*, 34(6):669–692.
- Payne, R. S. (1971). Acoustic location of prey by barn owls (*tyto alba*). *Journal of Experimental Biology*, 54(3):535–573.
- Peña, J. L., Cazettes, F., Beckert, M. V., and Fischer, B. J. (2019). Synthesis of hemispheric itd tuning from the readout of a neural map: Commonalities of proposed coding schemes in birds and mammals. *Journal of Neuroscience*, 39(46):9053–9061.
- Peña, J. L. and Konishi, M. (2001). Auditory spatial receptive fields created by multiplication. *Science*, 292(5515):249–252.

- Poganiatz, I., Nelken, I., and Wagner, H. (2001). Sound-localization experiments with barn owls in virtual space: influence of interaural time difference on head-turning behavior. *Journal of the Association for Research in Otolaryngology : JARO*, 2(1):1–21.
- Poganiatz, I. and Wagner, H. (2001). Sound-localization experiments with barn owls in virtual space: influence of broadband interaural level different on head-turning behavior. *Journal of Comparative Physiology A*, 187(3):225–233.
- Pombal, M. A. and Megías, M. (2020). The nervous systems of jawless vertebrates. In Kaas, J. H., editor, *Evolutionary neuroscience*, pages 77–99. Academic Press, Amsterdam.
- Popper, A. N. and Fay, R. R. (1993). Sound detection and processing by fish: critical review and major research questions. *Brain, behavior and evolution*, 41(1):14–38.
- Puelles, L. (2007). *The chick brain in stereotaxic coordinates: An atlas based on neuromeres*. Academic, Oxford.
- Puelles, L., Robles, C., Martínez-de-la Torre, M., and Martínez, S. (1994). New subdivision schema for the avian torus semicircularis: neurochemical maps in the chick. *Journal of Comparative Neurology*, 340(1):98–125.
- Putland, R. L., Montgomery, J. C., and Radford, C. A. (2019). Ecology of fish hearing. *Journal of fish biology*, 95(1):39–52.
- Rayleigh (1907). Xii. on our perception of sound direction. *The London, Edinburgh, and Dublin Philosophical Magazine and Journal of Science*, 13(74):214–232.
- Rice, W. R. (1982). Acoustical location of prey by the marsh hawk: Adaptation to concealed prey. *The Auk*, 99(3):403–413.
- Rogers, L. J. and Deng, C. (2005). Corticosterone treatment of the chick embryo affects light-stimulated development of the thalamofugal visual pathway. *Behavioural brain research*, 159(1):63–71.
- Rogers, L. J. and Rajendra, S. (1993). Modulation of the development of light-initiated asymmetry in chick thalamofugal visual projections by oestradiol. *Experimental brain research*, 93(1):89–94.
- Rogers, L. J. and Sink, H. S. (1988). Transient asymmetry in the projections of the rostral thalamus to the visual hyperstriatum of the chicken, and reversal of its direction by light exposure. *Experimental brain research*, 70(2):378–384.

- Rubel, E. W. and Parks, T. N. (1988). Organization and development of the avian brainstem auditory system. In Edelman, G. M., Gall, W. E., and Cowan, W. M., editors, *Auditory functions*, Neurosciences Institute publication, pages 3–92. Wiley, New York, N.Y.
- Salvi, R. J., Saunders, S. S., Powers, N. L., and Boettcher, F. A. (1992). Discharge patterns of cochlear ganglion neurons in the chicken. *Journal of Comparative Physiology A*, 170(2):227–241.
- Sato, T., Fukui, I., and Ohmori, H. (2010). Interaural phase difference modulates the neural activity in the nucleus angularis and improves the processing of level difference cue in the lateral lemniscal nucleus in the chicken. *Neuroscience Research*, 66(2):198–212.
- Schnupp, J. W. H. and Carr, C. E. (2009). On hearing with more than one ear: lessons from evolution. *Nature neuroscience*, 12(6):692–697.
- Schnyder, H. A., Vanderelst, D., Bartenstein, S., Firzlaff, U., and Luksch, H. (2014). The avian head induces cues for sound localization in elevation. *PloS one*, 9(11):e112178.
- Schwarz, I. M. and Rogers, L. J. (1992). Testosterone: A role in the development of brain asymmetry in the chick. *Neuroscience Letters*, 146(2):167–170.
- Singheiser, M., Gutfreund, Y., and Wagner, H. (2012). The representation of sound localization cues in the barn owl's inferior colliculus. *Frontiers in Neural Circuits*, 6:45.
- Skiba, M., Diekamp, B., and Güntürkün, O. (2002). Embryonic light stimulation induces different asymmetries in visuoperceptual and visuomotor pathways of pigeons. *Behavioural brain research*, 134(1-2):149–156.
- Smith, Z. D. (1981). Organization and development of brain stem auditory nuclei of the chicken: dendritic development in n. laminaris. *The Journal of comparative neurology*, 203(3):309–333.
- Smotherman, M. and Narins, P. (2004). Evolution of the amphibian ear. In Manley, G. A., Popper, A. N., and Fay, R. R., editors, *Evolution of the vertebrate auditory system*, volume 22 of *Springer Handbook of Auditory Research*, pages 164–199. Springer, New York.
- Stanford, T. R. and Stein, B. E. (2007). Superadditivity in multisensory integration: putting the computation in context. *NeuroReport*, 18(8):787–792.
- Stein, B. E. and Meredith, M. A. (1993). *The merging of the senses*. A Bradford book. MIT Press, Cambridge, Mass., 2. print edition.

- Strybel, T. Z. and Fujimoto, K. (2000). Minimum audible angles in the horizontal and vertical planes: effects of stimulus onset asynchrony and burst duration. *The Journal of the Acoustical Society of America*, 108(6):3092–3095.
- Takahashi, T. and Konishi, M. (1986). Selectivity for interaural time difference in the owl's midbrain. *Journal of Neuroscience*, 6(12):3413–3422.
- Takahashi, T., Moiseff, A., and Konishi, M. (1984). Time and intensity cues are processed independently in the auditory system of the owl. *Journal of Neuroscience*, 4(7):1781–1786.
- Takahashi, T. T., Bala, A. D. S., Spitzer, M. W., Euston, D. R., Spezio, M. L., and Keller, C. H. (2003). The synthesis and use of the owl's auditory space map. *Biological Cybernetics*, 89(5):378–387.
- Takahashi, T. T., Kettler, L., Keller, C. H., and Bala, A. D. S. (2021). Anatomy and physiology of the avian binaural system. In Litovsky, R. Y., Goupell, M. J., Fay, R. R., and Popper, A. N., editors, *Binaural Hearing: With 93 Illustrations*, pages 81–111. Springer International Publishing, Cham.
- Takahashi, T. T., Wagner, H., and Konishi, M. (1989). Role of commissural projections in the representation of bilateral auditory space in the barn owl's inferior colliculus. *Journal of Comparative Neurology*, 281(4):545–554.
- Verhaal, J. and Luksch, H. (2013). Mapping of the receptive fields in the optic tectum of chicken (*Gallus gallus*) using sparse noise. *PloS one*, 8(4):e60782.
- Verhaal, J. and Luksch, H. (2016). Multimodal integration in the chicken. *The Journal of experimental biology*, 219(Pt 1):90–95.
- Volman, S. F. and Konishi, M. (1989). Spatial selectivity and binaural responses in the inferior colliculus of the great horned owl. *Journal of Neuroscience*, 9(9):3083–3096.
- Volman, S. F. and Konishi, M. (1990). Comparative physiology of sound localization in four species of owls. *Brain, behavior and evolution*, 36(4):196–215.
- von Campenhausen, M. and Wagner, H. (2006). Influence of the facial ruff on the sound-receiving characteristics of the barn owl's ears. *Journal of comparative physiology. A, Neuroethology, sensory, neural, and behavioral physiology*, 192(10):1073–1082.

- Wagner, H. (1993). Sound-localization deficits induced by lesions in the barn owl's auditory space map [published erratum appears in *J Neurosci* 1993 apr;13(4):following table of contents]. *Journal of Neuroscience*, 13(1):371–386.
- Wagner, H., Kettler, L., Orłowski, J., and Tellers, P. (2013). Neuroethology of prey capture in the barn owl (*Tyto alba* L.). *Journal of Physiology-Paris*, 107(1):51–61.
- Wagner, H., Takahashi, T., and Konishi, M. (1987). Representation of interaural time difference in the central nucleus of the barn owl's inferior colliculus. *Journal of Neuroscience*, 7(10):3105–3116.
- Wagner, H., Weger, M., Klaas, M., and Schröder, W. (2017). Features of owl wings that promote silent flight. *Interface focus*, 7(1):20160078.
- Wang, Y. and Karten, H. J. (2010). Three subdivisions of the auditory midbrain in chicks (*Gallus gallus*) identified by their afferent and commissural projections. *Journal of Comparative Neurology*, 518(8):1199–1219.
- Wang, Y., Zorio, D. A. R., and Karten, H. J. (2017). Heterogeneous organization and connectivity of the chicken auditory thalamus (*Gallus gallus*). *Journal of Comparative Neurology*, 525(14):3044–3071.
- Welch, T. E. and Dent, M. L. (2011). Lateralization of acoustic signals by dichotically listening budgerigars (*Melopsittacus undulatus*). *The Journal of the Acoustical Society of America*, 130(4):2293–2301.
- Wightman, F. L. and Kistler, D. J. (1989). Headphone simulation of free-field listening. i: Stimulus synthesis. *The Journal of the Acoustical Society of America*, 85(2):858–867.
- Young, S. R. and Rubel, E. W. (1983). Frequency-specific projections of individual neurons in chick brainstem auditory nuclei. *Journal of Neuroscience*, 3(7):1373–1378.

# Acknowledgments

I would especially like to thank my supervisor Harald Luksch, who always supported me in these 4 years of work. His wise advises, endless energy and humor made my Ph.D. experience much more instructive and enjoyable than expected, and I hope to collaborate with him in the future.

I would like to thank Uwe Firzlaff, who always supported me in the technical aspects of my work with his wide expertise and knowledge.

Also, I would like to thank the technicians Christian Fink, Yvonne Schwarz and especially Birgit Seibel for the great support and patience in several occasions.

Additionally, I would like to thank the other PhD students for the great fun together - even in such a quiet town as Freising - and for sharing (small) joys and (big) sorrows of electrophysiology experiments and Matlab coding.


I thank all my colleagues at the Zoology in Freising for many good times together, including field trips, Christmas parties and the notorious Freibierfest.


I thank the students who helped me out in my behavioral experiments, persevering stoically in the arduous task of training chickens.

Finally, I would like to thank Nil for bearing and motivating me when things were not going too smoothly, as well as all my family for their presence - even from a distance.


The work in this thesis was supported by the Deutsche Forschungsgemeinschaft (DFG) Grant (Lu 622 13/1) awarded to Harald Luksch.

## **Supporting documents concerning copyright**

Log in 



**JNeurosci**  
THE JOURNAL OF NEUROSCIENCE

An Official Journal of  **SOCIETY for NEUROSCIENCE**

Advanced Search

Submit a Manuscript

---

HOME
CONTENT
ALERTS
FOR AUTHORS
EDITORIAL BOARD
ABOUT
SUBSCRIBE

## Rights and Permissions

Updated June 2020

Top

### AUTHOR LICENSE POLICY

Authors grant *JNeurosci* a license to publish their work and copyright remains with the author. For articles published after 2014, the Society for Neuroscience (SfN) retains an exclusive license to publish the article for 6 months; after 6 months, the work becomes available to the public to copy, distribute, or display under the terms of the [Creative Commons Attribution 4.0 International License \(CC-BY\)](#). This license allows data and text mining, use of figures in presentations, and posting the article online, provided that the original article is credited.

Material published from 2010 to 2014 is licensed under a [Creative Commons Attribution-Noncommercial-Share Alike 3.0 Unported License \(CC-BY-NC-SA\)](#). SfN holds copyright for material published before 2010.

#### Open Choice

Authors may pay a surcharge to make their article freely available under a CC-BY license immediately upon publication. Authors can select the Open Choice option at submission, revision, or acceptance.

#### Author Rights

Authors do not need to obtain permission to reuse their material, including to:

- ❖ Reuse figures and tables in future works
- ❖ Include articles in theses or dissertations
- ❖ Reprint articles in books or compilations of their work
- ❖ Deposit the accepted manuscript version of their manuscript in an institutional repository or on their personal website. The *JNeurosci*-formatted PDF may be used 6 months after issue publication, or immediately if published Open Choice.

The original article in *JNeurosci* must be cited and linked to, where appropriate.

#### Funder Mandates

*JNeurosci* automatically deposits all articles in PubMed Central regardless of funding status. Articles are deposited once they have appeared in an issue and will be freely available 6 months from the issue date, unless the authors selected Open Choice. Furthermore, authors may deposit their final, accepted manuscript file, including revisions made during peer review, to funder, institutional, or other repositories at any time.

### PERMISSION TO REUSE *JNEUROSCI* MATERIAL

Anyone may reprint original *JNeurosci* material without requesting permission. A full journal reference and link to the version of record, where appropriate, must be included.

For content published before 2010, a copyright statement ("Copyright [year] Society for Neuroscience") should be included.


Questions should be directed to [jnpermissions@sfn.org](mailto:jnpermissions@sfn.org).

#### Photocopies

*JNeurosci* is registered with the [Copyright Clearance Center \(CCC\)](#). Authorization to photocopy items for the internal or personal use of specific clients is granted by SfN provided that the copier pays the appropriate fee to the CCC.

Home

Alerts



Content

Early Release

Current Issue

Issue Archive

Information

For Authors

For Advertisers

For the Media

About

About the Journal

Editorial Board

Privacy Policy

**Figure A1** Authors permission for reproduction from *The Journal of Neuroscience*




[My Orders](#)
[My Library](#)
[My Profile](#)

 Welcome gianmarco.maldarelli@gmail.com [Log out](#) | [Help](#) | [FAQ](#)
[My Orders](#) > [Orders](#) > [All Orders](#)

**Credit cards saved to your account prior to June 17th, 2022 will no longer be accessible during check out and in your profile. You will need to re-enter your credit card information for future transactions on Rightslink.**

## License Details

This Agreement between Mr. Gianmarco Maldarelli ("You") and Elsevier ("Elsevier") consists of your license details and the terms and conditions provided by Elsevier and Copyright Clearance Center.

[Print](#)
[Copy](#)

|  |   |
|--|---|
| License Number                               | 5420800183783   |
| License date                                 | Nov 02, 2022  |
| Licensed Content Publisher                   | Elsevier  |
| Licensed Content Publication                 | Current Biology   |
| Licensed Content Title                       | Auditory perception: The near and far of sound localization   |
| Licensed Content Author                      | David R Moore, Andrew J King  |
| Licensed Content Date                        | May 20, 1999  |
| Licensed Content Volume                      | 9   |
| Licensed Content Issue                       | 10  |
| Licensed Content Pages                       | 3   |
| Type of Use                                  | reuse in a thesis/dissertation  |
| Portion                                      | figures/tables/illustrations  |
| Number of figures/tables/illustrations       | 1   |
| Format                                       | both print and electronic   |
| Are you the author of this Elsevier article? | No  |
| Will you be translating?                     | No  |
| Title  | Behavioral Performance and Neurobiology of Sound Localization in the Chicken  |
| Institution name                             | Technische Universität München  |
| Expected presentation date                   | Jan 2023  |
| Order reference number                       | 1   |
| Portions                                     | Figure 1  |
| Requestor Location                           | Mr. Gianmarco Maldarelli<br>Liesel-Beckmann-Strasse 4<br><br>Freising, 85354<br>Germany<br>Attn: Mr. Gianmarco Maldarelli<br>GB 494 6272 12 |
| Publisher Tax ID                             | GB 494 6272 12  |
| Total  | <b>0.00 EUR</b>   |

[BACK](#)

Copyright © 2022 Copyright Clearance Center, Inc. All Rights Reserved. [Privacy statement](#). [Data Security and Privacy](#). For California Residents. [Terms and Conditions](#). Comments? We would like to hear from you. E-mail us at [customer@copyright.com](mailto:customer@copyright.com)

**Figure A2** License for reproduction from *Elsevier*

PLOS ONE

[PUBLISH](#)
[ABOUT](#)
[BROWSE](#)

SEARCH Q

advanced search

OPEN ACCESS PEER-REVIEWED

RESEARCH ARTICLE

## The Avian Head Induces Cues for Sound Localization in Elevation

Hans A. Schnyder , Dieter Vanderelst, Sophia Bartenstein, Uwe Firzlaff, Harald Luksch

Published: November 12, 2014 • <https://doi.org/10.1371/journal.pone.0112178>

|               |                |
|---------------|----------------|
| 55<br>Save    | 19<br>Citation |
| 7,491<br>View | 40<br>Share    |

- Correction
- Abstract
- Introduction
- Results and Discussion
- Methods
- Supporting Information
- Acknowledgments
- Author Contributions
- References

---

- Reader Comments
- Figures

**Citation:** Schnyder HA, Vanderelst D, Bartenstein S, Firzlaff U, Luksch H (2014) The Avian Head Induces Cues for Sound Localization in Elevation. PLoS ONE 9(11): e112178. <https://doi.org/10.1371/journal.pone.0112178>

**Editor:** M. Fabiana Kubke, University of Auckland, New Zealand

**Received:** June 2, 2014; **Accepted:** October 13, 2014; **Published:** November 12, 2014

**Copyright:** © 2014 Schnyder et al. This is an open-access article distributed under the terms of the [Creative Commons Attribution License](#), which permits unrestricted use, distribution, and reproduction in any medium, provided the original author and source are credited.

**Data Availability:** The authors confirm that all data underlying the findings are fully available without restriction. All relevant data are within the paper and its Supporting Information files.

**Funding:** The project was supported by a Bernstein Center for Computational Neuroscience Munich (BMBF) fund to HL (FKZ01GQ1004B), <http://www.bccn-munich.de>; a postdoctoral fellowship from the Research Foundation – Flanders (FWO); and a Marie Curie Intra-European Fellowship to DV, <http://ec.europa.eu/research/mariecurieactions>. The funders had no role in study design, data collection and analysis, decision to publish, or preparation of the manuscript.

**Competing interests:** The authors have declared that no competing interests exist.

Figure A3 Copyright for reproduction from PLOS ONE

OPEN ACCESS PEER-REVIEWED RESEARCH ARTICLE

# Azimuthal sound localization in the chicken

Gianmarco Maldarelli, Uwe Firzlaff, Harald Luksch

Published: November 22, 2022 • <https://doi.org/10.1371/journal.pone.0277190>

|          |            |
|----------|------------|
| 1 Save   | 0 Citation |
| 360 View | 2 Share    |

- Abstract
- Introduction
- Materials and methods
- Results
- Discussion
- Supporting information
- Acknowledgments
- References
- Reader Comments
- Figures

|   |
|---|
| <p><b>Citation:</b> Maldarelli G, Firzlaff U, Luksch H (2022) Azimuthal sound localization in the chicken. PLoS ONE 17(11): e0277190. <a href="https://doi.org/10.1371/journal.pone.0277190">https://doi.org/10.1371/journal.pone.0277190</a></p>   |
| <p><b>Editor:</b> Doug Wylie, University of Alberta, CANADA</p>   |
| <p><b>Received:</b> March 18, 2022; <b>Accepted:</b> October 21, 2022; <b>Published:</b> November 22, 2022</p>  |
| <p><b>Copyright:</b> © 2022 Maldarelli et al. This is an open access article distributed under the terms of the <a href="#">Creative Commons Attribution License</a>, which permits unrestricted use, distribution, and reproduction in any medium, provided the original author and source are credited.</p>               |
| <p><b>Data Availability:</b> All raw data files and scripts for data analysis are available from the Open Science Framework database (DOI: <a href="https://doi.org/10.17605/OSF.IO/UBMY4">10.17605/OSF.IO/UBMY4</a>); link: <a href="https://doi.org/10.17605/OSF.IO/UBMY4">https://doi.org/10.17605/OSF.IO/UBMY4</a>.</p> |
| <p><b>Funding:</b> This work was supported by a fund from the Deutsche Forschungsgemeinschaft (DFG Lu 622 13/1) awarded to HL, <a href="https://www.dfg.de/">https://www.dfg.de/</a>. The funders had no role in study design, data collection and analysis, decision to publish, or preparation of the manuscript.</p>     |
| <p><b>Competing interests:</b> The authors have declared that no competing interests exist.</p>   |

Figure A4 Copyright for reproduction from PLOS ONE